UNIVERSITÀ DEGLI STUDI DI BARI
Facoltà di Scienze Matematiche, Fisiche e Naturali

DOTTORATO DI RICERCA IN FISICA
XX Ciclo

Settore Scientifico Disciplinare
fis/01

The ALICE Silicon Pixel Detector Control and Calibration Systems

Ivan Amos Calì

A.A. 2006 - 2007

UNIVERSITÀ DEGLI STUDI DI BARI
Dipartimento InterAteneo di Fisica

DOTTORATO DI RICERCA IN FISICA
XX Ciclo

Settore Scientifico Disciplinare
fis/01

The ALICE Silicon Pixel Detector Control and Calibration Systems

Coordinatore: Prof. Maria Teresa Muciaccia

Supervisori: Prof. Bruno Ghidini
Dott. Vito Manzari

Dottorando: Ivan Amos Calì

Contents

Introduction

The work presented in this thesis was carried out in the Silicon Pixel Detector (SPD) group of the ALICE experiment at the Large Hadron Collider (LHC). It is hosted at the European Organization for Nuclear Research (CERN), near Geneva (Switzerland).
The SPD is the innermost part (two cylindrical layers of silicon pixel detectors) of the ALICE Inner Tracking System (ITS). The ALICE experiment is one of the four experiments (the others being ATLAS, CMS, LHCb), which will operate at LHC starting by mid 2008.
In the LHC, particles (p, Pb, Ar, etc.) will be accelerated to reach energies in the TeV range and they will collide head on at very high luminosity ($10^{34} cm^{-2} s^{-1}$ for protons and $10^{27} cm^{-2} s^{-1}$ for lead ions).

During the last three years I have been strongly involved in the SPD hardware and software development, construction and commissioning.
This thesis is focused on the design, development and commissioning of the SPD Control and Calibration Systems. I started this project from scratch. The work described in this manuscript is the result of my work and of a small team of collaborators who I coordinated. After a prototyping phase now a stable version of the control and calibration systems is operative. These systems allowed the detector sectors and half-barrels test, integration and commissioning as well as the SPD commissioning in the experiment.
The integration of the systems with the ALICE Experiment Control System (ECS), DAQ and Trigger system has been accomplished and the SPD participated in the experimental December 2007 commissioning run.

This thesis is divided in five chapters. The first gives a general overview on LHC and its expected performance. The ALICE physics and the main features of the apparatus are described.

Chapter 2 describes the main SPD features and services. This chapter is not intended to describe the detector in details but it only recalls the main

functionality and systems structure needed for this thesis.

The actual work done as PhD activity and object of this thesis is described in chapters 3 to 5.
The complexity of the detectors, the high number of subcomponents and the harsh working environment make necessary the development of a control system parallel to the data acquisition. This online slow control, called Detector Control System (DCS), has the task of controlling and monitoring all hardware and software components of the detector and of the necessary infrastructures. The latter include the power distribution system, cooling, interlock system, etc. As the physics experimental apparatuses grow in size and complexity, the number of electronic channels and the sophistication of the auxiliary systems increase proportionally. In this scenario, the DCS assumes a key role. Its functionalities have extended well over the simple control and monitoring of the experiment. DCS, nowadays, are highly advanced and automated online data acquisition systems, with less stringent requirements compared to the DAQ.
Moreover the SPD DCS has the unique feature of not only controlling but also operating the SPD front-end electronics. These requirements impose a high level of synchronization between the system components and a fast system response. The DCS, in this case, is a fundamental component for the detector calibration.
The SPD DCS should be operated in the ALICE DCS framework hence a series of integration constraint should be applied to the system.
Furthermore, in complex experiments such as ALICE, the detector operation is tightly bound to the connection and integration of the various systems such as DAQ, DCS, trigger system, Experiment Control System (ECS) and Offline framework. The knowledge of these systems structure and interfaces is fundamental for the developing of the SPD DCS and calibration systems.
The operation of the SPD front-end electronics and services should be done at various levels of integration. At the first and bottom level it is required that each system runs safely and independently. At the second level the subsystem controls should be merged to form a unique entity. At this stage the components operation should be synchronized to reach the full detector operation. The third level requires the integration of the SPD control in the general ALICE DCS/ECS. These requirements have been fulfilled by designing the DCS with two main software layers. On the bottom a Supervisory Control And Data Acquisition (SCADA) layer controls and monitors the equipments. It is based on a commercial application, PVSS, and it also responsible of provide an user interface to the subsystem components.
On top a Finite State Machine (FSM) Layer performs the logical connection

between the SPD subsystems and it connects the SPD DCS with the ALICE DCS and ECS.
PVSS is designed for slow control applications and it is not suitable for the direct control of the fast SPD front-end electronics. I designed a Front-End Device Server (FED Server) to interface the SCADA layer with the front-end electronics. The server receives macro-instructions from the SCADA and it operates autonomously the complex front-end electronics.

Chapter 3 gives a general SPD DCS overview focusing on the SCADA and FSM layers. It describes the control of the power supplies, cooling and interlocks systems. Moreover it hosts the description of the FED Server control. The FSM hierarchy as well as the Configuration Database (CDB) structures is discussed.

Chapter 4 is oriented to the FED Server and it gives a general overview of its functionality. Moreover it gives a description of the FED Server internal structure.

Chapter 5 is dealing with the detector calibration. The detector calibration parameters are introduced and the general strategies adopted to evaluate them are described. The complexity of the detector calibration requires a high automation level and the integration of the calibration system with the ALICE calibration framework. In order to satisfy these requirements and provide the user with a simple and versatile interface, I decided to foresee two calibration scenarios. A calibration scenario, named DAQ_ACTIVE, allows the fast detector calibration but it needs the control of the full detector and subsystems. A second calibration scenario, named DCS_ONLY, slower than the DAQ_ACTIVE scenario, allows the calibration of a detector partition without interference with the normal detector operation.
The control and calibration systems have been used to characterize and test the SPD components before and after the integration in the detector, both in laboratory (DSF) and in the ALICE environment. This chapter concludes the manuscript reporting some calibration and control systems application examples as well as a brief overview of the detector performance evaluated during the commissioning phases.

Chapter 1

The Large Hadron Collider and the ALICE experiment

In this chapter the motivations and the main features of the Large Hadron Collider (LHC) as well as some details of the ALICE experiment will be introduced.
In the first section the relevant accelerator parameters and the physics program allowed by the machine potential will be reviewed. The section will focus on few aspects of the p-p physics and will give a brief overview of three LHC experiments such as ATLAS, CMS and LHCb.
In the second section the ALICE detector and sub-detectors structures will be described, with emphasis on the requirements imposed by the physics program, the machine features and the technology constrains.

1.1 The Large Hadron Collider (LHC)

1.1.1 Machine parameters and Physics Program

The Standard Model (SM) predicts the existence of a yet to be seen particle, the Higgs boson. In this theoretical model, the Higgs boson is held responsible for electroweak symmetry breaking. Many extensions of the SM, like Supersymmetry, foresee the existence of an entire new class of undiscovered particles. Moreover the QCD phases diagram foresees that few microseconds after the Big Bang the matter was forming plasma of Quark and Gluons named Quark Gluon Plasma (QGP). It was the quest for the Higgs boson, the desire to investigate the limits of the Standard Model and its possible extensions and the study of the QGP that brought to the construction of the Large Hadron Collider (LHC), the most powerful particle accelerator at

present.

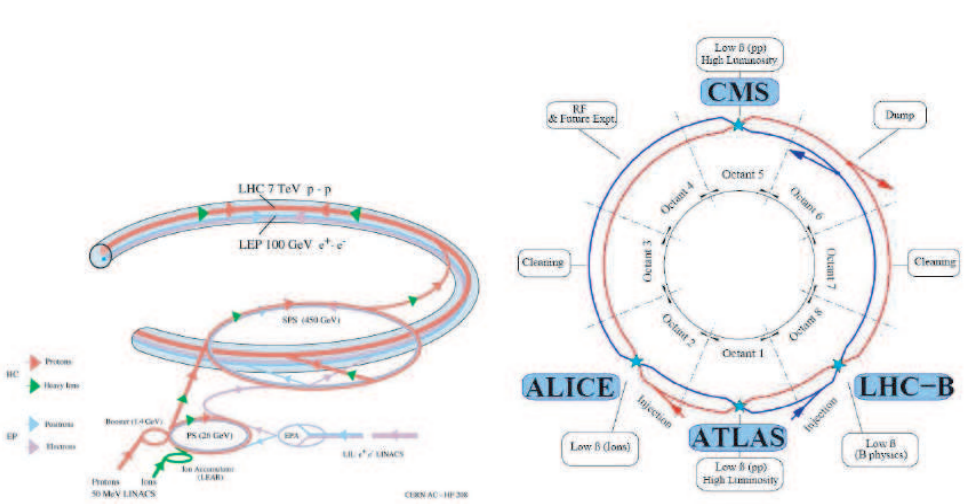

Figure 1.1: The LHC machine and its injection scheme (left). Layout of the LHC ring with the four interaction points (right).

The LHC at CERN is a proton-proton and heavy ions collider with a centre-of-mass energy of $\sqrt{s} = 14TeV$ when operating in the pp mode and $\sqrt{s} = 5.5TeV/A$ when operating in Pb-Pb mode. The accelerator is presently under construction and is currently being installed in the LEP tunnel. The first pp collisions at the LHC are expected to be observed in the middle of 2008. The circumference of the LEP tunnel is $\sim$ 27 Km and the magnetic field needed to keep the beam circulating in the machine is provided by 1232 superconducting dipoles providing a 8.4 Tesla magnetic field. A layout of the LHC injection and acceleration scheme is shown in Fig. 1.1. Protons will be produced in the 50 MeV proton linear accelerator (LINAC) and they will be injected into the 1.4 GeV Proton Synchrotron Booster. This will inject the protons into the Proton Synchrotron (PS) accelerating them to 25 GeV and delivering a beam of 135 bunches, containing $\sim 10^{11}$ protons. This beam is forwarded to the Super Proton Synchrotron (SPS) which will accelerate the protons to 450 GeV, ready to be injected into the LHC. Bunches of protons separated by 25 ns and with a RMS length of 75 mm intersect at four points where experiments are placed. ATLAS and CMS are general purpose experiments designed for searches for new physics and precision measurements. LHCb is B physics and CP violation dedicated detector while ALICE is a heavy ion experiment which will study the behavior of nuclear matter at very high energy densities.

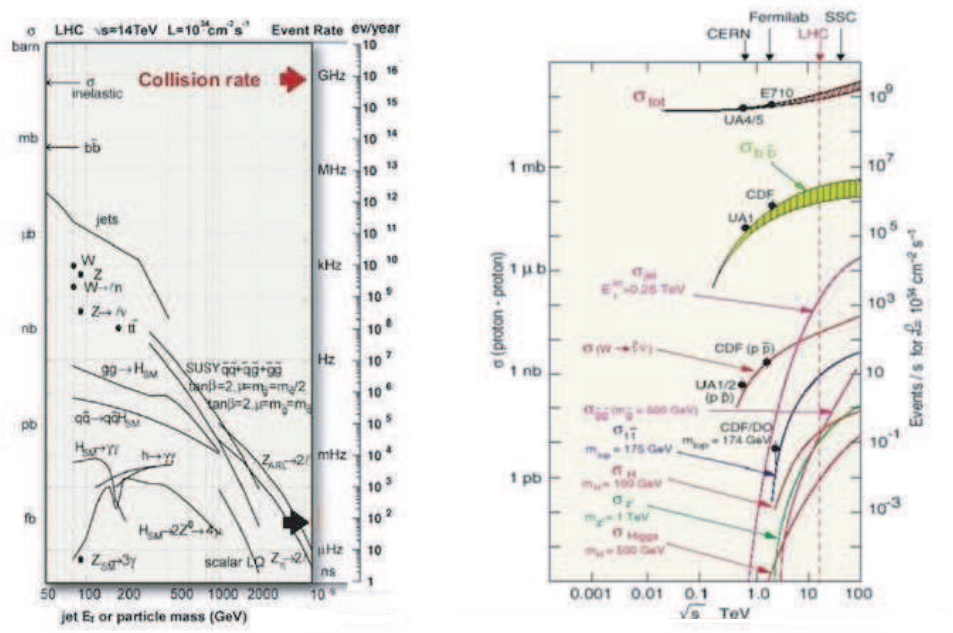

Figure 1.2: Production cross sections and event rates for various scattering processes at hadrons colliders as a function of the machine center-of-mass energy.

Two phases are foreseen for the LHC pp operation mode: in the first few years of operation (low luminosity phase) the nominal luminosity is expected to be $2 \times 10^{33} cm^{-2} s^{-1}$ and then should reach $1 \times 10^{34} cm^{-2} s^{-1}$ (high luminosity phase). At low luminosity approximately 10 fb^{-1} of data per calendar year will be provided while one year of operation at high luminosity will deliver 100 fb^{-1} of integrated luminosity. The machine will also be able to accelerate heavy ions allowing for example Pb-Pb collisions at 1150 TeV in the center of mass and luminosity up to $1 \times 10^{27} cm^{-2} s^{1}$.
The LHC machine will allow a broad and ambitious physics program. The main topics are briefly summarized in the following list:

- Search for a Standard Model Higgs boson from the LEPII low mass limit (114.6 GeV) up to the theoretical upper bound of 1 TeV. If a Higgs boson will be discovered, its mass, width and couplings could be measured.

- Search for Supersymmetry, Extra Dimensions and other signals of physics beyond the Standard Model up to masses $\sim 5TeV$.

- Precision measurements of the SM observables such as W and top quark masses and couplings.

- B physics and CP violation in the B hadrons system.

- Study of phase transitions from hadronic matter to plasma of deconfined quarks and gluons.

The LHC experiments will have to deal with complex working conditions due to high centre-of-mass energy and luminosity. The total cross section for inelastic, non-diffractive pp interactions at the LHC is expected to be around 80 mb at $\sqrt{s} = 14TeV$. Fig. 1.2 shows the cross sections for different processes as a function of the center-of-mass energy in p-p collisions. As it can be seen, the Higgs cross section increases steeply with $\sqrt{s}$, while the background remains almost constant.
At high luminosity the expected event rate is $\simeq 10^9 ev/s$. The physics events can be classified as follow:

- soft collisions: they are due to long range collisions between the two incoming protons. The final state particles from soft collisions have large longitudinal momentum and a small transverse momentum with $< p_T > \simeq MeV$. These events are also called minimum bias events and represent by far the majority of the pp collision.

- hard collisions: they are due to short range interactions in which head-on collisions take place between two partons of the incoming protons. In these interactions the momentum transfer can be large, allowing the production of final states with high-p_T particles and the creation of massive new particles. At the LHC the high-p_T events are dominated by QCD jet production from quarks and gluons fragmentation in the final state which has a large cross section. Rare events with new particle production have a cross section which is usually some orders of magnitude smaller than the jet production and therefore hadronic final states can not be used to detect rare events such as SM Higgs boson decay: in these conditions only decays into leptons and photons can

be used even if their branching ratio is much smaller than decays into quarks.

In the pp operation mode a bunch of $\sim 10^{11}$ protons will collide at each interaction point every 25 ns and therefore 25 soft collisions occur in average at each bunch crossing giving rise to a total number of 1000 charged particles in the region of $|\eta| < 2.5$. When an interesting high-p_T event takes place it is overlapped with $< 25 >$ soft interactions which constitute the pile-up. The detector parameters have been carefully tuned in order to reduce the impact of the pile-up on the physics searches. The AA physics program is described in section 1.2.1.

1.1.2 The Experiments at LHC

In total there are four experiments built to exploit LHC physics: ATLAS and CMS are designed as general p-p experiments; LHCb will focus on B-physics and ALICE is designed to study in details heavy ion collisions.

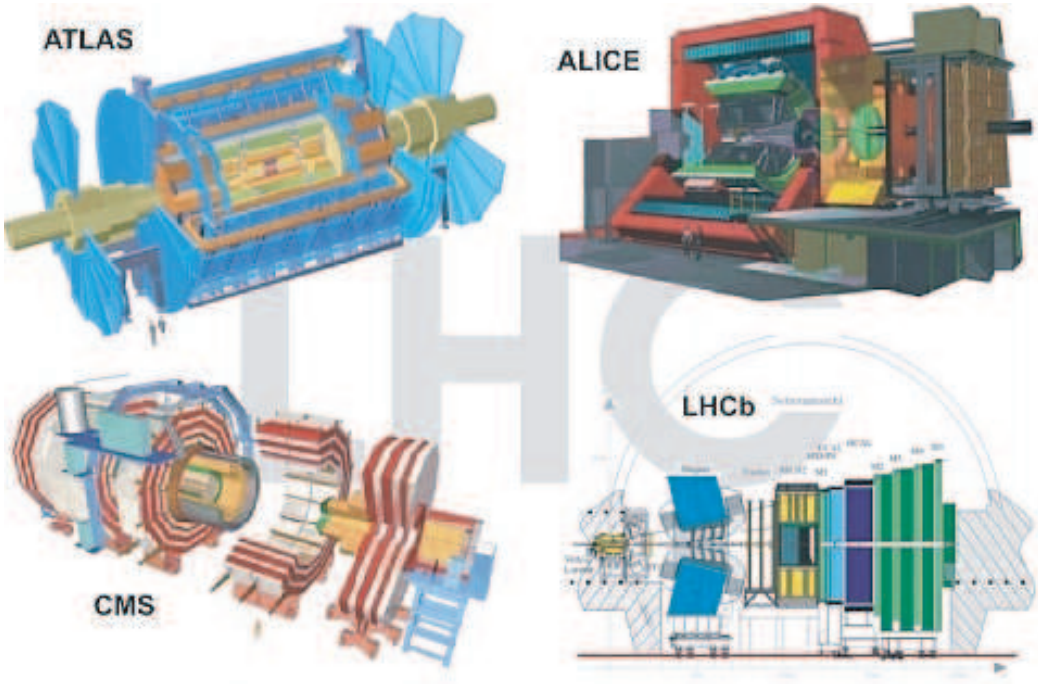

Figure 1.3: Schematic designs of the ATLAS, CMS, ALICE and LHCb experiments.

ATLAS and CMS are two general-purpose detectors and therefore they are designed to measure the broadest range of signals. Their main goals are to find the Higgs boson and to look for evidence of physics beyond the standard model, such as Supersymmetry, or extra dimensions.

ALICE is optimized for studying heavy ion collisions. The temperature and density at a collision of lead nuclei is expected to be high enough to generate a quark-gluon-plasma. In this phase quarks and gluons are almost free. ALICE will be able to investigate heavy ion collision at an unprecedented particle and energy density.

LHCb's specialty is the b-physics ('B factory'). In particular it will measure the parameters of CP violation in the interactions of b-hadrons.

In the next subsections a short description of the three experiments such as ATLAS, CMS and LHCb and their main goals is given. Section 1.2 is devoted to the ALICE experiment.

1.1.3 ATLAS

With a length of 46 m and a diameter of 25 m ATLAS (A Toroidal LHC ApparatuS) is the largest detector at the LHC.
The tracking detector of ATLAS consists of a Silicon Pixel Detector (SPD), Silicon Strip Detector (SSD) and a Transition Radiation Detector (TRD). It is surrounded by a solenoidal magnet which generates a uniform magnetic field. The Electromagnetic Calorimeter (ECal) and the Hadronic Calorimeter (HCal) build the next two layers of the detector. They are enclosed by the Muon Detector including the Muon Toroidal magnets. [1]

1.1.4 CMS

The main detector of CMS (Compact Muon Solenoid) is the Inner Tracker System. It consists of 10 layers of silicon strip and pixel detector with a total surface of $\sim 200\,\mathrm{m}^2$. The next layer, the Electromagnetic calorimeter(ECAL), is built of 80000 scintillating lead tungsten crystals. The Hadronic calorimeter (HCAL) consists of scintillators layers sandwiched with layers of brass or steel. The HCAL is surrounded by a super-conducting solenoid magnet which provides a 4 Tesla magnetic field. The outermost layer is the muon system and Return Yoke. It consists of Drift Tubes (DT), Cathode Strip Chamber (CSC) and Resistive Parallel Plate Chambers (RPC). For high precision trajectory measurements the DTs are placed in the central

barrels while the CSCs are mounted in the End Caps. The RPCs are placed in both the Barrel and the End Caps [2].

1.1.5 LHCb

LHCb is a fix target experiment using an LHC derived beam. It will look at CP-violation using the decay modes of b-mesons. LHCb will use the results coming from other experiments like KEK-B and PEP-II. With LHC it will be possible to measure precisely CP-asymmetry and processes which change the flavor of quarks and leptons. The two main detectors of LHCb are semiconducting trackers and a Ring-Imaging-Cherenkov detector (RICH).

1.2 A Large Ion Collider Experiment (ALICE)

1.2.1 ALICE Physics

ALICE will investigate equilibrium as well as non-equilibrium physics of strongly interacting matter in the energy density regime $\varepsilon \simeq 1-1000 GeV/fm^3$. In addition, the aim is to gain insight into the physics of parton densities close to phase-space saturation, and their collective dynamical evolution towards hadronization (confinement) in a dense nuclear environment. In this way, one also expects to gain further insight into the structure of the QCD phase diagram (Fig. 1.4) and the properties of the Quark Gluon Plasma (QGP) phase. In this plasma quarks and gluons do not exist in their compound state like in hadrons but they are free inside the plasma volume. The existence and the properties of this plasma can give answers to questions of QCD, a better understanding of the confinement and information about the transition from the hadronic state to the QGP. Due to the inner pressure the plasma expands and cools down until a critical temperature is reached where the hadronization starts. The QGP will also give information about the recreation of the chiral symmetry, the symmetry of right and left handed particles.

At high temperature T and vanishing chemical potential μ_B (baryon-number density), qualitative aspects of the transition to the QGP are controlled by the chiral symmetry of the QCD Lagrangian. This symmetry exists as an exact global symmetry only in the limit of vanishing quark masses. Since the heavy quarks (charm, bottom, top) are too heavy to play any role in the thermodynamics in the vicinity of the phase transition, the properties of 3-flavour QCD are of great interest. In the massless limit, 3-flavour QCD

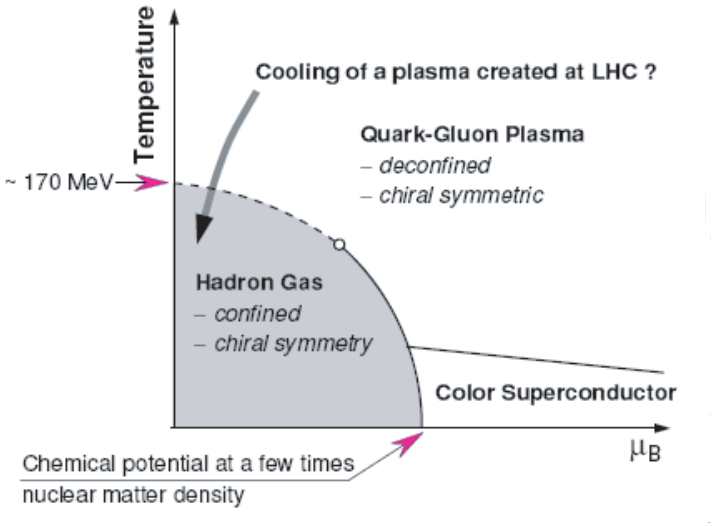

Figure 1.4: The QCD phase diagram.

undergoes a first-order phase transition. However, in nature quarks are not massless. In particular, the strange quark mass, which is of the order of the phase-transition temperature, plays a decisive role in determining the nature of the transition at vanishing chemical potential. It is still unclear whether the transition shows discontinuities for realistic values of the up, down and, strange quark masses, or whether it is merely a rapid crossover. Lattice calculations suggest that this crossover is rather rapid, taking place in a narrow temperature interval around $T_c \sim 170 MeV$. This high temperature and density can be reached by colliding ultra-relativistic heavy nuclei i.e. lead or gold nuclei in an accelerator like the LHC (but also at SPS energies).

The QGP cannot be observed directly due to the short life-time of this phase. Instead other signatures have to be used to measure this medium such as strangeness enhancement or J/Ψ suppression [3].
A series of SPS experiments were carried out using Pb projectiles of 160 GeV/A against lead (^{208}Pb) target. There are about 1500-2000 charged particles created in each of theses collision events and at the LHC this will go up to 50,000. Several thousands of them are expected in the central rapidity region, which is the region of interest for the QGP physics. The detector system thus has to have an extreme spatial resolution to separate the particle tracks and record electronically the track (and the ionization strength) of each traversing particle. In addition, the flight time of the particles has to be

measured. This allows identifying and determining momentum of all charged particles produced in Pb-Pb head-on collision. It is also possible to identify neutral "strange particles" by their secondary decay into charged particles.

ALICE will have also a proton-proton program that will be an intrinsic part of the experiment. The study of p-p collisions is essential as comparison and reference for the study of ion-ion collisions. It will also allow comparing results with previous experiments at SPS. It will provide first insights into pp physics in a new energy domain, to study soft hadronic physics and its gradual evolution for a better understanding of the perturbative QCD regime. Furthermore, the analysis of p-p data will provide low multiplicity data to commission and calibrate the various components of the ALICE detector [4].

1.2.2 The ALICE Detector

ALICE is a general-purpose detector designed to study the physics of strongly interacting matter and the quark-gluon plasma in nucleus-nucleus collisions at the LHC. The detector is designed to cope with the highest particle multiplicities anticipated for Pb-Pb reactions (dN/dy ∼8000) and it will be operational at the start-up of the LHC. In addition to heavy ions, the ALICE Collaboration will study collisions of lower-mass ions, which are a means of varying the energy density, and protons (both pp and p-nucleus), which provide reference data for the nucleus-nucleus collisions.
The ALICE detector (Fig. 1.5) consists of a central part, which measures event-by-event hadrons, electrons and photons, and a forward spectrometer to measure muons. The central part, which covers polar angles from 45^o to 135^o ($|\eta| < 0.9$) over the full azimuth, is embedded in the large L3 solenoidal magnet. It consists of an Inner Tracking System (ITS) of high-resolution silicon tracking detectors; a cylindrical Time Projection Chamber (TPC); three particle identification arrays based, respectively, on time-of-flight (TOF-PID), transition radiation (TRD) and Cerenkov counters (HMPID); two complementary electromagnetic calorimeters (PHOS, EMCAL). The forward muon arm (2-9^o , $\eta = 2.5$-4) consists of a complex arrangement of absorbers, a large dipole magnet, and 14 planes of tracking and triggering chambers. The set-up is completed by a set of zero-degree calorimeters (ZDCs) located far downstream in the machine tunnel, and a forward multiplicity detector (FMD) which covers a large fraction of the phase space ($|\eta| < 4$).
The most important components of the detector are briefly discussed in the next sections.

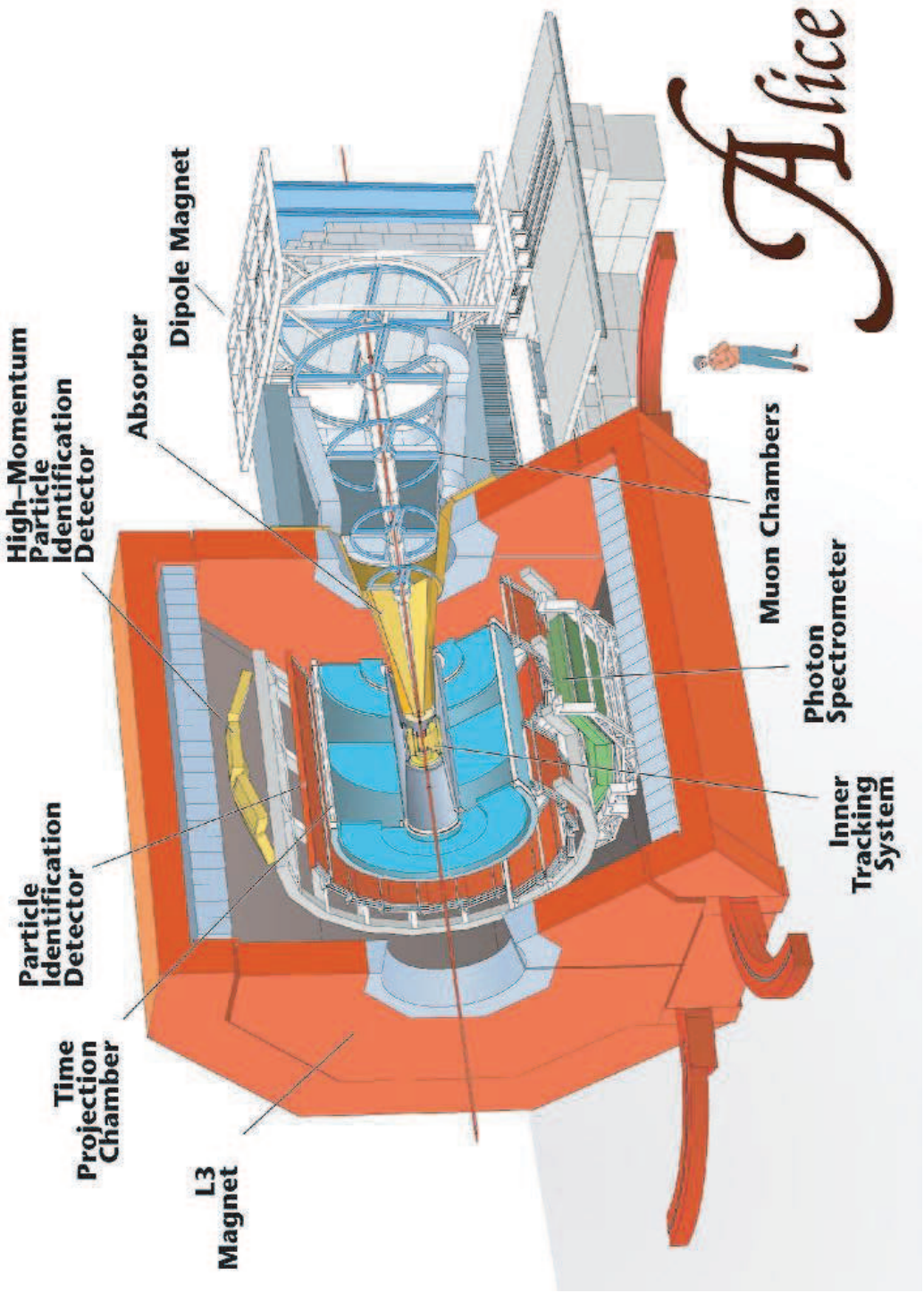

Figure 1.5: A ALICE detector schematic draw.

1.2.2.1 Magnet

The optimal choice for ALICE is the L3 large solenoid with a rather weak field (0.2 to 0.5 T) allowing full tracking and particle identification inside the magnet. The available space has to be sufficiently large to accommodate the PHOS, which must be placed at a distance of $\sim 5m$ from the vertex, because of the large particle density.

1.2.2.2 Inner Tracking System (ITS)

The basic functions of the inner tracker - secondary vertex reconstruction of hyperon and charm decays, particle identification and tracking of low-momentum particles, and improvement of the momentum resolution - are achieved with six barrels of high-resolution detectors. Because of the high particle density, the innermost four layers need to be truly two-dimensional devices, i.e. silicon pixel and silicon drift detectors. The outer layers at distance r $\sim$ 40 cm from the beam axis will be equipped with double-sided silicon micro-strip detectors. Four of the layers will have analogue readout for independent particle identification via dE/dx in the non-relativistic region, which will give the inner tracking system a stand-alone capability as a low p_T particle spectrometer. More details about the Inner Tracking System will be presented in section 1.3.

1.2.2.3 Time Projection Chamber (TPC)

The Time Projection Chamber is the main detector in the central barrel of ALICE. Its functions are:

- track finding with an efficiency better than 90 %;
- charged particle momentum measurement with a resolution better than 2.5% for electrons with a momentum of about 4 GeV/c;
- particle identification with a dE/dx resolution better than 10% and
- two-track separation in the region of $p_T < 10\,GeV/c$ and a pseudo-rapidity of $|\eta| < 0.9$

The TPC is a cylindrical gas detector with an active volume between 90 cm to 250 cm in radial direction and a length of 500 cm along the beam axis. A high voltage (HV) electrode is located at its center, which will be aligned to the interaction point, dividing the barrel into two symmetric drift volumes of 250 cm length. The HV electrode, which consists of an aluminized

stretched Mylar foil, and two opposite axial potential degraders create a highly uniform electrostatic field. The potential of the drift region is defined by Mylar strips wound around 18 inner and outer support rods [5], [6]. The design is optimized for good double-track resolution; in particular, the use of Ne/CO_2 (90/10) minimizes electron diffusion and reduces the space charge. The 72 pad-readout chambers are arranged in two end plates of 18 azimuthal sectors at both ends of the TPC, and feature 570,000 channels.

1.2.2.4 Particle Identification System (TOF, HMPID, TRD)

A special task of the ALICE experiment is to identify the mass of the particles emitted. If the low energy particles may be identified by the loss of energy, the higher ones are detected measuring the time it takes for a particle to fly from the collision point to the detector barrel which is 3.5 meters away. At even larger energies where the yield of particles is low, ALICE makes use, for PID, of a smaller detector ($14m^2$) called HMPID. This detector is based on the detection of Cherenkov photons emitted by the particles in a dielectric medium. Hence the detector is called a RICH (Ring Imaging CHernkov) because the pattern of the photons detected by a Cesium Iodide (CsI) photocathode is ring like. A Transition Radiation Detector (TRD) allows electron identification above 1 GeV/c.

The Time of Flight (TOF) will allow a separation of kaons from pions up to 2.5 GeV/c or protons from kaons up to 4 GeV/c, which requires a global time resolution of $\sim$ 100 ps. The ALICE TOF is arranged in 18 supermodules, covering 360^o in azimuth and a range in pseudo-rapidity of $|\eta| < 1$ with a total area of $\sim 150m^2$. Each supermodule consists of five modules, containing between 15 and 19 Multigap Resistive Plate Chambers (MRPC) strips. Each strip contains two stacks of resistive glass plates, separated with equal sized spacers, creating a series of uniform gas gaps with voltage applied to the external surfaces. The MRPC stack is made of 6 glasses forming 5 gaps with 250 μm width [7], [8].

The High Momentum Particle Identification Detectors (HMPID) consists of seven $1.5\,m \times 1.5\,m$ RICH proximity focusing counters, mounted at a radial distance of 4.7 m from the interaction point on a space frame, covering 5 % of the ALICE barrel acceptance. Each of these modules contains six $0.64\,\mathrm{m} \times 0.4\,\mathrm{m}$ CsI photocathodes (PCs) covering a total active area of $11\,\mathrm{m}^2$. The HMPID identifies pions and kaons in the range of $1 < \mathrm{p_T} < 3\mathrm{GeV/c}$ and protons and kaons in the range of $2 < \mathrm{p_T} < 5\mathrm{GeV/c}$. The low yield of high-

momentum particles in Pb − Pb collisions at the LHC energy regime justifies the single-arm geometry of the HMPID [9], [10].

The Transition Radiation Detector (TRD) will be installed between the space frame and the Time Projection Chamber. The TRD barrel has a radius range between 2.9 m and 3.7 m from the beam axis and 7 m length along the beam axis covering the central rapidity region of $|\eta| < 0.9$. The TRD is divided into 540 modules organized in 18 sectors and 6 layers. The detector has a total area of 750 m^2 of gas chambers with radiators for particle tracking and electron identification above 1 GeV/c. The TRD will also contribute to the trigger system on high-p_T e^+e^- pairs in order to reduce the collision rate to the readout event rate, by increasing the statistics on rare signals such J/Ψ and Υ [11], [12].

1.2.2.5 Photon Spectrometer (PHOS)

The Photon Spectrometer is optimized to measure photons with a high resolution and to detect light neutral mesons (π^0 and η) through their two-photon decay. The PHOS has been designed to cover the pseudorapidity range $|\eta| = 0.12$ and an azimuthal domain of 100 degrees. The detector consists of 5 identical modules, each with 3584 channels, 17920 in total. Each detection channel consists of a $2.2 \times 2.2 \times 18\,cm^3$ lead-tungsten crystal, $PbWO_4$ (PWO), coupled to an Avalanche Photo-Diode (APD) and a low-noise preamplifier [13].

1.2.2.6 Electromagnetic Calorimeter (EMCAL)

The Electromagnetic Calorimeter is a large Pb-scintillator sampling calorimeter with cylindrical geometry, located ∼4.5 m radial from the beam axis inside the L3 magnet. Covering a range in pseudo-rapidity of $|\eta| < 0.7$ the EMCAL is positioned opposite in azimuth to the PHOS. The calorimeter is segmented into 12672 projective towers, each covering $\delta\eta \times \delta\phi \sim 0.014 \times 0.014$. The Readout fibers are coupled to an Avalanche Photodiode (APD) sensor. The EMCAL provides level 0 and 1 triggers for photons, electrons and jets [5].

1.2.2.7 Forward Detectors (ZDC, PMD, FMD, FMS, T0, V0)

The Forward Muon Spectrometer (FMS) is designed to cover the complete spectrum of heavy quarkonia states (c $\bar{c}$, b $\bar{b}$) i.e. J/Ψ, Ψ', Υ, Υ", Υ" through their decay channels in two muons, both in proton-proton and in heavy-ion collisions. The angular acceptance of the muon spectrometer is from 2^o to

9^o ($|\eta| = 2.5 - 4$). Its mass resolution will be better than 100 MeV at about 10 GeV, sufficient to separate all quarkonia states. It consists of a composite absorber, made with layers of both high- and low-Z materials, starting 90 cm from the vertex, a large dipole magnet with a 3 Tm field integral placed outside the L3 magnet, and 10 planes of thin, high-granularity tracking stations. A second absorber at the end of the spectrometer and four more detector planes are used for muon identification and triggering. The spectrometer is shielded throughout its length by a dense absorber tube, of about 60 cm outer diameter, which surrounds the beam pipe.

The pre-shower Photon Multiplicity Detector (PMD) has a fine granularity and full azimuthal coverage in the pseudo-rapidity region $1.8 \leq \eta \leq 2.6$. It will be mounted on the L3 magnet door 5.8 m from the interaction point. Charged particles are rejected using a charged particle veto (CPV) in front of the converter. Both the CPV and the pre-shower converter are based on a honeycomb proportional chamber design. There are $\sim 2 \times 10^5$ cells each having an area of $1\,\mathrm{cm}^2$. The honeycomb wall forms a common cathode, operated at a high negative voltage. The signal will be readout from the anode wires at ground potential using GASSIPLEX front-end electronics. The PMD will be able to take data in conjunction with the dimuon spectrometer and other high rate detectors [14].

The FMD consists of 51,200 silicon strip channels distributed over 5 ring counters. There are two types of ring counters which have 20 and 40 sectors each in azimuthal angle. The main function of the FMD is to provide precise charged particle multiplicity measurements in the pseudorapidity range of $-3.4 \leq \eta \leq -1.7$ and $1.7 \leq \eta \leq 5.0$, respectively. Due to the readout time of $\approx 13\,\mu$s the FMD will only contribute to the level 2 trigger in ALICE. Together with the pixel detector system the FMD will provide charged particle multiplicity distributions for all collision types in the pseudorapidity range of $-3.4 \leq \eta \leq 5.0$ [15].

The T0 detector consists of 2 arrays of PMTs equipped with Cherenkov radiators and positioned on the opposite side of the IP. The main task of the T0 is to supply a signal for the level 0 trigger for ALICE, in particular for the TRD and delivering a reference time for the TOF. The T0 has a time resolution better than 50 ps and covers a range in pseuo-rapidity of $-3.3 \leq \eta \leq -2.9$ and $4.5 \leq \eta \leq 5.0$, respectively.

The V0 consists of 2 disks of segmented plastic scintillator tiles (8 segments) readout by optical fibers. It covers approximately the same range in pseudo-rapidity as the FMD. The main functionality of the V0 system is to provide the online L0 centrality trigger for ALICE by setting a threshold on deposited energy, and to provide a background rejection capability for the dimuon arm.

The event by event determination of the centrality plays a basic role in heavy ion collisions. It is used at the trigger level to enhance the sample of central collisions and to estimate the energy density reached in the interactions. The Energy E_S carried away by non-interacting nucleons (spectators) is the measurable quantity most directly related with the centrality of the collision. The ZDC consists of two radiation hard calorimeters, one for the spectator neutrons, the other for the spectator protons made of quartz-fiber, which allows a very compact design of the detector [16].

1.2.2.8 Computing and Core Software

For complex systems, such as the ALICE detector (and the other CERN detectors), an object oriented approach, implemented in C++, is now the choice of software developers. The move to this mainstream software technology will help to manage the process of change over the long lifetime of the experiment. C++ releases have been made of the functional prototypes of the most important software components. The data storage, networking and processing power needed to analyze data is in excess of those of today's facilities. Technological advances will help to make the data analysis possible in a distributed environment. Several groups were started with the aim of developing the reconstruction and selection procedures (algorithms and software) starting from the output of the Level-1 trigger, and aiming ultimately at the full offline reconstruction.
In the original ALICE design the scope of the trigger system was very limited, essentially providing a gate to the TPC for central events and protecting against pileup. With the increasing importance of low-cross section, high-pt observables, and the successive addition of the muon arm and especially the TRD, the demands on the trigger system have increased dramatically. It now includes a pretrigger, three hardware trigger levels (L0, L1 and L2) and a processor based High Level Trigger (HLT). The pretrigger, essentially detecting an interaction using the small angle counters (T0, V0), provides in less than 100 ns a wake-up signal to the TRD front-end, thus allowing

its digital electronics to be in a low-power mode most of the time. The L0 (at 1.2 μs) and L1 (at 6.5 μs) triggers gate the fast detectors, while only at the end of the TPC drift time (after about 100 μs), a L2 decision can be reached, which includes an elaborate and flexible past-future protection scheme. After the L2 decision the readout of all detectors is initiated.
The HLT implements features of online analysis of the full event during the data readout, by using both a dedicated computer farm and distributed intelligence in the data receivers and local data concentrators. HLT functions will include flexible trigger algorithms, data compression, and advanced online tracking possibilities.
A general framework called the ALICE Data Acquisition Test Environment (DATE) system has been developed to operate the DAQ system. The communication between the DAQ system and the detectors electronics is performed via optical link: the ALICE Detector Data Link or DDL. In order to collect a sufficient number of events for physics analysis in the short heavy-ion running period (roughly one month per year), and given the large amount of information carried for each event (up to several 10 Mbytes) the DAQ system is designed to have a very large bandwidth of up to 1.25 Gbytes/s on mass storage.

1.3 The ALICE Inner Tracking System (ITS)

The ITS consists of six cylindrical layers of coordinate-sensitive detectors. It covers the central rapidity region ($|\eta| \leq 0.9$) for vertices located within the length of the interaction diamond ($\pm 1\sigma$), i.e. 10.6 cm along the beam direction (z). The detectors and front-end electronics are held by lightweight carbon-fiber structures. Fig. 1.6 displays the ITS structure.
The number and position of the layers are optimized for efficient track finding and impact parameter resolution. In particular, the outer radius is determined by the track matching with the TPC, and the inner one is the minimum compatible with the radius of the beam pipe (3 cm).
The silicon detectors feature the high granularity and excellent spatial precision required. Because of the high particle density, up to 90 per squared centimeter, the four innermost layers ($r < 24$ cm) must be truly two-dimensional devices. For this task Silicon Pixel Detectors (SPD) and Silicon Drift Detectors (SDD) were chosen. The two innermost layers of the ITS are fundamental in determining the quality of the vertexing capability of ALICE (determination of the position of the primary vertex, measurement of the impact parameter of secondary tracks from the weak decays of strange, charm and beauty particles).

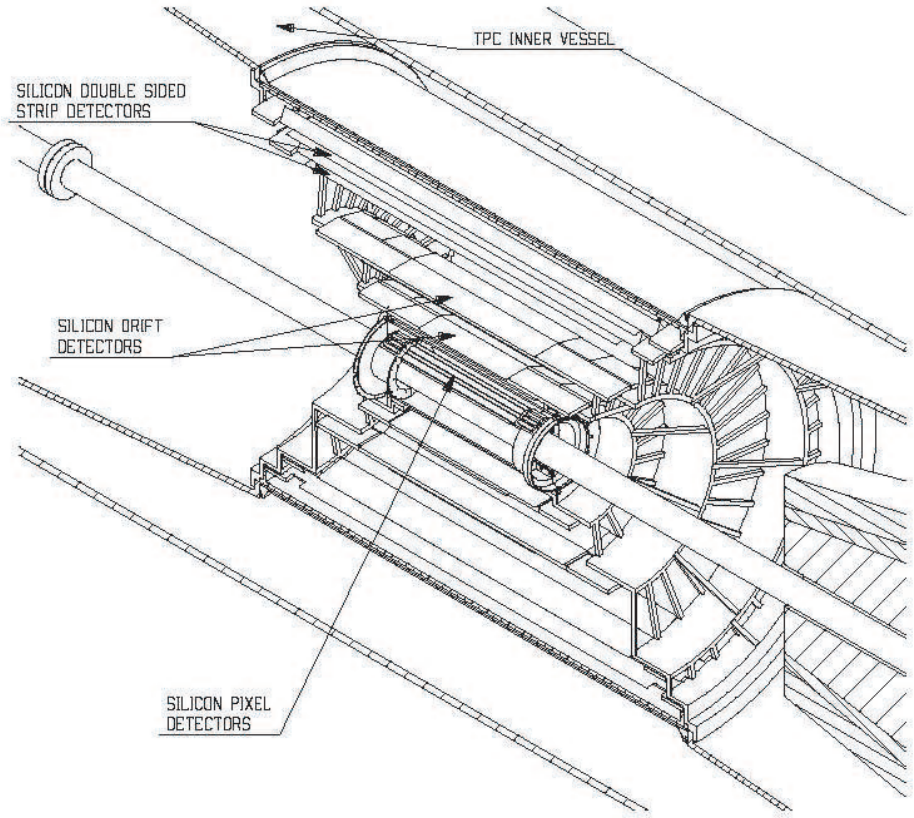

Figure 1.6: General view of the Alice Inner Tracking System. It consists of six cylindrical layers of silicon detectors.

Several motivations led to the choice of equipping ALICE with a barrel of two layers of Silicon Pixel Detectors. A silicon detector with a two-dimensional segmentation combines the advantages of unambiguous two-dimensional readout with the characteristics of silicon microstrip detectors such as: geometrical precision, double-hit resolution, speed, simplicity of calibration and the ease of alignment. In addition, a high segmentation leads naturally to a low individual diode capacitance, resulting in an excellent signal-to-noise ratio at high speed. The SPD will be described in more detail in chapter 2.

Silicon Drift Detectors (SDD) have been selected to equip the two intermediate layers of the ITS, since they couple a very good multi-track capability with dE/dx information.
At least three measured samples per track, and therefore at least four layers carrying dE/dx information are needed. The SDDs, each $7.0 \times 7.5\,\mathrm{cm}^2$ in active area, are mounted on linear structures called ladders, each holding six detectors for the inner and eight detectors for the outer layer. The detector consists of two barrel layers located at radii 14.9 and 23.8 cm, respectively. The inner layer is composed in total of 14, the outer layer of 22 ladders[17].

The two outer layers, where the track densities are below 1 per cm^2, are equipped with Silicon Strip Detectors (SSDs). They are crucial for the connection of tracks from the ITS to the TPC. The two layers of the detector at radii 39.1 and 43.6 cm are made of double-sided strip detectors (SSD) and have a length of 45.1 and 50.4 cm, respectively. The sensors, each with 768 strips of 25 - 50 μm wideness and 95 μm pitch, have an area of $75 \times 42\,\mathrm{mm}^2$ and a thickness of 300 μm. The stereo angle between the strips on one sensor is $\pm$17.5 milliradians. The SSD also provides dE/dx information to assist particle identification for low-momentum particles [18], [19].
Double-sided microstrips have been selected rather than single-sided ones because they introduce less material in the active volume. In addition they offer the possibility to correlate the pulse height readout from the two sides, thus helping to resolve ambiguities inherent in the use of detectors with projective readout.

With the exception of the two innermost pixel planes, all the ITS layers will have analogue readout for particle identification via a dE/dx measurement in the non-relativistic region. This will give the inner tracking system a stand-alone capability as a low-p_T particle spectrometer.

The large number of channels in the layers of the ITS requires a large number of connections from the front-end electronics to the detector and to the read-out. The requirement for a minimum of material within the acceptance does not allow the use of conventional copper cables near the active surfaces of the detection system. Therefore TAB bonded aluminum multilayer micro-cables are used.
The ITS four outer layers are assembled onto a mechanical structure made of two end-cap cones connected by a cylinder placed between the SSD and the SDD layers. Both the cones and the cylinder are made of lightweight sandwiches of carbon-fiber plies and Rohacell. The carbon-fiber structure includes also the appropriate mechanical links to the TPC and to the SPD layers.
The latter are assembled in two half-cylinder structures, specifically designed for safe installation around the beam pipe. The end-cap cones provide the cabling and cooling connection of the six ITS layers with the outside services.

Chapter 2

The Silicon Pixel Detector (SPD)

This chapter gives a general overview on the Silicon Pixel Detector (SPD) components and services. Its main goal is to introduce the SPD features needed for the understanding of this thesis. A detailed SPD description can be found in ALICE literature such as reported in this manuscript references. Chapter 1 introduced the ALICE apparatus and explained the physics reasons that lead to the need of an Inner Tracking System. The introduction of this chapter recalls the system specification whereas in section 2.1 the detector modules (Half-Staves) are described. Sections 2.2 and 2.3 are intended to introduce the SPD off-detector electronics and services.

The Silicon Pixel Detector (SPD) constitutes the two innermost layers of the ALICE Inner Tracking System (ITS) at radii of 3.9 cm and 7.6 cm, respectively. It is a fundamental element for the determination of the position of the primary vertex as well as for the measurement of the impact parameter of secondary tracks originating from the weak decays of strange, charm, and beauty particles [53]. The SPD will operate in a region where the track density could be as high as 50 tracks/cm^2, and in relatively high radiation levels: in the case of the inner layer, the integrated levels (10 years, standard running scenario) of total dose and fluence are estimated to be 2.5 kGy and 3×10^{12} n/cm^2 (1 MeV neutron equivalent), respectively [61].

The SPD design implements several specific solutions to minimize the material budget. Therefore, the materials used are as thin as possible using wherever possible light weight materials. As a result the average material traversed by a straight track perpendicular to the detector surface is less than 1 % X_0 per layer. It is the lowest value for pixel detectors at the LHC.

Moreover a unique feature of the SPD is that it can provide a prompt multiplicity trigger within the latency of the L0 trigger (850ns) [20].

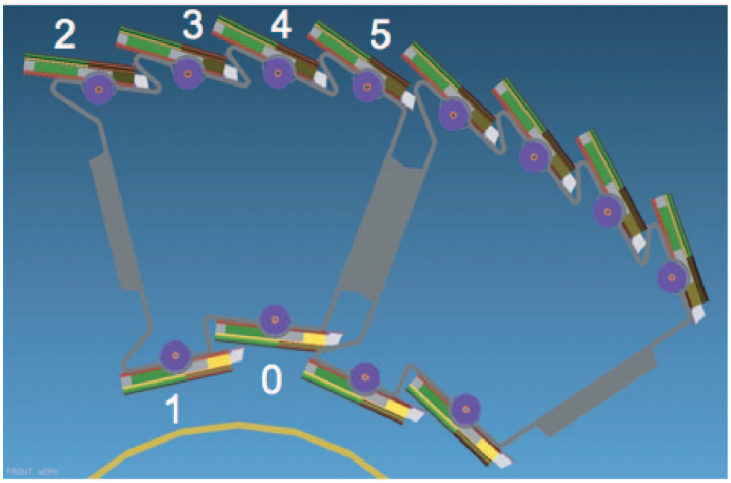

Figure 2.1: A schema of two adjacent sectors. On the bottom the beam-pipe is visible. The HS numbering schema is reported.

The SPD is based on hybrid silicon pixels, consisting of a two-dimensional matrix (sensor ladder) of reverse-biased silicon detector diodes bump-bonded to readout chips. Each diode is connected through a conductive solder bump to a contact on the readout chip corresponding to the input of an electronics readout cell. The readout is binary: in each cell, a threshold is applied to the pre-amplified and shaped signal and the digital output level changes when the signal is above a set threshold. This technique had already been successfully applied in the WA97 and NA57 experiments at CERN.
The ladder consists of a silicon sensor matrix bump bonded to 5 front-end

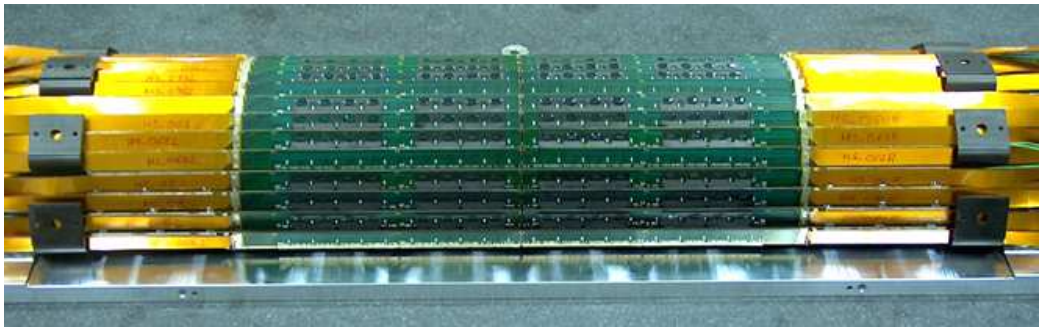

Figure 2.2: Half-barrel assembled on reference table.

chips [45]. The sensor matrix includes 256 $\times$ 160 cells measuring 50 μm ($r\varphi$) by 425 μm (z).
The basic detector module is the Half-Stave (HS). A HS is an assembly of two ladders glued and wire-bonded to a high density aluminum/polyimide multi-layer interconnect cable (Pixel Bus) that distributes power and connect the Pixel Chips to a readout Multi Chip Module (MCM) [21].
The MCM controls the front-end electronics and is connected to the off-detector electronics readout system via optical fiber links.
Two Half-Staves are attached head-to-head along the z direction to a Carbon Fiber Support Sector (CFSS), with the MCMs at the two ends, to form a stave.

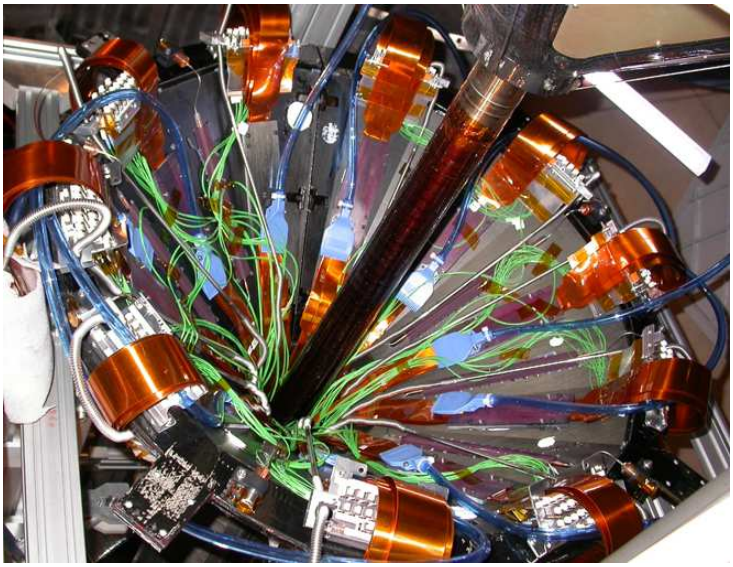

Figure 2.3: The SPD installed around the beryllium beam pipe.

Each sector supports six staves: two on the inner layer and four on the outer layer (Fig. 2.1). Ten sectors are then mounted together around the beam pipe to close the full barrel. In total, the SPD (60 staves) includes 240 ladders with 1200 chips for a total of 9.8×10^6 cells.
Fig. 2.2 shows a half-barrel assembled and ready to be integrated in the pixel mechanics. Fig. 2.3 shows the SPD installed around the beryllium beam pipe in the experiment.
In counting room zero suppression and data encoding are performed in the Link Receiver mezzanine cards (LinkRx card) in the VME based Router readout modules (Router cards)[23]. One Router card with three LinkRx cards serves a Half-Sector (6 HSs) and has optical links to the experiment

DAQ and trigger system.
Fig. 2.4 displays the block diagram of the full SPD electronics and connections. The next sections describe in details the various elements of this diagram.

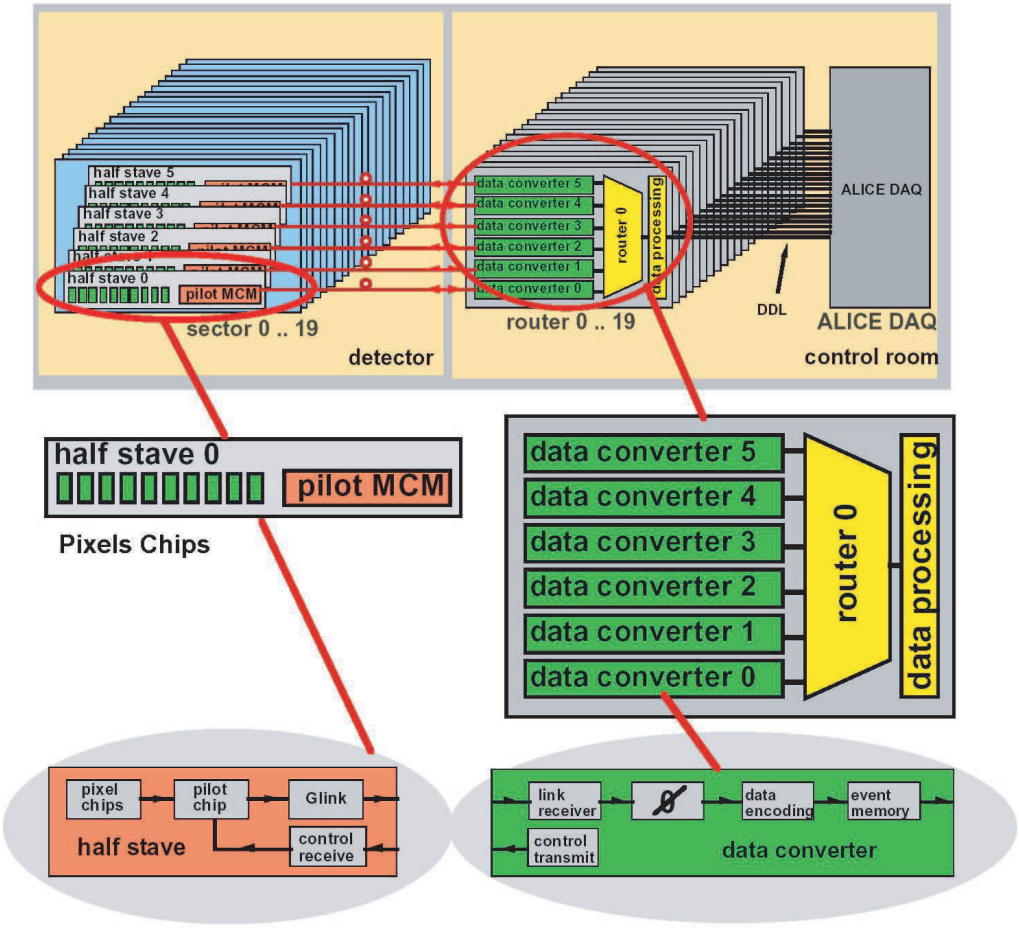

Figure 2.4: The SPD electronics block diagram.

2.1 The Detector Modules

The basic detector module is the Half-Stave (HS) which consists of one MCM and two sensor ladders glued on a Pixel Bus [24]. The connections between the Pixel Bus, readout chips and the MCM are carried out via ultra-sonic wire-bonding using 10 × 103 (32 data lines, 71 lines for control, test and power purposes) aluminum wire bonds of 25 μm diameter. The edge of the

pixel bus is connected to the MCM, which controls the entire communication from and to the off-detector electronics. A grounding foil, consisting of an aluminum/polyimide laminate (25 μm and 50 μm thick, respectively), which is glued between the carbon fiber and the readout chip, completes the layout of the HS. The grounding foil provides electrical isolation with respect to the carbon fiber support.
Two copper/polyimide laminates are connected to the Pixel Bus and the MCM to provide power to the readout electronics and the sensors. Each Half-Stave is supplied with 1.85 V/ 5.5 A for the Bus and 2.6 V/ 0.5 A for the MCM, respectively [25]. Fig. 2.5 shows the HS structure (a), components (b) and the HS cross section (c).

2.1.1 Ladders

One sensor ladder consists of 5 ALICE Pixel Chips which are flip-chip bonded to one p-in-n sensor. The flip-chip bonding is carried out at VTT[1] using Pb-Sn bump bonds of $\approx 25\,\mu$m diameter [26]. The next sessions give more details on the ladder components.

2.1.1.1 The Front-End Readout ASIC

The ALICE pixel readout chip is a mixed signal ASIC developed in an IBM 0.25 μm CMOS process (6 metal layers) with radiation-tolerant layout design [48]. Each chip contains 8192 readout cells of 50 μm $\times$ 425 μm arranged in 32 columns and 256 rows. Each readout cell is connected via bump bonds to a sensor cell.
The size of the chip is 13.5 mm $\times$ 15.8 mm including internal DACs, JTAG controller, chip controls and wire bonding pads. The chip clock frequency is 10 MHz. A detailed description of the chip architecture can be found in [51], [45] whereas Fig. 2.6 shows the readout pixel cell block diagram.

Each readout cell contains a preamplifier-shaper with leakage current compensation, followed by a discriminator. A signal above threshold generates a logical 1 which is propagated through a delay line during the L1 trigger latency ($\sim$6 μs). A four-hit-deep multi-event buffer in each cell allows derandomization of the event arrival times. Upon arrival of the L1 trigger, the logical level present at the end of the delay line is stored in the first available of the 4 multi event buffer locations.

[1] VTT Center for Microelectronics, Espoo, Finland, http://www.vtt.fi/index.jsp.

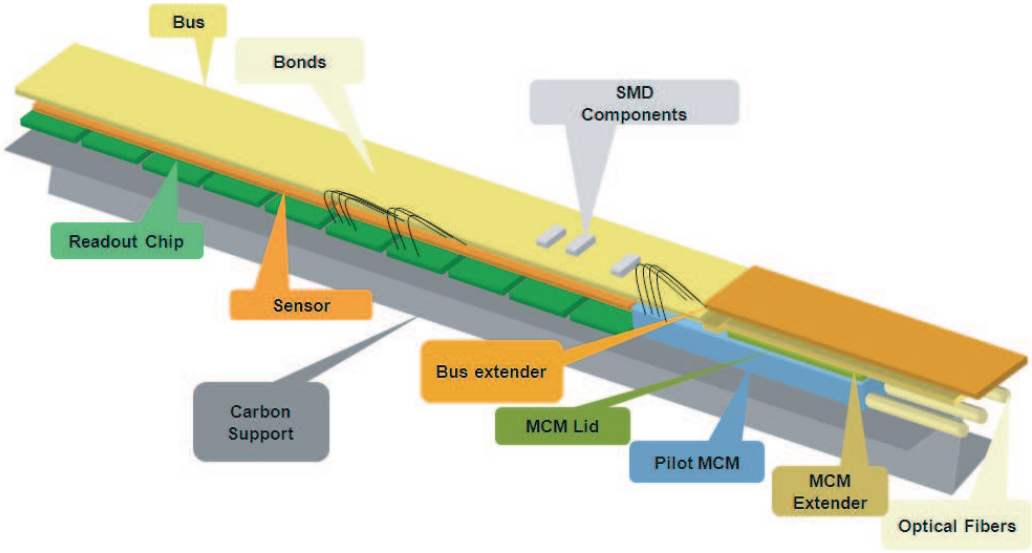

(a)

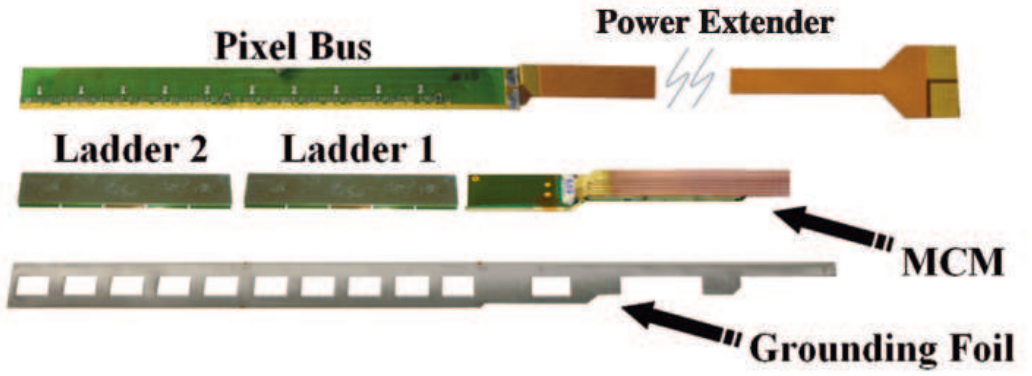

(b)

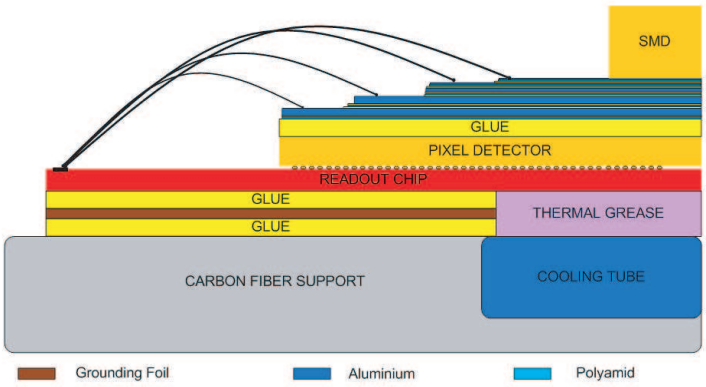

(c)

Figure 2.5: The HS structure (a), components (b) and cross section (c).

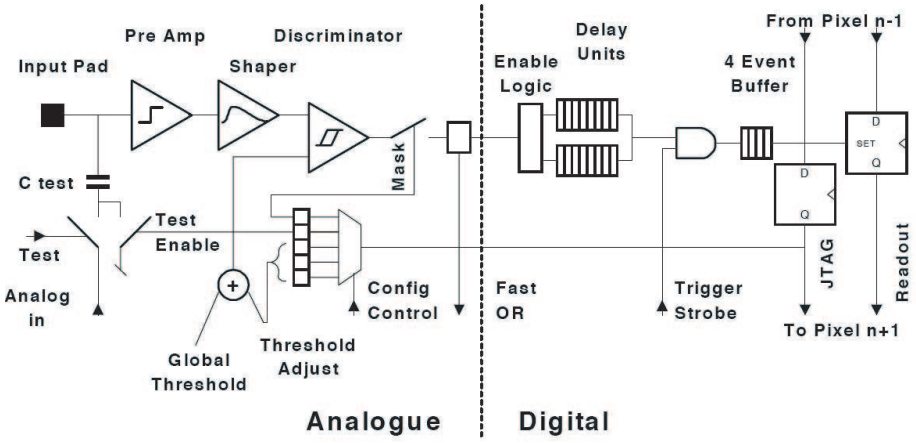

Figure 2.6: The readout pixel cell block diagram.

Upon arrival of the second level trigger (L2), the data contained in the multi event buffer locations corresponding to the first (oldest) L1 trigger are loaded onto the output shift registers. Then, for each chip, the data from the 256 rows of cells are shifted out during 256 cycles of a 10 MHz clock. At each cycle, a 32-bit word containing the hit pattern from one chip row is output on the 32-bit data bus where it is processed by the MCM and sent optically to the readout electronics located in the control room.
One pixel chip is readout in 25.6 μs. The 10 chips on each Half-Stave are readout sequentially.

The Pixel Chip includes many operation parameters remotely adjustable. The on-chip global registers include 42 8-bit DACs that adjust current and voltage bias references, L1 trigger delay, global threshold voltage, and leakage compensation. In each pixel cell a 3-bit register allows individual tuning of the threshold; there is also provision to enable the test pulse input and to mask the cell. All configuration parameters are controlled by the Digital Pilot via the serial interface following the IEEE JTAG standard[27].
The chips are in daisy chain respect to the JTAG lines. Each Pixel Chip has two JTAG circuitry input (TDI) lines for redundancy in the chain. In case of a faulty chip the configuration data can be bypassed to the subsequent chip. Fig. 2.7 displays JTAG connection between chips.

The Pixel Chip has proven to be insensitive to a total ionization dose (TID) of 10 Mrad. The main specifications of the ALICE SPD front-end chip are summarized in Tab. 2.1.

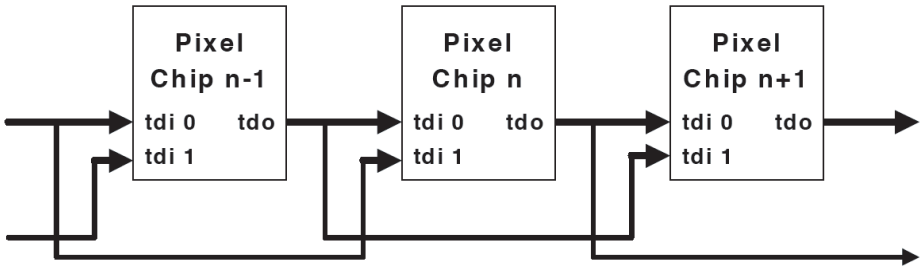

Figure 2.7: The Pixel Chips JTAG daisy chain.

Cell size	50 μm ($r\varphi$) $\times$ 425 μm (z)
Number of cells	256 ($r\varphi$) $\times$ 32 (z)
Minimum threshold	1000 e
Threshold uniformity	200 e
L1 latency	up to 51 μs
Operating clock frequency	10 MHz
Radiation tolerance	$>$ 10 Mrad
Power consumption	$\sim$ 990 mW

Table 2.1: Main specifications of the ALICE SPD front-end chip [46].

A special feature of the ALICE SPD is the Fast-OR (FO) signal. Whenever a pulse above the threshold is produced by a hit it will trigger a Fast-OR signal. This signal is produced after the threshold discrimination and sent to the off-detector electronics without further processing in the readout cells allowing a fast response. The individual cells are ORed together to generate one Fast-OR pulse for each chip. Thus, the SPD can provide 1200 independent Fast-OR signals to the L0 trigger decision (800 from the outer and 400 from the inner layer) [28].

2.1.1.2 The Silicon Sensor

The pixel sensors (Fig. 2.8) have an active size of 70.7 mm $\times$ 12.8 mm. They are produced on 5" high resistivity n-type silicon wafers of 200 μm thickness to comply with the material budget constraints. The sensors contain a pixel matrix of 5 $\times$(32 $\times$ 256) pixel cells of 50 μm $\times$ 425 μm elongated to 625 μm in the boundary region to assure coverage between readout chips.

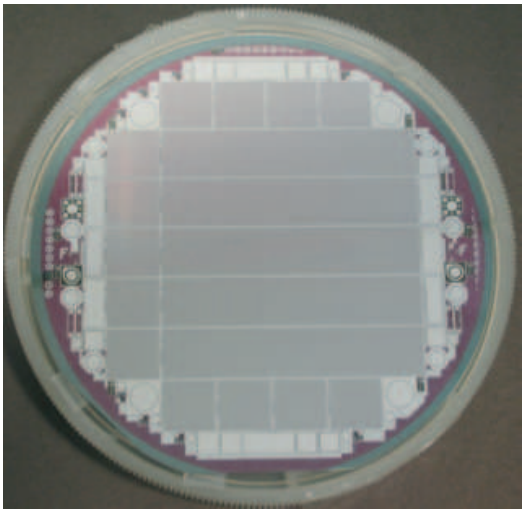

Figure 2.8: The 5" sensor wafer. The picture shows the front side of the sensor with large pixel sensors in the center of the wafer. Different test structures and single chip sensors are placed around the sensor edge.

2.1.2 Readout Multi Chip Module (MCM)

A Multi Chip Module (MCM) is located at the outer end of each Half-Stave. It houses the readout and control electronics and consists of four ASICs: the Analog Pilot, the Digital Pilot, the GOL and the RX40. These ASICs have been developed in the same IBM 0.25 μm CMOS process used for the Pixel Chip. Fig. 2.9 shows an MCM picture.
The MCM is based on a 5-metal-layer sequential build-up substrate (polyimide/copper). The floorprint is 110 mm x 12 mm. Due to space constraint the thickness is less than 1.5 mm. This has been achieved by mounting bare die ASICs and by the development of a custom optical package[2].
The MCM data/signal lines are wired bonded to the Pixel Bus. Power is supplied to the Pixel Bus and the MCM using two independent flexible copper/polyimide laminates (power extenders). The communication between the MCM and the counting room is via optical links on three single-mode fibers.

The Analog Pilot [29] chip provides reference voltages to the 10 pixel chips and contains an ADC for monitoring the currents and voltages. Two ADCs read also the Pt1000 temperature sensor chains on the Half-Stave.
The Digital Pilot [30] transmits the signals and configuration data to the

[2]STMicroelectronics, Milan, Italy.

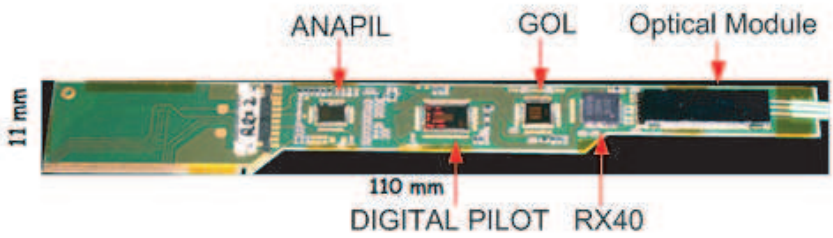

Figure 2.9: Multi Chip Module (MCM). Left to right: wire bonds connecting the MCM ASICs via the Pixel Bus to the readout chips, MCM ASICs, optical package with three optical fibers.

Router cards located in the control room and provides timing, control and readout for the Half-Stave. The Digital Pilot receives serial trigger, configuration data and clock via the two PIN diodes in the optical package and the receiver chip RX40. The Digital Pilot initiates the Pixel Chip readout, performs data multiplexing and sends the data to the G-link compatible 800 Mbits/s serializer GOL (Gigabit Optical Link) [31] which drives the laser in the Optical component.
The latter is a custom designed optical transceiver housed in a silicon package and contains two PIN diodes and one laser diode. The module is extremely compact with a floorprint of 116 mm $\times$ 6 mm and a thickness of 1.2 mm and has bond pads for electrical connections.

The MCM carries the reference analogue voltages with an accuracy of 10 mV and digital data streams at speeds of 800 Mbits/s without any observable cross-talk effects. The incoming 40 Mb/s clock is recovered with a maximum jitter of 42 ps allowing proper functionality of the 800 Mbits/s G-Link. The jitter on the 800 Mbit/s stream is as low as 11 ps. The optical noise margin for the incoming and outgoing data is higher than 14 and 9 dB, respectively, and is adequate to compensate for radiation effects and ageing.

2.1.3 Multi-Layer interconnect cable (Pixel Bus)

The Pixel Bus (Fig. 2.10) is a 250 μm thick 5-metal layer sequential build-up (SBU) substrate (aluminum/polyimide). It provides the connection between the 10 Pixel Chips and the MCM. Two Al layer are used for the power supply and three for the signal routing. The layers are separated by a polyimide

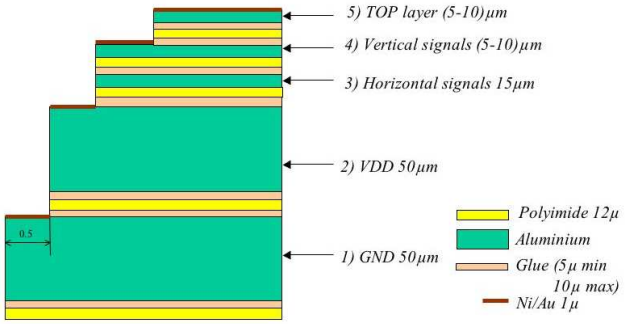

Figure 2.10: Pixel bus layers structure.

foil. Each subsequent layer is 500 μm shorter than the layer below in order to make it accessible for wire bonds. In total approximately 1000 wire bonds are used on each Half-Stave. The connection of the three aluminum signal layers is carried out with micronvias. The use of aluminum in place of copper is dictated by the low-mass requirements; it is not an industrial standard and has required a custom development[3]. The overall thickness of the Pixel Bus is $\sim$280 μm. A picture of the wire bonding of ladders to the bus is shown in Fig. 2.11.

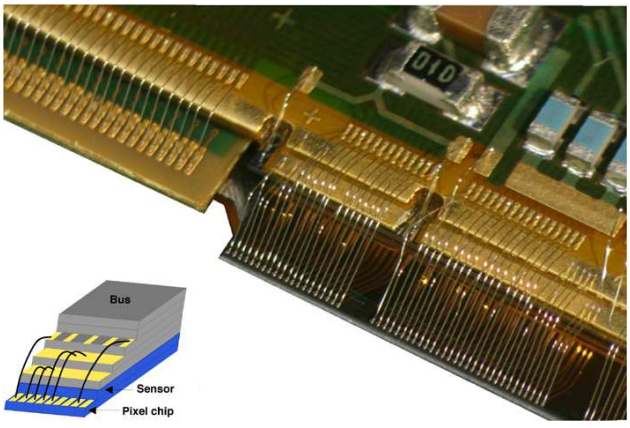

Figure 2.11: Wire bonding of ladders to Pixel Bus .

[3]CERN TS-DEM Workshop.

2.2 Off-detector electronics

The SPD off-detector readout electronics is located in the control room. Twenty Router cards (Fig. 2.12), each carrying three 2-channel LinkRx cards, provide the interface between the on-detector electronics and the ALICE DAQ, Detector Control System (DCS) and trigger systems. Each LinkRx card channel is connected to a HS. The channels consists of three optical fiber links, one for receiving the data and two for transmission of clock, control and configuration signals.

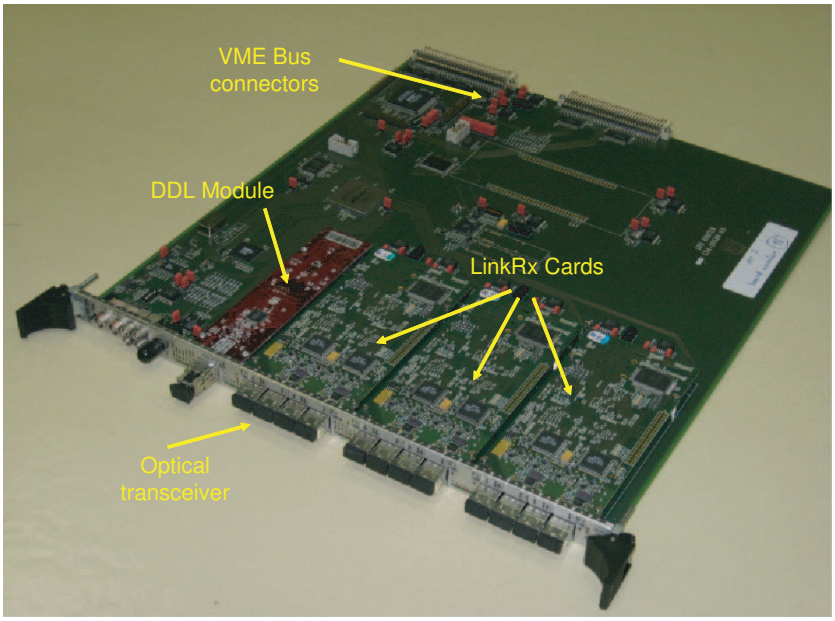

Figure 2.12: SPD Router card with three LinkRx cards and a DDL module.

In the LinkRx card the pixel data stream is de-serialized, the received data is checked for format errors and stored in a FIFO for subsequent hit encoding. Afterward the data is zero-suppressed, encoded, reformatted and written in the Dual Port Memory (DPM) of the LinkRx card. When all data belonging to one event is stored in the dual memory the LinkRx card provides an event ready flag for the Router processor. The LinkRx card confirms the error flags that are identified in the data stream coming from the detector. The Router card multiplexes the data incoming from the six Half-Staves into one ALICE Detector Data Link (DDL) and it attaches trigger and status information. The trigger information is delivered to the Router card by the Trigger, Timing and Control (TTC) system via optical fibers.

Moreover the Router cards contributes to the temperature interlock by controlling the second Pt1000 chain. Each Router card produces an interlock signal whenever one of the six HSs temperature passes a certain limit.
The Router cards are 9U VME and FPGA based modules having six channels in order to connect all the optical links for the operation of one Half-Sector.
A schematic diagram of the SPD electronics system is shown in Fig. 2.13.

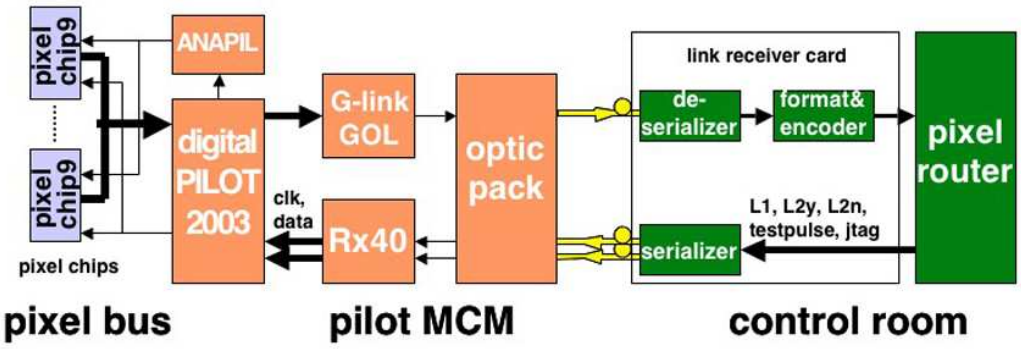

Figure 2.13: The readout electronics block diagram.

The 20 DDLs are connected to Local Data Concentrators (LDCs) housed in 4 PCs. The data access from the DCS to the Router cards is established via the router VME ports. The same port also allows monitoring and copying the data flow during data taking (data spy mode).
The 120 Half-Staves are readout in parallel. The system is able to readout data with an average rate of $\sim 3.3KHz$

2.3 Detector Services

In order to operate the SPD needs a series of support systems such as Power Supply (PS), Cooling (CS) and Interlock (IS) Systems. The next sessions give more details on these systems.

2.3.1 Power Supply System

The Low Voltage (LV) power supply requirements for the front-end electronics on each HS are 1.85V ($\sim 6A$) for the pixel bus and 2.6V ($\sim 0.5A$) for the MCM. The LV Power Supply (PS) System is based on 20 CAEN[4] A3009B

[4]CAEN, Viareggio, Italy.

LV dc-dc converter modules (12 independent LV channels each), housed in 4 CAEN Easy3000 crates located in the ALICE cavern. The distance between the LV PS and the detector is ∼40 m.

Each Half-Sector is powered by one LV module using the odd channels

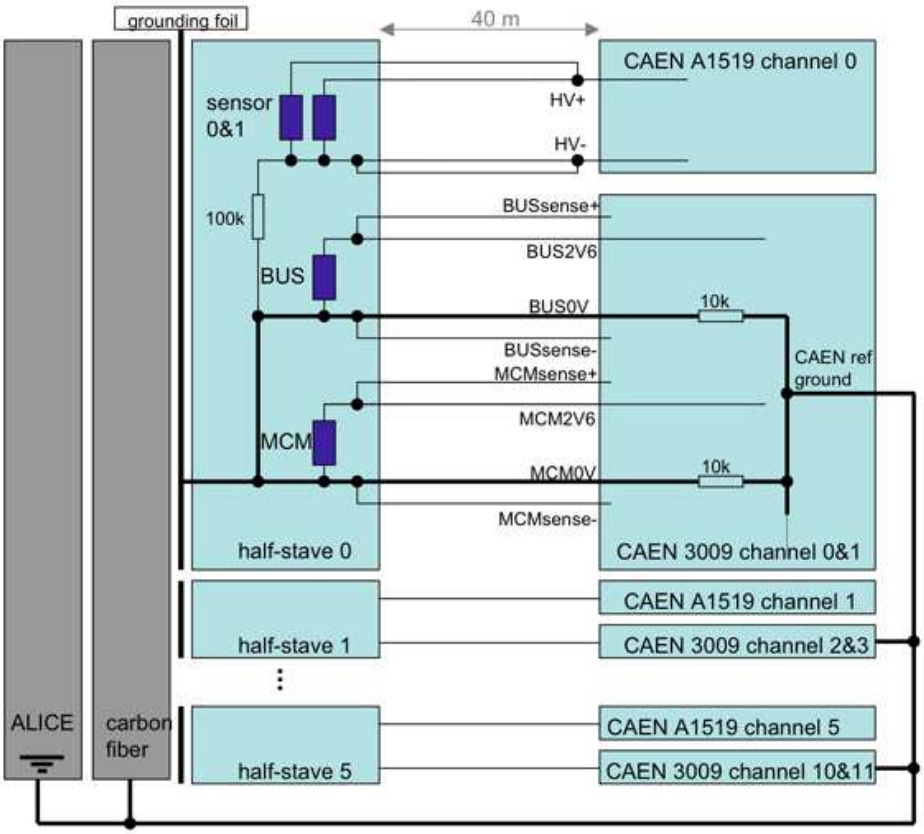

Figure 2.14: Power supply and grounding scheme.

for the MCM and the even channels for the Pixel Bus. Remote sensing is used throughout. In each module the Pixel Chip/MCM supply return lines are shorted and define the Half-Stave ground. In the CAEN A3009A, all return lines are connected via 10 kOhm resistors to a power supply reference ground that is connected to the ALICE ground (on the absorber and the space frame).

The detector bias voltage (High Voltage (HV) and 50V typical at start of detector operation) is provided by CAEN A1519 modules (12 independent HV channels each) housed in a CAEN SY1527 mainframe and located in the control room at a distance of ∼120 m. One HV module is used for each sector. The two sensor ladders in one Half-Stave share one HV module output

but are connected by one coaxial cable each to the HV module in the control room. This allows the individual connection of a sensor ladder to the bias voltage. The return line of the high voltage is connected to the Half-Stave ground via a 100 kOhm resistor. The Half-Stave ground is isolated from the carbon fiber support using a 25 μm thick aluminum/polyimide laminate (grounding foil). The carbon fiber support itself is connected to the ALICE ground.
The SY1527 mainframe is the system brain and it communicates with the software layer via ethernet (TCP/IP, OPC protocol). The DCS downloads in the mainframe the devices configurations and the mainframe monitors and configures the system. In case of errors such as over-current, over-voltage, trip, etc. the mainframe switches off the corresponding channels/boards. The SY1527 communication with the LV modules is via a CAEN A1676 branch controller.
The Easy3000 crates are supplied by remote controllable CAEN power converter (48 V).
Fig. 2.14 illustrates the power supply and grounding scheme.

2.3.2 Cooling System

The power dissipated in the front-end electronics is $\sim$ 1.35 kW hence efficient cooling is vital for this very low mass detector.
The cooling system is of the evaporative type and is based on C_4F_{10}. The sectors are equipped with cooling capillaries embedded in the sector support and running underneath the staves (one per stave). The heat transfer from the front-end chips is assured with high thermal conductivity grease. The SPD barrel is surrounded by an Al-coated carbon-fiber external shield to prevent radiation of heat towards the SDD layers.
The major contribution to the on-detector power dissipation is due to front-end chips; they generate a heat load of $\sim$23 W (nominal) in each stave. The design of the cooling system has been driven by various constraints such as low material budget, long-term stability against corrosion, chemical compatibility, minimal temperature gradients, cooling duct temperature above the dew point.

Several possible solutions based on different coolants have been considered [62]. An evaporative system with C_4F_{10} as coolant has been chosen to fulfill the requirements. The C_4F_{10} follows a Joule-Thomson cycle (rapid expansion at constant enthalpy and subsequent evaporation).

The liquid, overcooled and compressed by a pump, is brought to the coex-

istence phase inside the cooling duct by a pressure drop inside the capillaries (0.5 mm internal diameter, 550 mm long). Heat abduction through phase transition takes place inside the cooling tube at 15-18 °C (1.9-2.0 bar); a compressor raises then the pressure pushing the gas towards a condenser, where the liquid phase is re-established by heat transfer to cold water (∼6 °C).
The evaporation temperature can be controlled by regulating the pressure in the return line, setting then the coexistence conditions of the mixed phase. Each stave is put in thermal contact with the cooling duct mounted in a groove on the CFSS by a thermal grease layer. The cooling duct is obtained using Phynox tubes with a wall thickness of 40 μm and an initial diameter of 2.6 mm, squeezed down to flat profile with an overall thickness of 600 μm in the thin dimension. Each sector is equipped with cooling collectors at the two ends, one functioning as an inlet and the other as an outlet for the whole sector. Extensive corrosion tests have been performed on tubes, together with the choice of surface treatment and of fitting materials. The cooling plant provides one main cooling line for each sector.
The cooling plant is controlled by a Programmable Logic Controller (PLC). The communication with the DCS is via ethernet (TCP/IP) using the OPC Server-client protocol.

2.3.3 Interlock System

The detector has very low mass and high heat dissipation. In normal operation, if a sudden failure of the cooling were to occur, the Half-Staves temperature would increase at a rate of 1 °C/s. Continuous monitoring and a fast, reliable safety interlock on each Half-Stave are therefore mandatory. They are based on Pt1000 temperature transducers mounted on the Pixel Bus, next to the Pixel Chips. Two daisy chains of 5 transducers each (interleaved positions) provide redundant measurements of the average temperature. One chain is readout in the MCM that sends the resistances values to the off-detector electronics in the counting room. The other chain is hard-wired to the remote interlock system, based on a Programmable Logic Controller (PLC) that is part of the detector control and safety system. Temperature values and trends are logged. If the temperature reaches a preset threshold (40 ^oC), the low-voltage power supply is promptly switched off by the safety interlock and an alarm is generated.
The PLC scans the 120 chains in less than 1s and communicates with the software layer via ethernet and using OPC Server-Client Protocol. All the temperature readouts are also sent online to the counting room.
The cooling plant provides 11 interlock lines informing on the general status

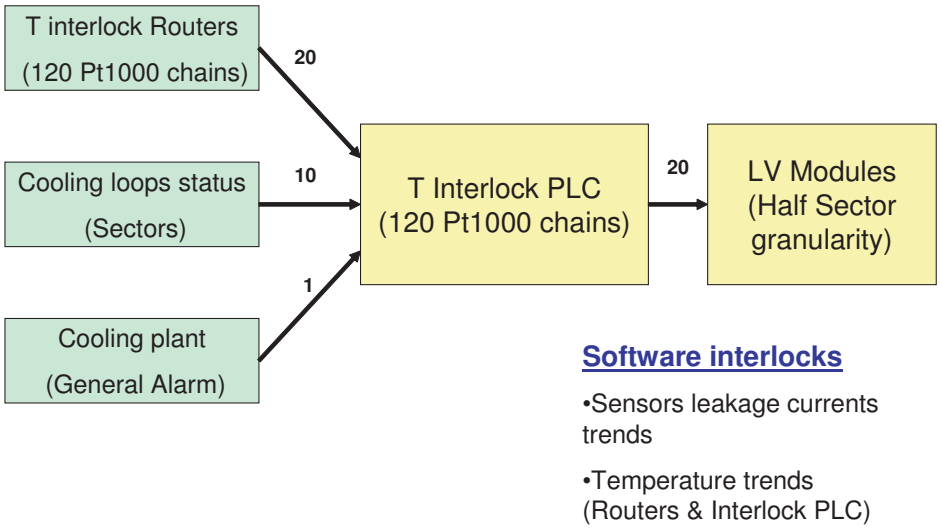

Figure 2.15: A block diagram of the SPD interlock schema.

of the plant and on the activation status of the cooling lines. Whenever either the plant is not running or the lines are not opened an interlock is issued. Moreover the system foresees also two level of software interlock based on currents and temperatures trending such as described in section 3.2.2.
The block diagram of Fig. 2.15 displays the SPD interlock schema.

Chapter 3

The SPD Detector Control System

The SPD Detector Control Systems (DCS) is complex software application designed to operate and monitor the SPD. The primary function of the DCS is the overall control of the detector status. It takes appropriate corrective actions to maintain the detector stability and ensure high quality data. It provides an adequate user interfaces for experts or simple shifters. In addition, it communicates with external systems such as the databases and the control systems of the accelerator.
Another main task of the DCS is the control and monitoring of the systems environment at and in proximity of the experiment. These tasks are historically referred to as "slow controls" and include: handling the electricity supply to the detector, control of the cooling facilities, environmental parameters, crates and racks. Also safety related functions such as detector interlock are foreseen by the DCS in collaboration with the Detector Safety System (DSS). Many functions of the DCS are needed at all time. Thus the technologies and solutions adopted must ensure a 24-hour functioning for the entire life of the experiment.
Moreover the SPD DCS should be integrated in the general ALICE DCS and Experiment Control System (ECS) in order to operate the SPD as an ALICE subsystem.
The SPD DCS has also the unique feature of not only controlling but also operate the SPD front-end electronics. These requirements impose a high level of synchronization between the system components and a fast system response. The DCS in this case is also a fundamental component for the detector calibration. These needs strongly influence the system design as described in the next sections.
The SPD DCS needs to configure roughly 20 M parameters, calibrate the

$\sim$ 50 k front-end electronics DACs and monitor $\sim$ 5000 variables. Moreover the detector performance are evaluated by means of $\sim$ 10000 calibration parameters. The huge amount of elements to be controlled imposes high system automation and an intuitive user interface. System performances are critical issues in the system design.

The ALICE DCS needs to fulfill a series of requirements in order to operate the full experiment built up of 18 sub-detectors and the experiment services. The requirements can be summarizes as:

Partitionability: The ability to partition the DCS system is essential for a detector like ALICE, which has a large number of sub-detector elements. Partitioning implies that a specific sub-element can be cut off from the rest of the system and operated independently. This operation mode is useful for maintenance and calibration.

Modularity: Modularity is achieved through a hierarchical structure of the DCS.

Homogeneity: This characteristic will facilitate integration, maintenance, and upgrading. The usage of commercial hardware and software follows this guideline.

Scalability: An important uncertainty for the DCS is the exact size of the system to be installed for the first physics run, as well as the evolution of the accelerator and experiment performance. Scalability makes the system flexible enough to facilitate the introduction of select new technologies in its various parts.

Automation: Automation features speed up the execution of commonly performed actions and avoid human mistakes typical in repetitive routines.

Radiation tolerance The DCS hardware components placed in proximity of the detector will suffer high radiation levels. Therefore, radiation tolerant components are mandatory and sensitive equipment should be placed as far as possible from the interaction point.

Each ALICE sub-detector should follow these guidelines for the specific DCS implementation. Moreover, besides these general requirements, each sub-detector has some specific ones resulting from its unique design and implementation.

In order to fulfill the mentioned system requirements, the ALICE DCS has a hierarchical two software layers structure as displayed in Fig. 3.1. The bottom

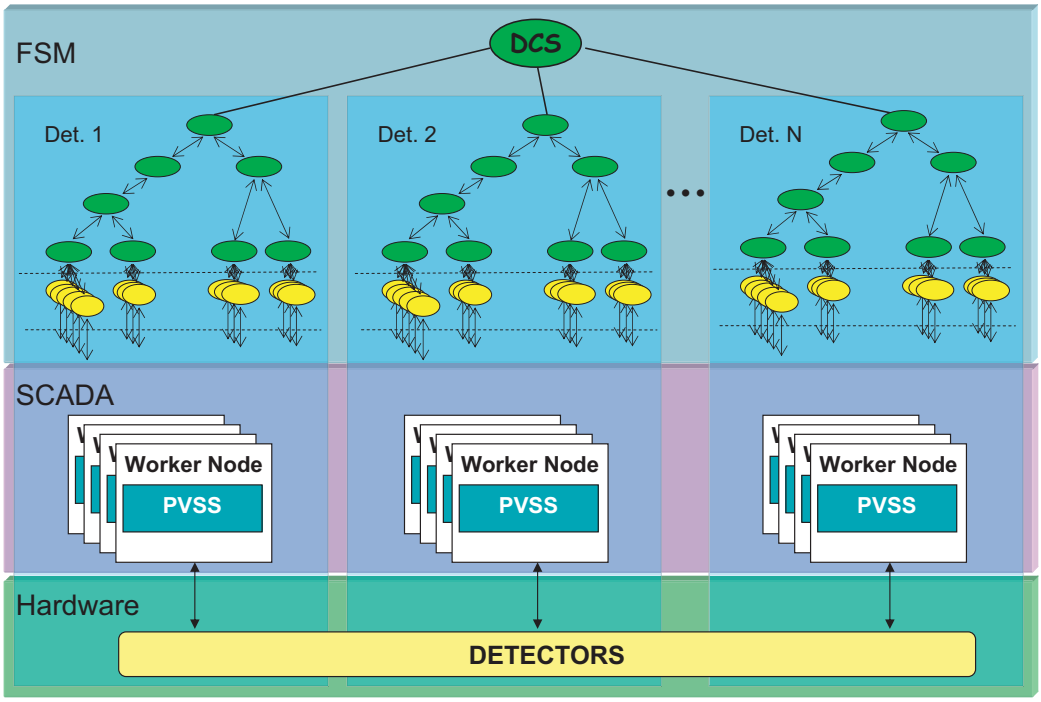

Figure 3.1: The DCS software layers. On top the FSM controlling logically the devices monitored and controlled by the SCADA applications.

software layer is a supervisory layer (SCADA layer) devoted to control and to operate the detector subsystems individually. It is responsible for stable and safe operation of the equipments and it also provides low level user interfaces. The operators can access directly the equipments using these interfaces. The supervisory layer is based on a Supervisory Control And Data Acquisition (SCADA) application and CERN standardized PVSS (see section 3.1.1 for more details) as SCADA for all the LHC experiments. PVSS is an industrial SCADA product from the Austrian company ETM and the acronym PVSS is the German abbreviation for "Process visualization and control system". It is a SCADA system designed specifically for the operation and supervision of technical installations and industrial processes. Nevertheless some of its features, described in the next sections, make it interesting for high energy physics applications.
The upper DCS software layer hosts a Finite State Machine (FSM) performing the logical control of the full system. The FSM merges the subsystems control to form a unique entity. It is also responsible of the systems syn-

chronization and high level DCS automation. All the ALICE detectors have their own FSM however the FSM top level, named top-node, is common to all the detectors. This is a common interface used to integrate the detectors control with the global ALICE DCS/ECS. The FSM is implemented using the State Management Interface (SMI++)[75] (more details in section 3.1.2).

The PVSS layer (also called SCADA layer in this thesis) receives commands from the FSM and communicates with the detector hardware. Moreover PVSS hosts a FSM GUI.
All the ALICE detectors should provide the ALICE DCS with an FSM and a SCADA (PVSS) layer. Furthermore the SPD DCS hosts a third software layer, named Front-End Device Servers layer, connecting the SCADA layer with the SPD front-end electronics. This layer will be widely described in section 3.2.1 and chapter 4.
The configurations parameters needed by the DCS and by the detector hardware components are stored into a specific Configuration Database (CDB). It is introduced in section 3.4.

In order to support the intensive computing load required by the control system, the DCS software is scattered on a series of PCs. Each of them runs PVSS projects, FSM elements and control support applications (e.g. 10 PCs are used by the SPD DCS). The communication between the software elements and the PCs is via ethernet. The DCS PCs are divided in two families: Worker Nodes (WNs) and Operator Nodes (ONs). The WNs monitor and control the hardware/software components supporting the DCS computing load. The ONs host the system user interface and they are used by the operator to access and operate the system. The system can be operated at various levels such as full DCS level or detector level. Each detector has its own Operator Node and Fig. 3.2 (a) displays a typical detector DCS structure. Fig. 3.2 (b) show the operator access at the ALICE DCS level.

The control system is designed to operate automatically in stand-alone and to inform the operator only when an error condition is verified. However, the operator can monitor and manually operate the system logging to specific ONs. Fig. 3.3 shows the flux of information generated by the operator accessing a hardware component using an ON and the FSM. The ONs have a PVSS interface displaying the FSM communicating with the various subsystems. The FSM forwards the operator commands to the appropriate PVSS system that applies the required actions on the hardware components.

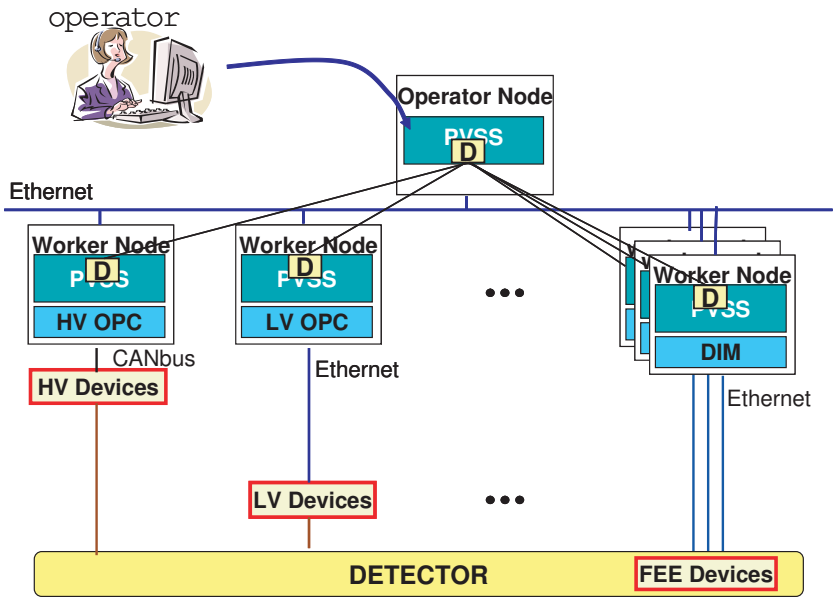

(a)

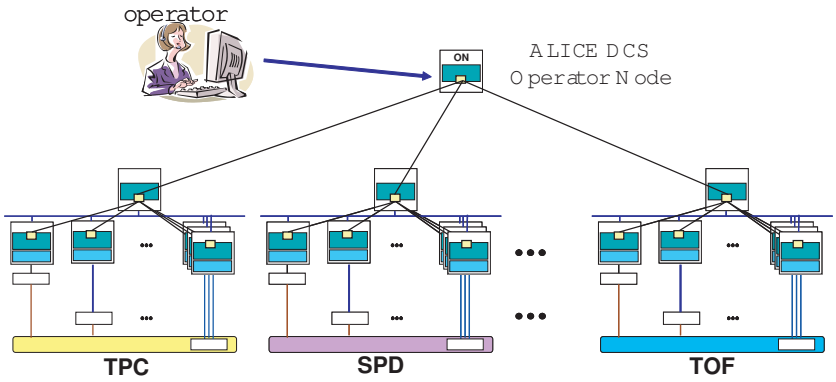

(b)

Figure 3.2: A typical detector DCS structure (a). The control schema used by the global ALICE DCS to access the detectors control systems (b).

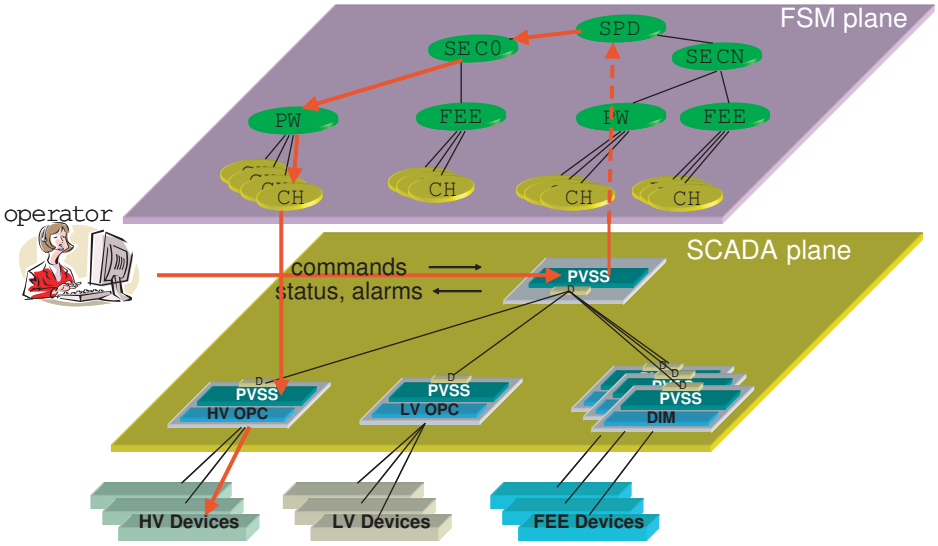

Figure 3.3: The information flux generate by an operator accessing a hardware component via ON. In this example the operator sends commands to a HV channel using the FSM visible in the operator node. The FSM address the corresponding driver in the various PVSS systems.

3.1 The DCS software tools

The Detector Control System has been developed using PVSS for the SCADA layer and the State Management Interface (SMI++) for the FSM layer. This section[1] reports the main features of these two developing tools in order to understand the structures and conventions used in this thesis. Moreover in section 3.1.2 FSM implementation strategies are discussed.

3.1.1 PVSS and the JCOP Framework

PVSS is a Supervisory Control And Data Acquisition application designed by ETM of the Siemens group[66]. SCADAs are commercial software systems used extensively in industry for the supervision and control of industrial processes. SCADA systems are used in a wide variety of industrial domains and therefore typically provide a flexible, distributed and open architecture to allow customization to a particular application area. In addition to a set of basic SCADA functionalities, these systems also provide a set of standard interfaces to both hardware and software as well as an Application Program-

[1]The DCS experts already aware of the PVSS, FSM and SMI++ functionality and implementations, can skip this section without loosing the thesis flow.

ming Interface (API) to enable integration with other applications or software systems.
PVSS is used to connect to hardware (or software) devices, acquire the data they produce and use it for their supervision, i.e. to monitor their behavior and to initialize, configure and operate them. A wide documentation on SCADA applications and PVSS can be found at [106] and [36] whereas in this section only the information needed for the understanding of this thesis are reported.

PVSS has a highly distributed architecture and a PVSS application is composed of several software processes called Managers. A PVSS system (named also PVSS project) is an application containing one Event Manager, one Data Manager and any number of other Managers. An example of a PVSS system is shown in Fig. 3.4.

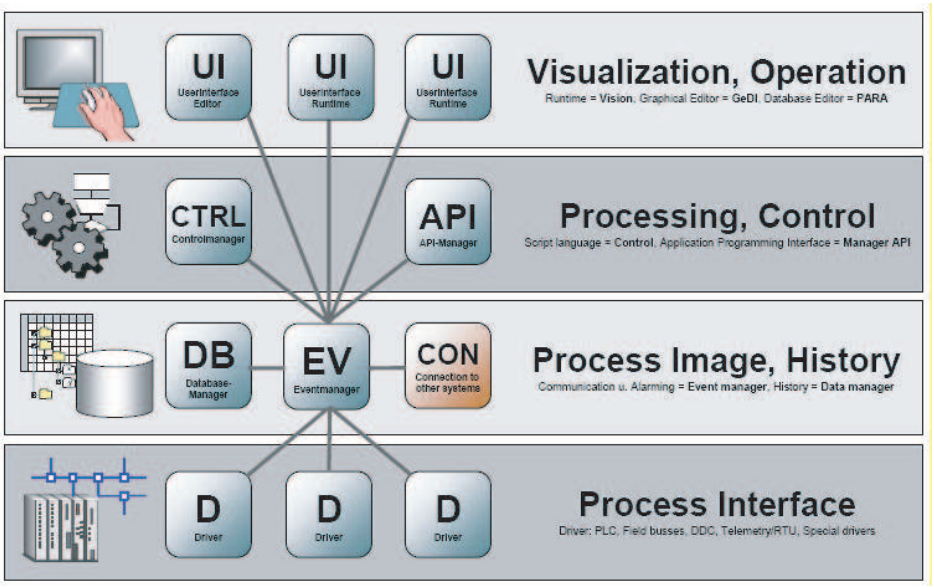

Figure 3.4: An example of PVSS system in which the main manager types are reported.

The Event Manager (EV) is the PVSS central processing unit. This unit holds the current image of all process variables in the memory. Every other Manager, which want to access the data, receives these data from the process image of the Event Manager and do not have to communicate directly with a controller. Viceversa a command from a control station is set as a value change in the process image of the Event Manager in the first instance. Afterwards the responsible driver forwards the value to the specific target

device automatically. The EV is a central data distributor, the communication center for PVSS. Additionally this manager executes also the alert handling and it is in a position to make different calculation functions automatically. Managers subscribe to data and they are only sent by the Event Manager, on change. Indeed data processing and communication between the individual Managers is normally performed purely on an event-oriented basis. Conversely, in steady-state operation with no changes in values, there is neither communications nor processing load.

The Data Manager (DB) constitutes the link to the PVSS internal database. It handles the parametrization data of an application to be saved in such a database and the archiving of value changes and alerts.

The Drivers (D) are special programs providing the connection between PVSS and hardware or software devices to be supervised. They convert a specific protocol into the form of communications used internally by PVSS. The driver can be e.g. Profibus, OPC, CanBus, Modbus, DIM, etc.

The User Interface (UI) Managers form the interface with the user. These include a graphical editor (GEDI), a database editor (Graphical Parametrization, PARA) and the general user interface of the application (Native Vision, UI). The PARA allows the users to define the structure of the database, define which data should be archived and define which data coming from a device should generate alarms.
In the User Interface, values are displayed, commands issues or alerts tracked in the list of alerts. In PVSS, the user interaction software runs completely separately from the processing executing in the background. It merely provides a window on the live data from the process image or the archived data in the history.

The Control Managers (CTRLs) run background scripts for any data processing. The scripting language has largely the same syntax as ANSI-C with extensions. It is an advanced procedural higher-level language that uses multithreading. The code is processed interpretively so does not need compiling. Any user functions that are repeatedly needed can be stored in PVSS libraries for use by panels and scripts.

The API Managers (API) allow the users to write their own programs in C++ using a PVSS Application Programming Interface (API) to access the data in the PVSS database.

Several instances of a manager for all manager types (UI, CTRL, D, API, etc.) can be added to a PVSS system. Thus a number of user interfaces or drivers can be run from one Event Manager for example. These Managers communicate via a PVSS-specific protocol over TCP/IP and this means that a PVSS system can be distributed across a number of computers.
PVSS allows interconnecting a number of autonomous systems into an overall system. As shown in Fig. 3.5 a Distributed System is built by adding a Distribution Manager (Dist) to each system and connecting them together.

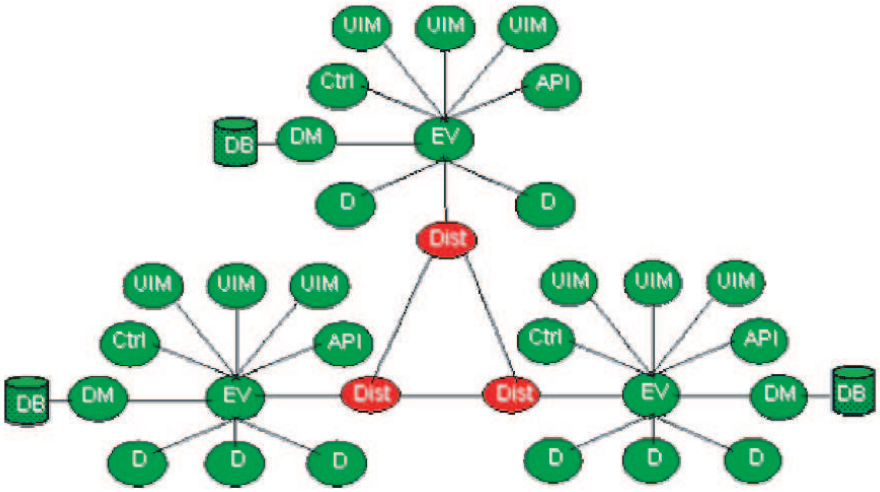

Figure 3.5: An example of Distributed System.

PVSS allows users to design their own user interfaces (panels), in a "drag and drop" fashion. By using the Graphic Editor, the user can first design the static part of a panel, by placing widgets like buttons, tables, plots, etc. Actions can then be attached to each widget. Depending on the widget type, actions can be triggered on initialization, user click or double click, text input, etc. Moreover PVSS provides the possibility to create a single symbol or panel and to use it many times. This is called a Reference Panel. Changes to this Reference Panel are inherited by all instances of the panel.

The device data in the PVSS database is structured as Data Points (DPs) of a pre-defined Data Point Type (DPT). PVSS allows devices to be modelled using these DPTs. A DPT (DPTs are similar to structures in OO terminology) describes the data structure of the device and a DP contains the information related to a particular instance of such a device (DPs are

similar to objects instantiated from structure in OO terminology). The DPT structure is user definable and can be as complex as one requires and may also be hierarchical. The elements forming a DPT are called Data Point Elements (DPEs) and are user-definable. After defining the data point type, the user can then create data points of that type which will hold the data of each particular device. The creation and modification of DPTs and DPs can be done either using the Graphical Parametrization tool (PARA), or programmatically using ctrl scripts.

The use of PVSS has been standardized at CERN and given the evident similarity in technical requirements for controls amongst the experiments, the Joint Controls Project (JCOP) [107] was created. This project provides the PVSS users with guidelines and PVSS components, which can be devices or tools commonly used for the experiment controls. The series of components produced by this project are called JCOP Framework components. The SPD DCS uses some of the Framework components. In this thesis will be noticed the uses of these elements in the various sessions.

3.1.2 The State Management Interface (SMI++) language

The SPD control has a complex structure and this characteristic impose a high rate of automation to control processes, to reduce human errors and to optimize recovery procedures. Automation comes with the need to describe the behavior and evolution of the system in the most accurate way. A solution is to view all system sub-elements (either abstract or physical) as controllable objects whose behavior is defined through finite state automaton. A finite state automaton, or more simply a Finite State Machine (FSM), is a model of behavior for any complex or simple object with a finite number of states, transitions and actions. A state stores information about the past, i.e. it reflects the input changes from the system start to the present moment. A transition indicates a state change and is described by a condition must be met to enable the transition. An action, instead, is a description of an activity that is to be performed at a given moment. The action may be executed when entering the state, exiting it or during the transition.
State Management Interface (SMI++)[75] is a custom CERN language CERN oriented to control systems FSM. CERN standardized the use of SMI++ for all the LHC experiments.
The language is object oriented and it allows 3 basic object types: Device Units (DUs), Logical Units (LUs) and Control Units (CUs) described in the

next sections. These FSM objects can be connected together to form hierarchies. The data flow is only being vertical: commands (actions) flowing downwards, states and alarms going upwards. A command may trigger state changes at lower hierarchy level that in return may cause state changes at higher hierarchy ones. Fig. 3.6 displays an example of FSM hierarchy.
In the FSM hierarchy various levels are foreseen and the connections between the objects define the roles. The objects at the same level are named *children* of the object at the higher level named *parent*. The higher hierarchy level is named top-node.

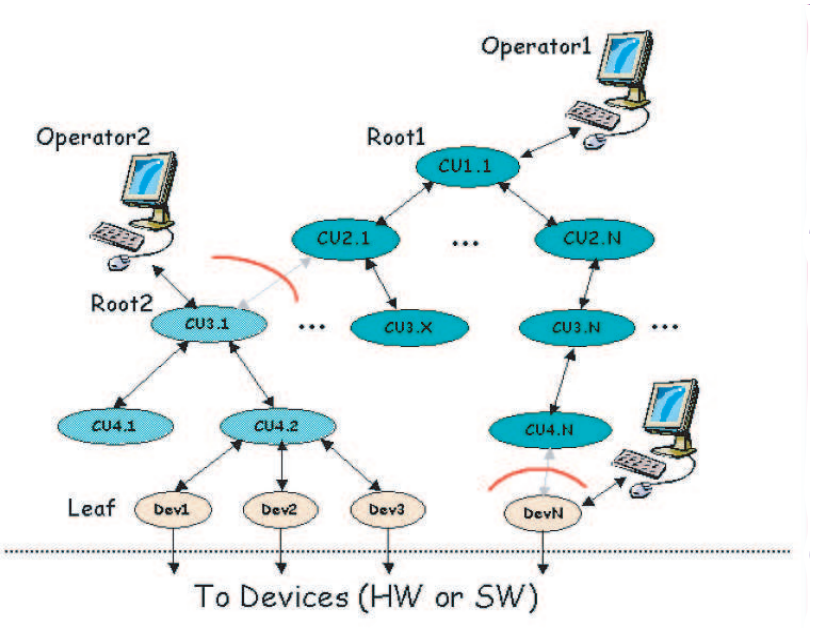

Figure 3.6: An example of FSM hierarchy.

An important advantage of having a hierarchical structure is the possibility to partition the command hierarchy, essential for a detector like the SPD. Partitioning implies that a branch of the main tree is cut off. In this way components can be operated independently from the rest of the tree: the corresponding partition operate independently from the rest of the system. This mode of operation will be used mainly for maintenance, calibration, system testing and trouble shooting. The partitioning modes available are the following: Included, Excluded, Manual, and Ignored. The meaning of each is clearly illustrated in Fig. 3.7.

PVSS hosts a FSM toolkit provided by the JCOP Framework and based

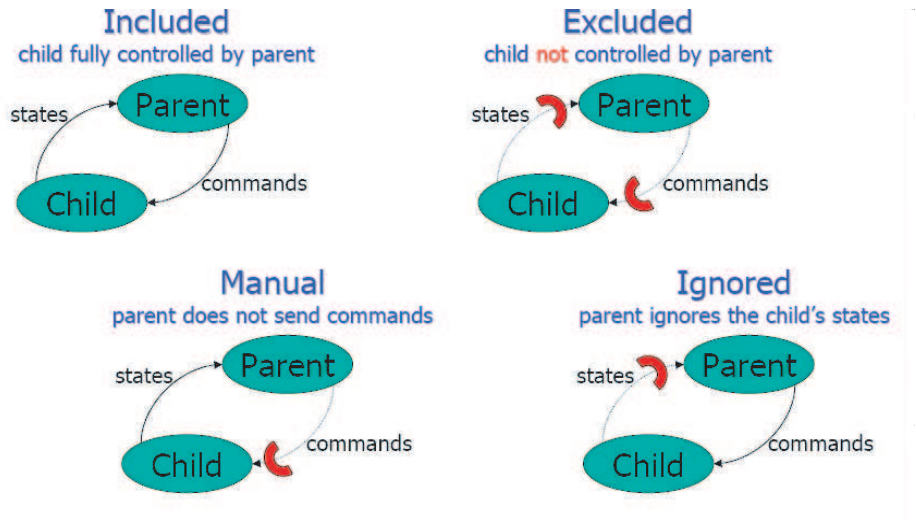

Figure 3.7: An example of FSM hierarchy.

on SMI++. A friendly user interface allows defining the FSM structure for every node. It is possible to specify the states, the accepted commands, the allowed transitions between states and the eventual actions to undertake. Moreover the Device Units can host PVSS scripts.

3.1.2.1 Device Units

The specific tasks of a Device Unit (DU) are to interface to the actual hardware device, implement the actions to be taken on the device and retrieve the devices state. In addition it must be able to generate alarms.
The DUs are the bottom layer objects in the FSM hierarchy indeed they cannot have children. They are communicating with the hardware devices via PVSS datapoints (DPs) and producing a state as function of the DPs values retrieved. The state is re-calculated each time the DPs are updated and the DUs are not allowed to modify autonomously their states. This characteristic is fundamental for a device control system.
Inside the DUs is possible to use PVSS functions and run PVSS scripts. This functionality gives strength to these objects allowing also complex sate calculation operations from a series of DPs. The DUs are the only FSM object capable of manage operation timeout.
The DUs accept user defined commands in strings format. These commands can be translated inside the DU to a series of operation to apply on PVSS DPs. The list of commands is unique for all the states and the user can decide their visibility in the different states. The DUs cannot run in stand-alone,

they need to be inserted in a hierarchy in which a CU is present in the higher levels.

3.1.2.2 Control and Logical Units

The Control Units and Logical Units are pure logical FSM objects able to configure, monitor and control its children, recover errors, handle alarms. The difference between these object resides in the partitioning capability. The CUs form domains containing all the elements below in the hierarchy. They can run autonomously on a PC allowing the hierarchy scattering on various PCs. However CUs are high memory consuming ($\sim 7Mb$ each) objects. This limitation strongly influences the hierarchy design and performances, indeed, a CU should be used only when the system partitioning is strongly needed. LUs can be used instead when this requirement is not stringent.
The LUs and CUs actions are state dependent and they can set parameters, send commands to the children and change their own state.
LUs and CUs contain a list of user defined condition dependent on the children state. Whenever a child change its state, this list is checked and these objects can either call a state action or change their state.

3.2 The SPD supervisory software layer

The SPD SCADA layer should provide monitoring of the detector conditions, of front-end electronics, and all SPD subsystems (high voltage, low voltage, cooling system and interlock system). All monitored data should be recorded and archived in a common ALICE database. Furthermore the DCS should provide early warnings in case of abnormal conditions, issue alarms and execute automatic control actions to protect the detector.
The main challenges for this layer are the large number of channels (10 M) and parameters (more than 5000 among temperatures, voltages, currents electronics configurations, cooling pressures, etc.) to monitor, the large data volume, and the necessity to run the DCS during the whole ALICE detector lifetime.
My contribution to the SPD SCADA layer was the conceptual system design and the architectural layer structure. Moreover I coordinated the system design activity.
The main concept in designing the DCS SCADA layer is the modularity and the autonomous and self-consistency operation of the various subsys-

tems. Each component should operate safely independently. The exchange of information between subsystems must be performed only trough a specific interface. Hence every module should be able to accept requests by the others and publish its results without allowing the changes of its parameters by other subsystems. Moreover the SCADA systems design is Object Oriented (OO) in which every subsystem and component is seen as a self-consistent element.
Innovative design patterns have been applied to optimize system performances, scalability and maintenance. For example each subsystems (cooling, power supply, FE electronics, etc.) control part is divided in three main blocks such as hardware interface, user interface and automatic control to archive these goals. This separation allows the decoupling of the three blocks that can have an autonomous, robust, light and easy to upgrade structure. The global system performance are strongly enhanced in term of stability, speed and equipments operation safety. The actual details of the implementations are reported in the corresponding subsystems sections.

In order to understand the structure given to the control system is important to bear in mind that commands and status should be completely independent. In control systems indeed a command to the hardware can bring the system in a state completely different from the expected. This effect can be produced as consequence of the command issued or function of unexpected factors. Hence the control system should have two separate architectures: the command to the hardware and the status information. The two should communicate only when automatic actions should be taken.

The SPD SCADA layer can be logically separated in four main subsystems as displayed in Fig. 3.8. This block diagram shows the connection between the hardware and the software components. For schematize the full DCS, the four subsystems CSs are represented as separated elements but actually they are strongly interacting. The Service Control (SCS) is not displayed in the block diagram but it is responsible of establishing the link between the various subsystems. Moreover it manages the services needed to operate the various CSs.
The Power Supplies Control (PSCS) communicate with the CAEN mainframe managing the 360 detector power channels.
The Front-End and Read Out electronics (FERO) Control (FECS), using two FED Server (see chapter 4 for more details), controls the off-detector electronics and on-detector electronics. Moreover the FECS is not only a control system but it also embeds the detector calibrations functionalities (see chapter 5 for more details).

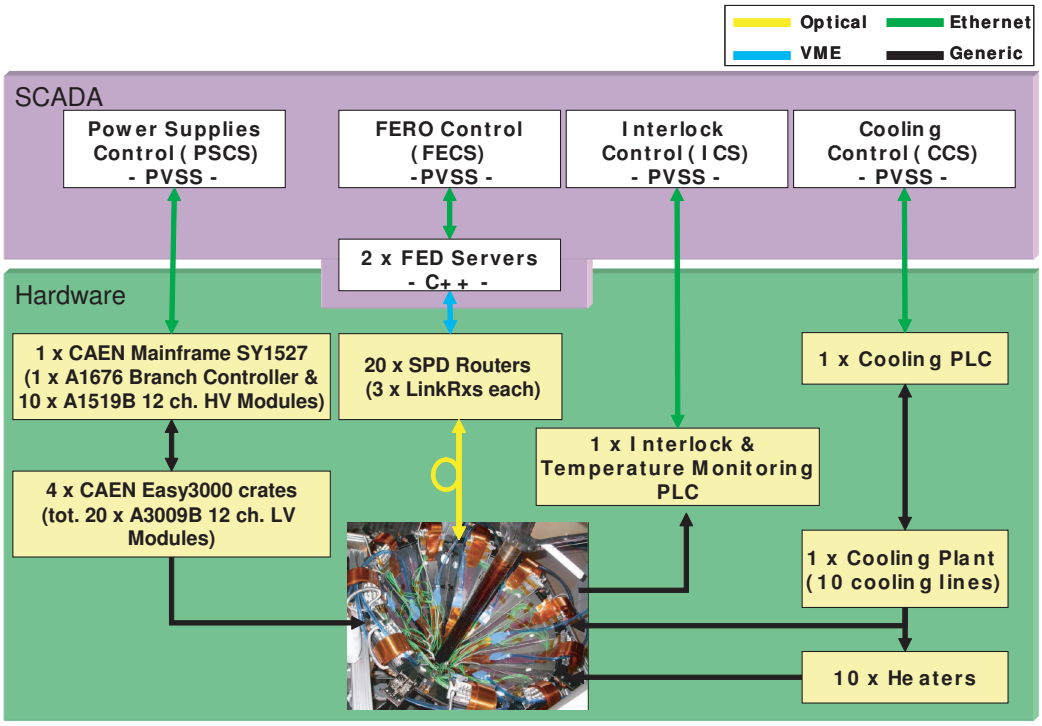

Figure 3.8: A logical block diagram displaying the SPD control system branches. In white are displayed the software components whereas in yellow the hardware components.

The Interlock Control (ICS) manages the SPD interlock system and it monitors the detector temperature. The parameters readout via the ICS are widely used also by the other CSs.
The Cooling Control (CCS) operates the cooling system and a series of heaters used to compensate the variation of heating produced by various detector powering configurations.
In the future it is also planned to integrate the control of the Pixel Trigger (PIT) electronics in the SPD DCS.
Each CS contains translator scripts capable of converting macro-instructions into the sequence of operations required for the hardware. Background scripts monitor continuously the status of the hardware and take automatic actions to protect the system in case of abnormal states. Most processes are fully automated in order to obtain the required reliability and safety of operation.

3.2.1 Front-End and Read Out Electronics Control System (FECS)

The FECS is the software used to control and operate the Front-End and Read Out Electronics (FERO) such as Router cards, LinkRx cards and HSs. It should monitor the actual electronics status of the off-detector electronics and on-detector electronics. Moreover the FECS configure the detector ($\sim$ 50 k Pixel Chips DACs and 10 M pixels matrices in term of TP and pixel masking), the Router cards and the LinkRx cards ($\sim$ 1600 registers). The FECS monitors the detector temperature and it performs the detector calibration procedure.
The FECS is built up of two software layers (Fig. 3.9). On top the PVSS layer communicating via TCP/IP with the bottom Front-End Device Server (FED Server) layer. In this section the PVSS layer is described whereas chapter

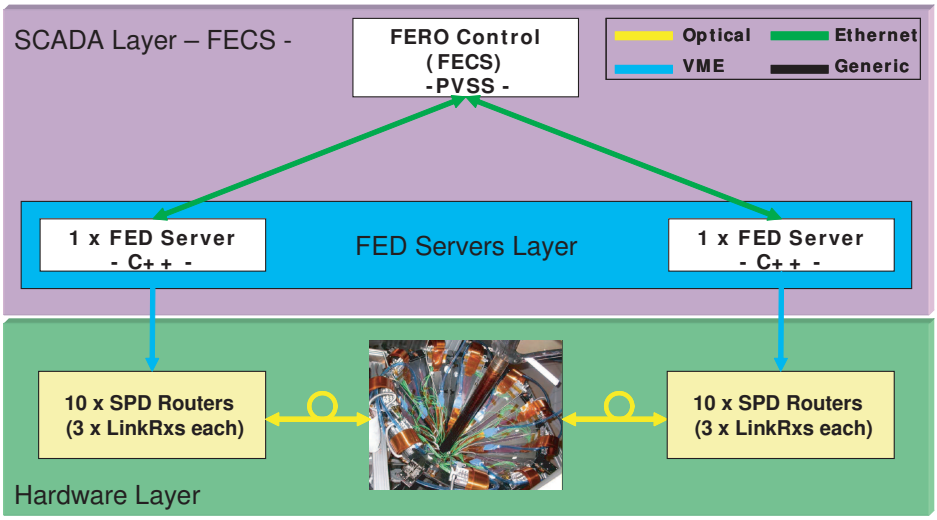

Figure 3.9: A block diagram displaying the connection between the FECS-PVSS, FECS-FED Servers layer and the hardware layer.

4 is dedicated to the FED Server. In order to understand this section it is only important to bear in mind that the PVSS is not designed for high speed control applications and it would not suit with the complex SPD electronics control. Hence the FED Servers receive macro-instructions from the PVSS layer and they publish the actual detector status and configuration.
For convenience, in this chapter, FECS means FECS-PVSS layer.

The FECS is designed to operate the FED Servers in automatic and manual mode. It provides the human interface to the detector configura-

tion parameters and to the detector calibration functions. Hence the system has been designed Object Oriented and with high modularity. This design pattern is fundamental for an application such FECS requiring data managements and often updates. The main concept in designing the FECS is to provide the users with a common interface to the detector configuration and calibrations passing trough either the FED Servers or the Configuration Database.
The FECS is composed of three main blocks such as Local Configuration Storage, Driver Layer and Human Interface. These blocks operate asynchronously and they run in specific and separated control loops. The communication between the various elements is performed only through dedicated interfaces and the data exchange uses the Local Configuration Storage as main gateway. The FECS structure separates the information fluxes in two main blocks as displayed in Fig. 3.10.

The top block foresees the communication between the Human Interface

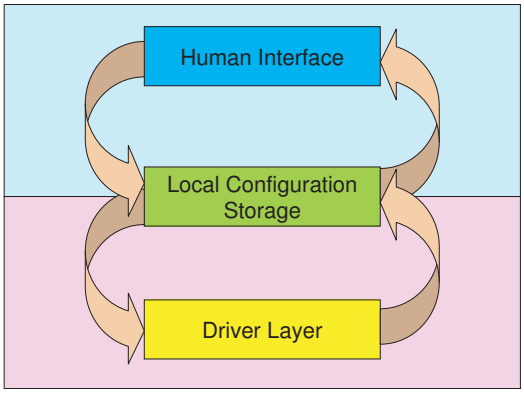

Figure 3.10: A simplified FECS PVSS layer block diagram.

and the Local Configuration Storage elements whereas the bottom block establishes the communication between the Driver Layer and the Local Configuration Storage. This structure makes the system very robust and it strongly simplify the system maintenance. Moreover the Human Interface designers and users are not obliged to know the full system structure but only the Local Configuration Storage structure. Viceversa the Driver Layer needs to communicate with only one block to store and retrieve information. The information centralizing into the Local Configuration Storage allows expanding easily the control system adding control loops plugged directly to the Local Configuration Storage. This design pattern also optimize system performances because all the control processes can run in separate PVSS managers, hence easily managed.

Fig. 3.11 displays a simplified FECS collaboration diagram. In the next sections the three main blocks will be described.

3.2.1.1 The FECS Local Configuration Storage

The Local Configuration Storage is the FECS core in which the information on the hardware status and configuration is stored. The FECS uses the FERO DPs as information collectors and main gateway to the different applications. Hence the FERO DPs are mapping the hardware configuration parameters such as electronics registers, DACs and noisy pixel maps. Moreover each DP store information on the electronics status such as temperature, activation status, TPs activation, dead pixels, etc. The FERO DPs are: 120 DPs of type HS, 60 DPs of type LinkRx card, 20 DPs of type Router card and a series of support DPs defining the calibration parameters to be used. All the FERO DPs have three main parts: Settings, Actual and DefaultConfig (same structure of the FED Server storage classes described in section 4.3.2). The Settings elements specify which configuration should be downloaded into the electronics whereas the Actual elements store the actual electronics configuration. The DefaultConfig memorize the information either retrieved from the Configuration Db (CDB) or to store in the CDB. In Fig. 3.12 is displayed the Half-Stave DP type as FERO DP example. The Analog Pilot (API) Actual and Settings DP elements have been expanded .

The Local Configuration Storage block hosts also a DataDistributor script used to forward data to other systems. For example the detector temperatures readout via FECS and used by the PSCS to switch off hot channels. The DataDistributor runs on a dedicated PVSS control manager reading cyclically the FERO DPs. When a DP changes, the script forwards the data to the appropriate system.

The StatusScripts are a series of scripts running on independent PVSS control managers and checking online the electronics and control system status. These scripts read cyclically the information stored in the FERO DPs Actual and Status parts and they asserts alarms, e.g. the FED Server alive status, when an error condition is found. If one of the FED Servers either stops operating or the communication is closed, the FED Server hearth bit DP stops to be updated. In this case the StatusScripts generate a message on the PVSS log and it inform the FECS thought specific FECS status DPs.

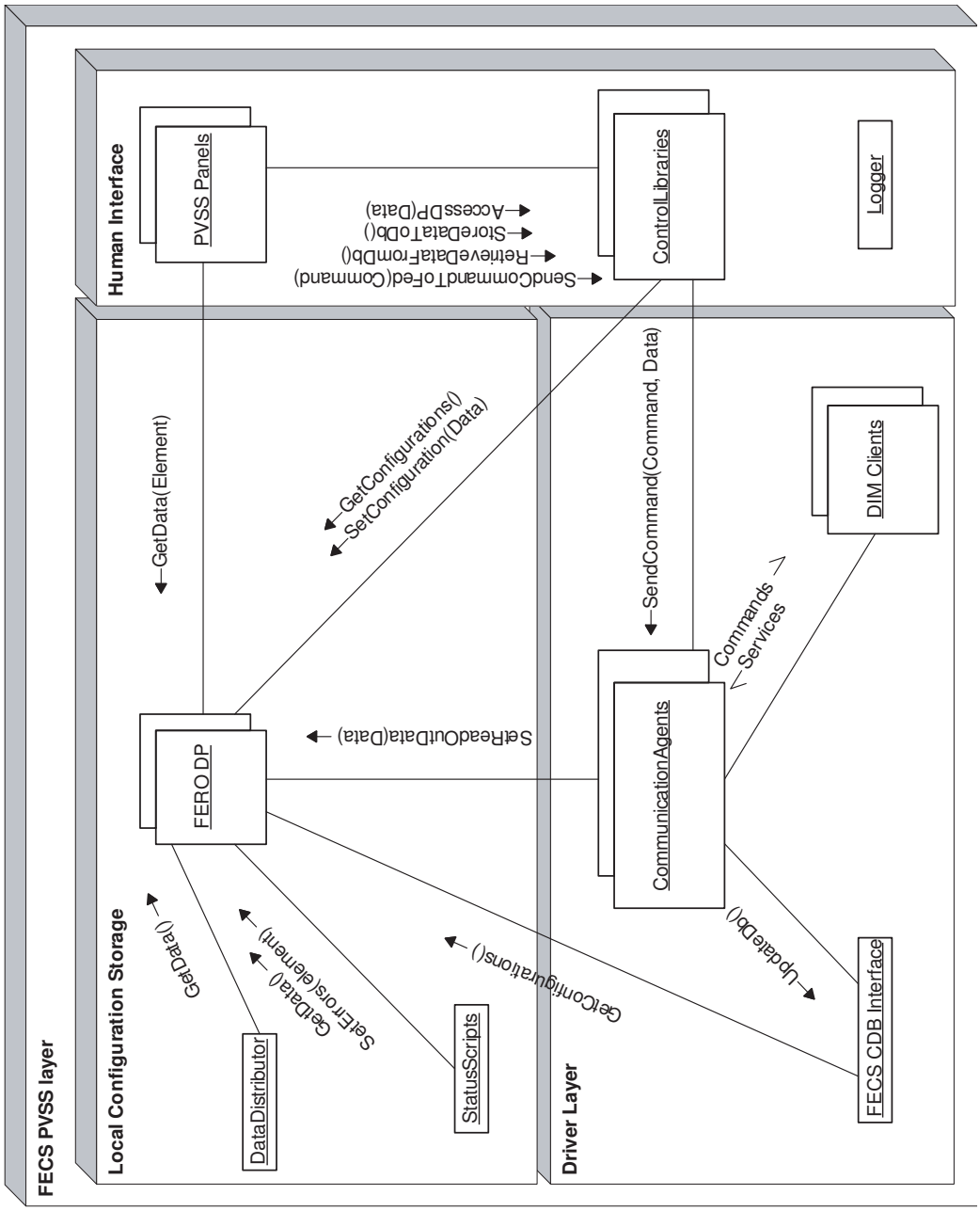

Figure 3.11: A simplified FECS PVSS layer collaboration diagram.

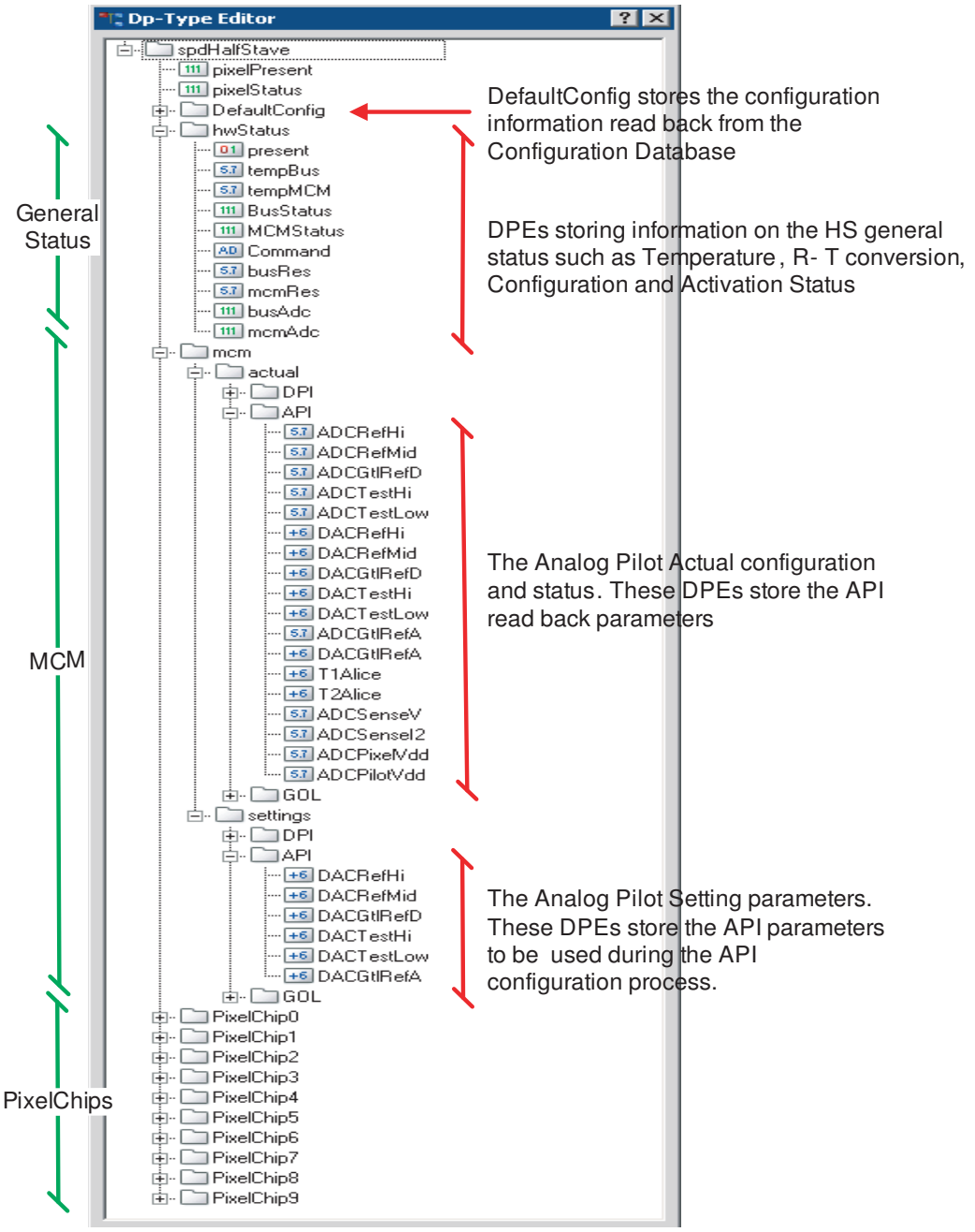

Figure 3.12: An example of FERO DP displayed using the PVSS PARA. The DPs of type HS (spdHalfStave) store information on the HS configuration and status. In correspondence of the + the menu can be expanded and the DP elements become visible. This example shows the Analog Pilot (API) Actual, the API Settings and the hwStatus elements.

Sensitive FERO DPs such as detector temperature, voltages and currents monitored by the FED Servers, are archived, on change, on an ALICE DCS centralized archival Oracle Database. The connection to the Db is performed running a specific PVSS manager.

3.2.1.2 The FECS Driver Layer

The FECS Driver Layer establishes the FECS communication with the FED Servers and the Configuration Database. Two type of clients such as DIM Client and FECS CDB Interface are managed by the Communication Agents. These Agents synchronize the clients operation and they represent the interface with the other FECS blocks.

Two DIM Clients communicate respectively with the two FED Servers to control the detector side A and side C (more details on DIM can be found in section 4.2.1). The JCOP Framework provides a DIM manager establishing the communication between the DIM clients and PVSS DPs. When the DPs associated to commands are updated, the corresponding DIM commands are sent using the DPs values as parameter. Viceversa when a service is published, the corresponding DPs are updated. The FECS uses two DPs as DIM Clients and each of them manage the communication with one FED Server. These DPs are separated in three parts: one for the FED Server commands, one for the FED Server services and one for store information on the communication status (more details on the FED Server commands and services structure can be found in section 4.2).
A third DIM Client is used to communicate with the DCS Online Data Analysis Tool (CDT) during the detector calibration procedures. More details on this tool and on the communication schema between FECS and CDT can be found in section 5.2.2.

The FECS CDB Interface updates the Configuration Database using the configuration information stored in the FERO DPs. When the Communication Agents issue the Db update command, the FECS CDB Interface connects to the FERO DPs and it generates a file of type Configuration Data containing all the FERO DPs DefaultConfig parts. Further the FECS CDB Interface calls the CDB client to perform the actual access to the CDB (see section 3.4.2 for more information on CDB client and Configuration Data files).
The CDB reading procedure is implemented inside the FED Servers and it

is managed by the Communication Agents (see below).
The mechanism described to update the CDB is very powerful because detaches completely the human interface by the Db connection. The users should only write in the FERO DPs DefaultConfig parts the information to be updated and the FECS CDB Interface manages the full process.

The Communication Agents are a series of background scripts, running in dedicated PVSS control managers, to interface the FECS blocks with the actual system drivers. The Communication Agents use two main channels to communicate with the FECS blocks: one publishes the incoming DIM data to the FERO DPs whereas the second channel receives commands by the Human Interface block. Whenever the DIM Clients update the services DPs, the Communication Agents decode the incoming information and, using the services Command and ID fields (see section 4.2.4 for more details), they forward the data to the specific FERO DPs Actual part. In case of error messages coming from the FED Server, alarms are also generated using the system Logger.
When the Communication Agents receive a command to FED Server request, they pack the incoming Command and Data in a unique data stream. Moreover these Agents add to the stream a unique ID that is also stored in an internal buffer. The steam is then forwarded to the DIM Clients. If after a certain timeout the Communication Agents do not receive a FED Server service with the ID stored in the buffer, an alarm is asserted.
More details on the communication protocol between FECS and FED Servers are reported in section 4.2.2. The main feature to bear in mind is that the system has two completely independent data flows: one directed to the detector and one coming from the detector.

3.2.1.3 The FECS Human Interface

The users can interact and operate the FECS using either a series of PVSS panels or methods contained in a set of Control Libraries.
The panels provided in the FECS package manage and display the electronic configurations, they monitor the detector temperature and configure the FED Servers. The FECS contains also a series of panels to perform the detector calibrations.
The FECS panels are divided in two classes: the user panels and the expert panels. The user panels are designed to be intuitive also to not system experts and they have a high level of automation. They are oriented to display

system parameters and system status. The actions to the system allowed by the users panels are only a subset of the FECS commands. These panels should be used by remote users or shifter.
The expert panels allow the full system control but with the drawback of a low automation and they are not user friendly.
The scope of this section is not to describe the FECS panels but to explain the Human Interface operational mechanism. However in Fig. 3.13 an expert panel (a) and a user panel (b) are displayed. This example shows the difference between these two panels; it is immediately visible the panels complexity difference. The two panels allow the MCM configuration. In the expert panel all the settings are visualized and can be adjusted but the panel is without automation. The user panel displays only the MCM components configuration status using 3 led. All the configuration operations are automatically performed. Moreover the expert panels can modify the electronics configuration online whereas the user panels can only update the configuration parameters stored in the CDB. In this latter case, to update the electronics configuration, a global detector configuration function should be started by the operator using the FSM.

The detector configuration policy foresees, indeed, that only the detector experts can modify online the detector configuration. The users should apply the configuration changes only to the CDB. The main reason to use this policy is to keep track of the effective detector configuration. Moreover the electronics configuration using the CDB information is performed only when a request of the FSM is issued. The configuration policy assures also the synchronization of the detector configuration with a detector state capable of receive it. The expert panels do not guarantee this synchronization because the detector configuration can be performed anytime, also during the detector run.
Furthermore in the new DCS release are already planned consistency scripts running on the data to be updated to the CDB. If a user tries to update the CDB with an armful configuration, these scripts should avoid the update.
The CDB has been designed taking in account this policy. The CDB client (see section 3.4.2 for more details) and the FECS CDB Interface are responsible of minimize the Db resources involved. This policy has the drawback of increase quickly the global version number but the amount of data stored does not grow correspondingly. However it is already planned to have a garbage collector script running regularly on the CDB data and delete duplicated data. Fig. 3.14 displays the information flux when a configuration using a user panel is performed.

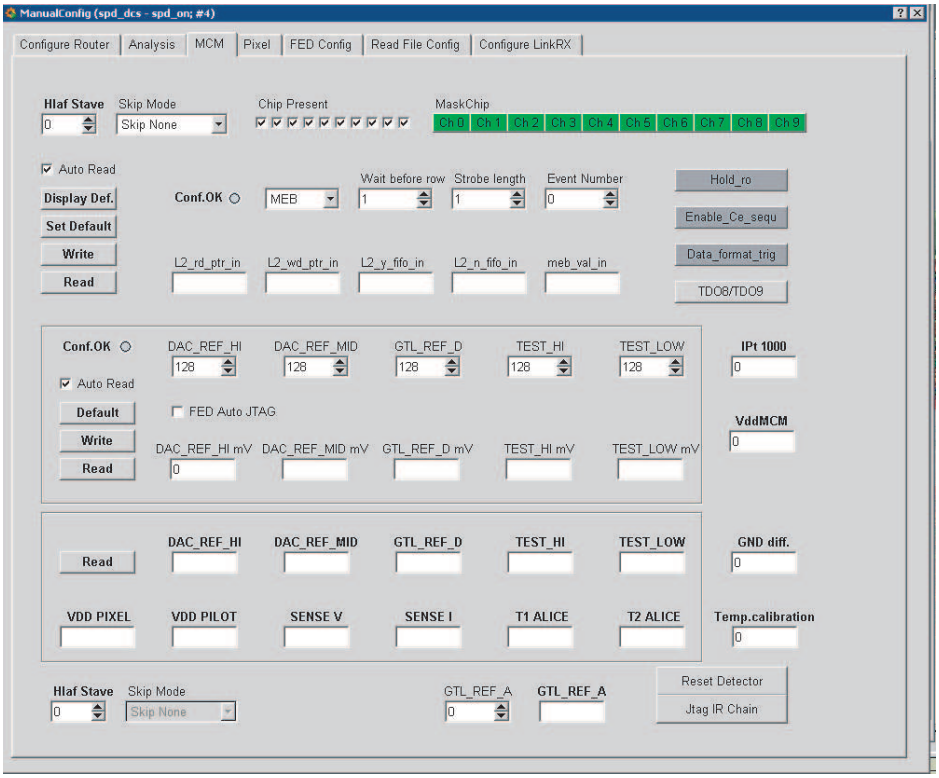

(a)

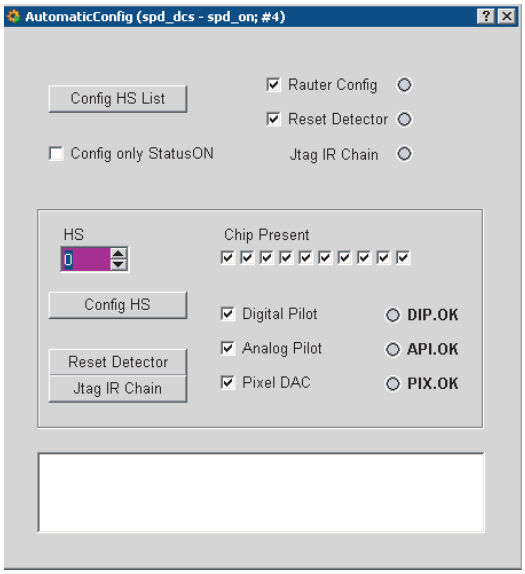

(b)

Figure 3.13: The two PVSS panels allow the MCM configuration. The (a) is an expert panel and all the MCM parameters can be directly configured. The (b) is a user panels performing automatically the configuration.

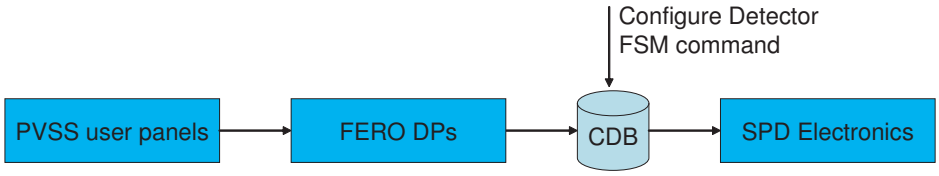

Figure 3.14: The detector configuration information flux when a user panel is used. The panels write into the FERO DPs and the data are forwarded to the CDB. The new configuration is uploaded into the electronics when the FSM sends the detector configuration command.

All the FECS panels are designed following an OO structure using the PVSS reference panel functionality. More than 100 objects panels have been designed and they have been used to build up the main FECS panels. The actual code and functionalities are contained inside the object panels whereas the main control panels are almost only a collage of the different objects. In the panels design it has been minimized the actual code because the functions contained in the Control Libraries have been widely used. This implementation schema allowed a reduced coding effort and the capability to reuse the same code among different panels and inside the FSM methods.

The Control Libraries are a series of SPD PVSS libraries designed to operate the FERO. The functions contained in these libraries are used inside the panels, control scripts and FSM objects.
The libraries are divided in three main families: the hardware access libraries, the FERO DPs access libraries and the automatic configurations/calibrations libraries.
The hardware access libraries send commands, e.g. configure, calibrate, reset, etc. to the Driver Layer. These functions can be directed to a single detector element or to the full detector at a time.
The FERO DPs access libraries have a series of interface functions to store or retrieve either simple or complex structures from/to the FERO DPs. This set of libraries is the main gateway to the Local Configuration Storage and they are widely used in the FECS panels. The only direct link between panels and FERO DPs is used to display sensitive parameters contained in the FERO DPs Actual parts. In cases of simple reading operation the libraries are bypassed and the panels are plugged directly to the reading DPs. The use of the FERO DPs access libraries interface has the advantage to allow modifying the DPs structure without re-edit the panels and the higher level

functions. A change in the interface functions is automatically propagated to all the code.
The automatic configuration/calibrations libraries contain high level functions to configure and calibrate automatically the detector. They use functions of the FERO DPs access to retrieve the required information and the hardware access libraries to communicate with the FECS hardware layer.
This section is not meant to give a full description of the Control Libraries but only to explain the main functionality concepts. Moreover a detailed description can be found in the user manual [34].

3.2.2 Power Supply Control System (PSCS)

The Power Supply system is based on modules manufactured by CAEN [37]. A CAEN mainframe SY1527 controls 120 HV channels and 240 LV channels (more details on the hardware structure can be found in section 2.3.1). The PSCS is designed to operate and monitor the status of:

- 1 x Mainframe SY1527
- 4 x Easy3000 Crates
- 2 x Power Converter (48 V)
- 10 x HV Modules A1519B with 12 HV channels each
- 20 x LV Modules A3009B with 12 LV channels each

The Mainframe is the gateway to the powering system and it communicates via OPC [110] with the PSCS. CAEN provides also an OPC server to be run in each PC willing to communicate with the Mainframe. A general conceptual schema of the system is displayed in Fig. 3.15.
The CAEN modules are widely used at CERN hence the JCOP Framework group provides the users with a PVSS CAEN package containing the CAEN DPTs and a PVSS OPC client. This client allows establishing a direct connection between the PSCS DPs and the hardware. Whenever a control DP is updated by the user, the value is sent via OPC to the Mainframe. Viceversa

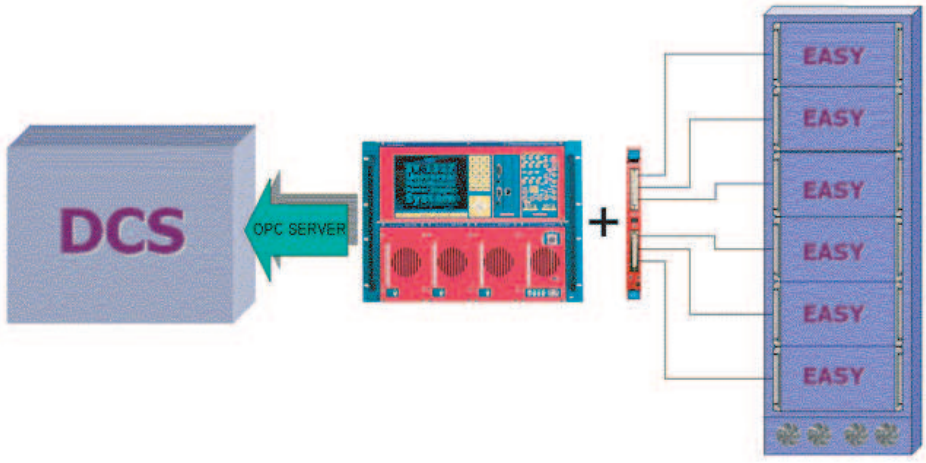

Figure 3.15: The CAEN mainframe can operate independently the power channels and it communicates with the DCS via OPC. The DCS monitors the system status and sends commands to the Mainframe.

whenever the Mainframe sends information to the PVSS client, the corresponding DPs get updated.

The PSCS block diagram is displayed in Fig. 3.16. The information on

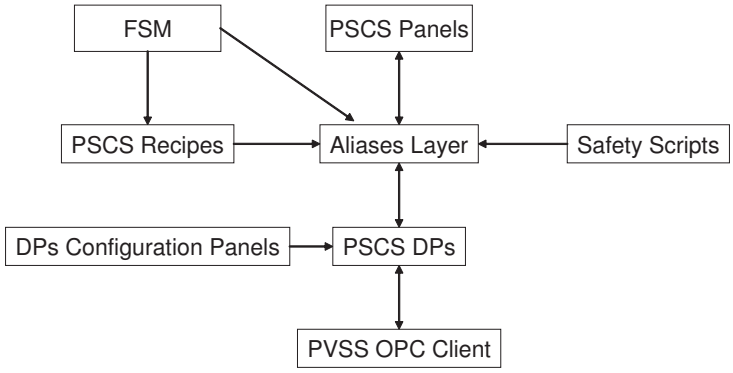

Figure 3.16: The PS Control System block diagram.

the hardware status and configuration is stored in a list of PSCS DPs corresponding to the various hardware elements described in the list above. All voltages and currents DPs are archived on change (variation $> 2\%$) into an ALICE DCS centralized archival Oracle Database. The connection to the Db is performed running a specific PVSS manager. Alarms are automatically issued by the PSCS DPs when voltages and currents are exceeding specific

alarm thresholds.

A translator layer, named Alias Layer or Logical Layer , is connected to the PSCS DPs to associate an alias to each power channel. The HS is supplied via three separate power channels: two LV channels are respectively for the MCM and for the Pixel Bus, a HV channel is used for the detector sensor. The aliases define the type of object to power and its physical position inside the detector. They have the structure: spdTYPE_x_y_z where TYPE can be BUS (the HS readout chips), MCM or HV (the detector). x is the detector sector number, y is the detector side (A, C) and z is the HS position number in the Half-Sector (the numbering schema is displayed in Fig. 2.1).
The aliases are used in all the PSCS blocks to refer to the specific elements. This strategy allows swapping hardware power channel with the simple redefinition of the aliases; the PSCS functionalities remain unchanged. The PSCS uses the Logical Layer as hardware gateway.

The Safety Scripts are a series of low level scripts to guarantee the detector safety constantly monitoring the detector status and taking corrective actions if necessary. Each script runs on a dedicated PVSS control manager and loops continuously on the PS channels. The scripts are plugged directly to the FECS DPs to assure the maximum efficiency and speed of response. For redundancy the checks performed by these scripts are repeated also at FSM level. However, if the FSM is disable these scripts remain operational and they guaranty anyway the detector safety.
In order to understand the Safety Script functionality is important to bear in mind that the HS can be damaged if a wrong powering combination of the three HS power channels is applied. Tab. 3.1 resumes the available combinations and the HS powering up/down sequences.

Sequence step	LV MCM	LV Pixel Bus	HV sensor
0	OFF	OFF	OFF
1	ON	OFF	OFF
2	ON	ON	ON (2V)
3	ON	ON	ON

Table 3.1: HS power up/down sequence and the HS powering stable states allowed.

The Safety Scripts switch off HSs elements or the full HSs in case of critical conditions such as:

HSs Channels Trip: If one or more channels associate to a HS trips, the scripts bring the HS to a stable powering condition switching off the appropriate HS channels. The script acts also when the wrong power up sequence is performed.

Temperature software Interlock: If the HS temperature is either increasing too quickly or it is too high, the HS is switched off.

Temperature monitoring faulty: If the PSCS does not receive the update of the detector temperatures for a certain time, the HS is switched off.

The JCOP Framework provides a series of panels used to operate the CAEN channels. However these panels are generic and they are orient to system experts only. Hence, I decided to develop a series of user friendly SPD oriented panels to operate the PS system. The goal of these panels is to provide the user with a simple interface where only the SPD required settings and statuses are displayed. Moreover the panels reorganize the information structure to be suitable for the SPD user case. The system experts can anyway access the JCOP Framework panels.
Now the PSCS has four main control panels to operate the Mainframe, the power converters and the power channels (HV and LV). These panels allow the devices switch on/off and the configuration of their operational parameters. The same panel is used for all the power channels of a certain type (HV, LV). A selector allows choosing of which channel perform the control. Fig. 3.17 displays the panels used for the control of HV (a) and LV (b) channels. The top panels section is used to display the monitored parameters whereas the bottom one is used to specify the channel settings. Fig. 3.18 displays the panels for the Mainframe SY1527 (a) and the power converter (b) control.
The PSCS have also a set of panels and libraries used to configure the system and DPs behavior. These panels allows to set automatically the DPs aliases, the archiving and the DPs alarms.
The OPC communication packages the parameters to be transmitted in groups and send them all at once. If an OPC group contains many parameters the full communication is slowed down. By default PVSS groups

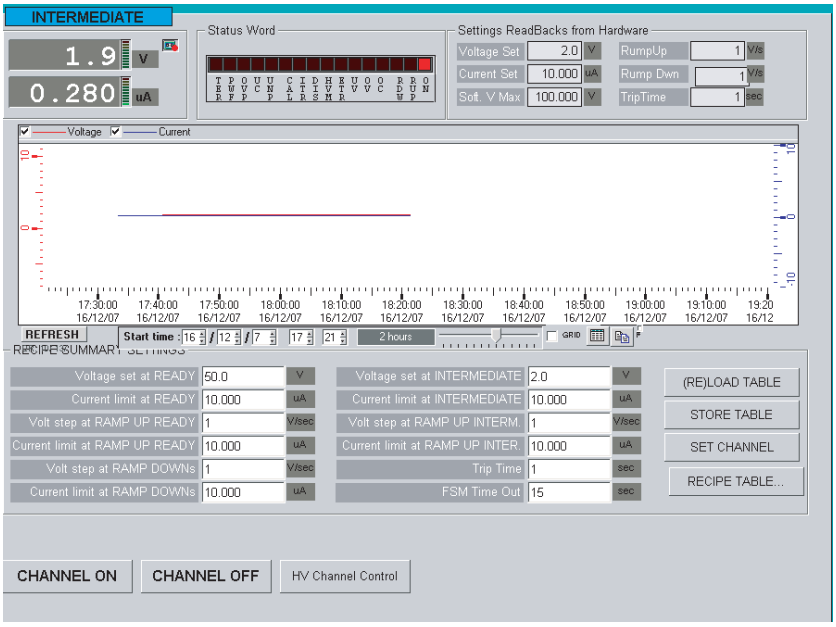

(a)

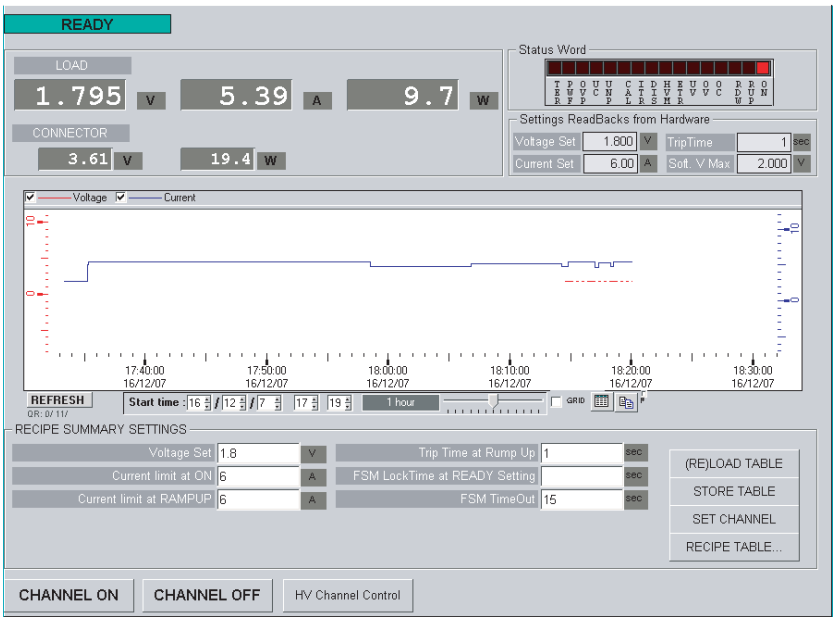

(b)

Figure 3.17: The PSCS control panels to operate a HV (a) and a LV (b) channel. The central and top panels sections are used for monitor the channel whereas the bottom part is used to specify the channel setting.

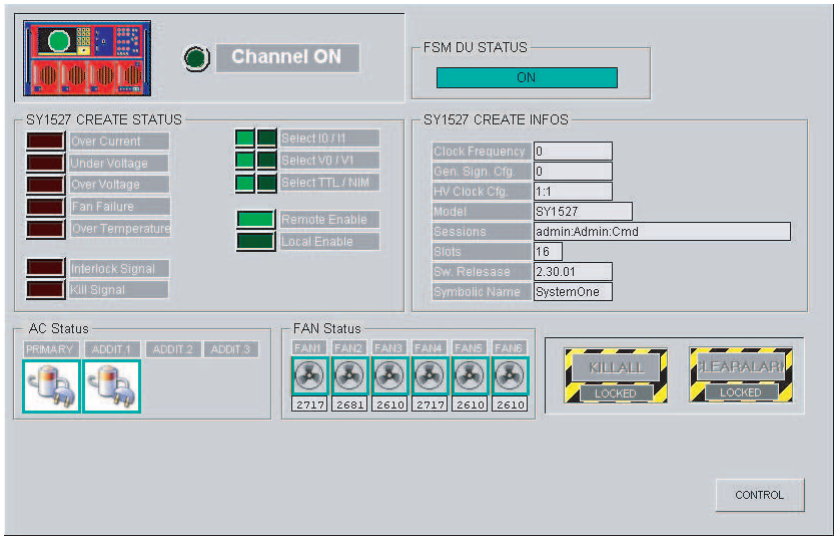

(a)

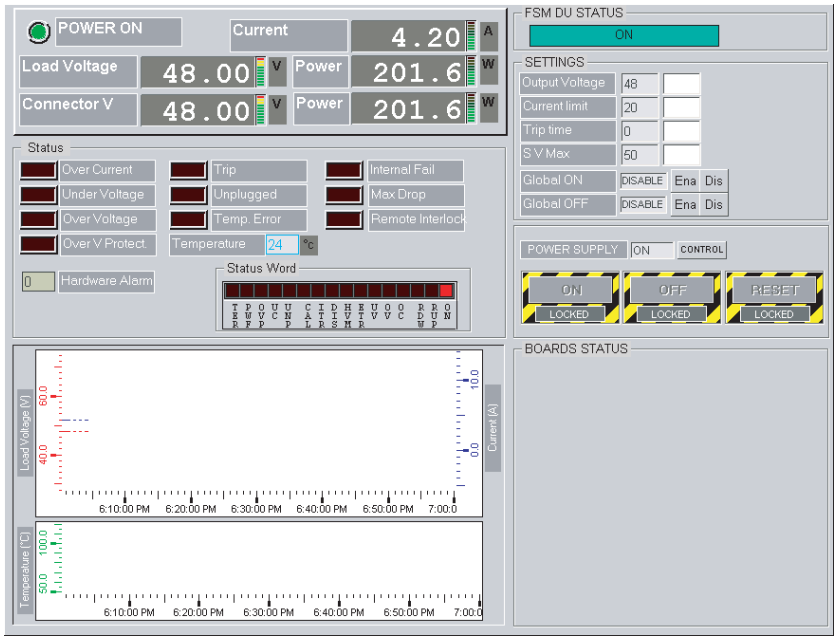

(b)

Figure 3.18: The Mainframe SY1527 (a) and the power converter (b) control panels.

all the CAEN parameters in a unique OPC group. In order to prevent this conditio, the PSCS has a series of functions to reorganize the OPC groups information. One OPC group is associated to every HS containing the parameters of the 2 LV and one HV channel. The PSCS has also panels to modify the addressing associated to each DP. The addressing is used by the OPC to associate a hardware component to a DP.

The devices configuration parameters are stored in the CDB and the JCOP Framework provides tools to organize the information in logical objects called 'recipes'. The PSCS has three recipe types such as spdMCM, spdBUS and spdHV. Each type contains the configuration parameters needed to configure the SPD Half-Sector power channels of the specified type. Moreover, each Half-Sector has a recipe associated to each HS powering state as described in section 3.3. This operation mode allows following the channel transient and stable phases with the appropriate configuration. For example, during the HV rump-up phases, it is possible to measure a small current overshot. This is a normal condition not dangerous for the detector. The overshot is disappearing as soon as the channel reaches the operational state. In this condition the channel would be switched off automatically by the system because of the trip current limit. In order to prevent this effect I foresee a configuration change between rump-up and stable state. During the rump-up the current limit is increased to avoid the channel trip whereas it is restored to the nominal value during normal operation. This mechanism is allowed by associating a recipe to each channel state. The other solution to prevent the channel switching off would be to keep a high trip current limit during all the channels states but this could be dangerous for the detector. Section 3.3 describes also the mechanism used by the FSM to load the recipes in the PSCS DPs and to control the PS system. More details on the recipes structure can be found in section 3.4.3.
The PSCS embeds also custom recipes editor panels such as displayed in Fig. 3.19. These panels allow either to generate new recipes or to update existing recipes. The panel of Fig. 3.19(a) updates all the Half-Sector recipes of a specific type and device. The panel of Fig. 3.19(b) updates the states recipes of a specific type and device.

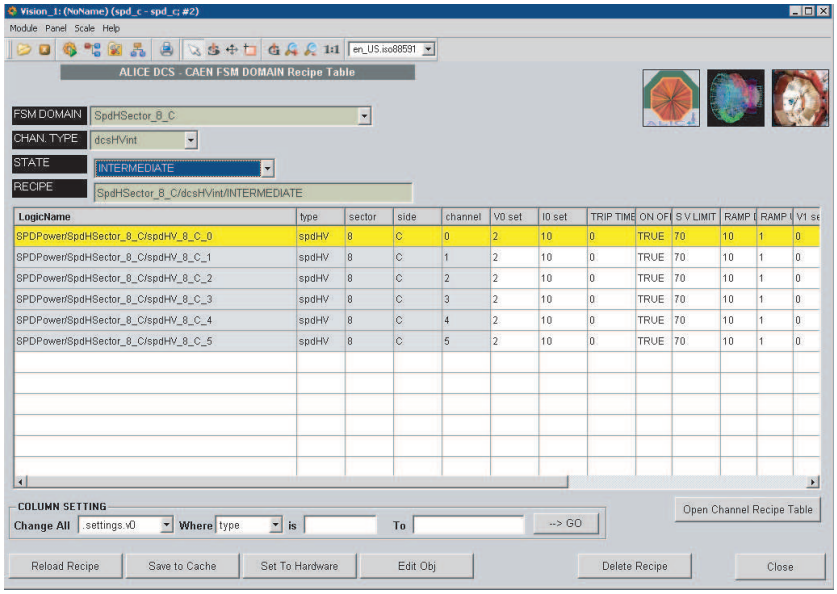

(a)

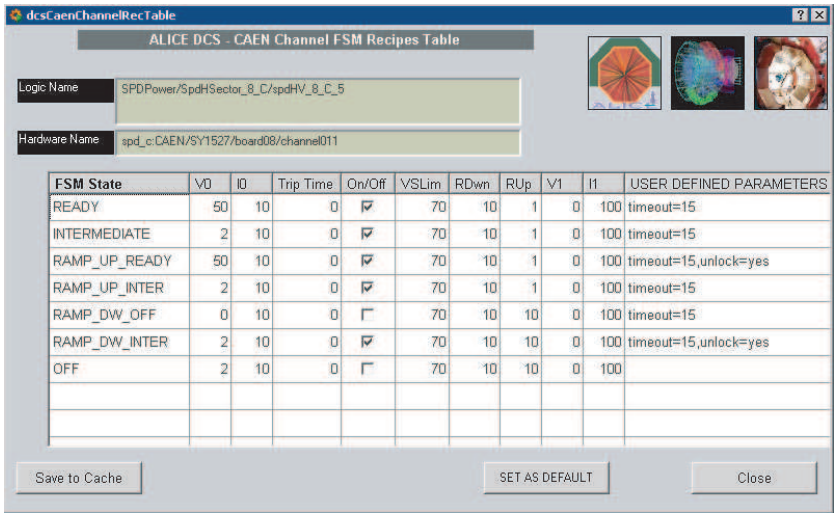

(b)

Figure 3.19: (a) The panel for the Half-Sector recipes editing. The selectors on top identify the Half-Sector and the recipe type. On the bottom part the devices list is displayed with the corresponding settings. These table fields can be edited. (b) The panel for edit the power channel recipes as function of the corresponding states.

3.2.3 Cooling, Interlock and Support Services Control Systems (CCS, ICS and SCS)

The SPD cooling plant has a CERN standard hardware interface. The communication between the cooling devices and the software is via OPC Server-Client protocol. The JCOP Framework group provides a Cooling and Ventilation (CaV) package to operate and monitor the cooling plant and the cooling loops. The package contains the CCS DPs, the OPC PVSS client and few main user panels. Using a configuration file (.SCY file) provided by the plant constructor, the CCS configure automatically the DPs and establishes the communication with the devices. The cooling system parameters should be adjusted only by experts, hence, I decided to use the standard JCOP Framework panel to operate the cooling system. The users can retrieve monitor the system using an external synoptic panel, named bitmap, connects to the CCS DPs. It shows intuitively the cooling system parameters. Fig. 3.20 (a) displays the plant control panel whereas (b) displays the loop control panel. The bitmap is displayed in Fig. 3.21. The actual cooling system control can also be performed automatically via FSM as it is described in section 3.3.

The ten cooling loops have three states i.e. OFF, ON and LOCKED while the cooling plant has four states i.e. OFF, STANDBY, RECOVERY and RUN. A 32 bit control register defines the main plant functionality.

The CCS monitors also the ten stabilizing heater added to each cooling lines. The cooling plant activates automatically the heater corresponding to a cooling line opened. Twenty temperatures sensors (Pt100), two for each heater, monitor the heater temperature. The CCS uses an Embedded Local Monitor Board ELMB[2] [38] to reads the temperature sensors. In case of anomalies the CCS informs the cooling plant that promptly disables the corresponding heater.

All the cooling system monitored parameters are archived on change into an ALICE DCS centralized archival Oracle Database. The connection to the Db is performed running a specific PVSS manager. Alarms are automatically issued by the ICS DPs when the operational parameters are outside a specified range.

The interlock system has been entirely designed and developed in the SPD group but, due to the fundamental role of this system in the SPD safety, it is now running in the ALICE Detector Safety System (DSS) framework. This

[2]The ELMB is a board able to measure in parallel up to 32 analog inputs and it communicates with the CS via MODBUS.

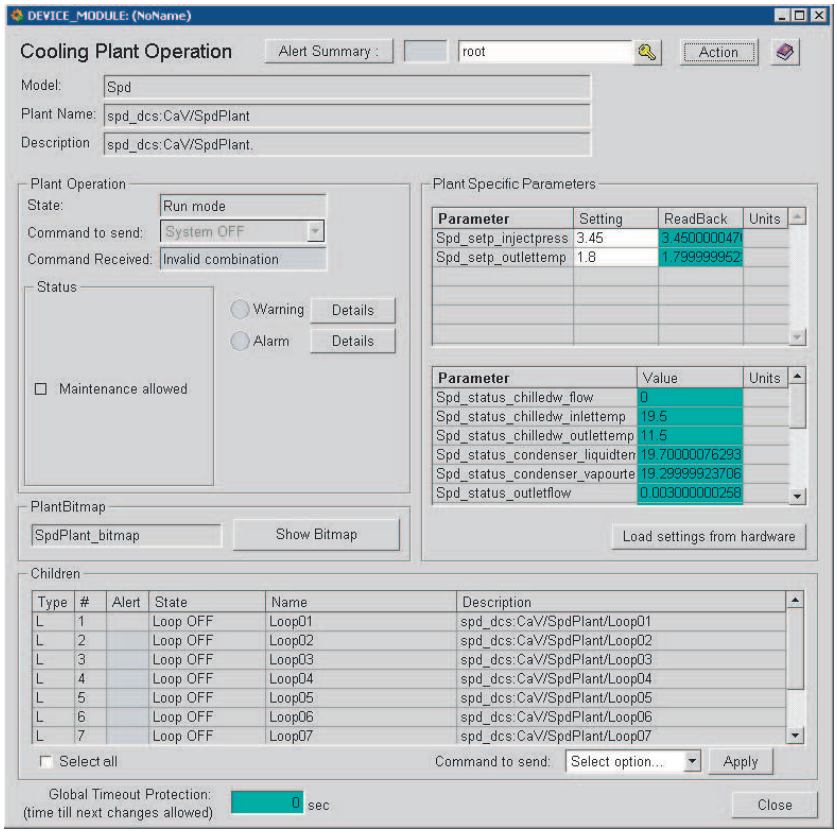

(a)

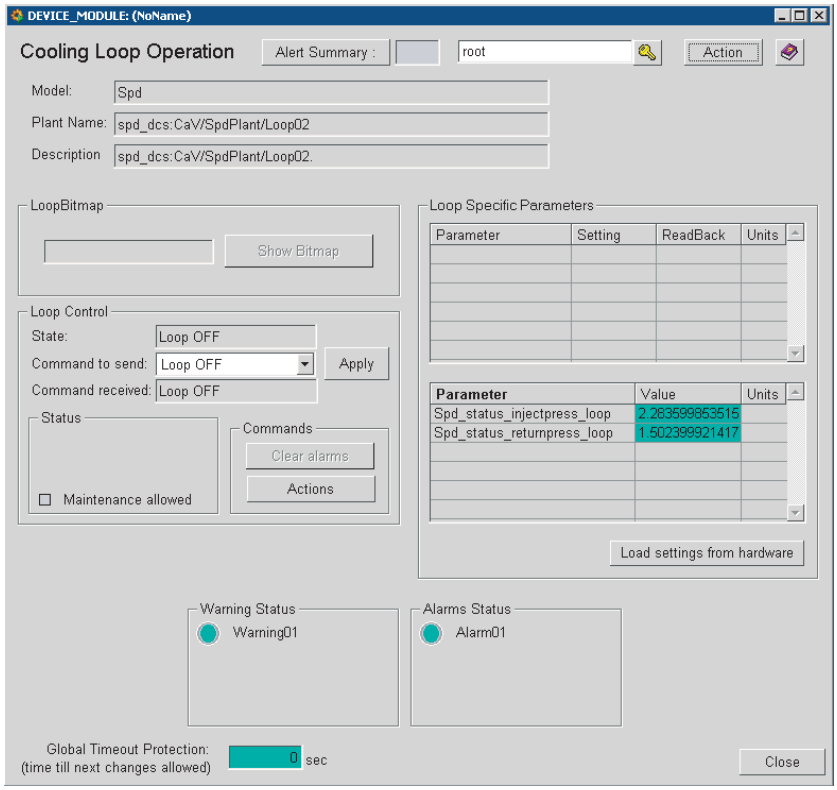

(b)

Figure 3.20: The cooling plant (a) and the cooling loop (b) control panels.

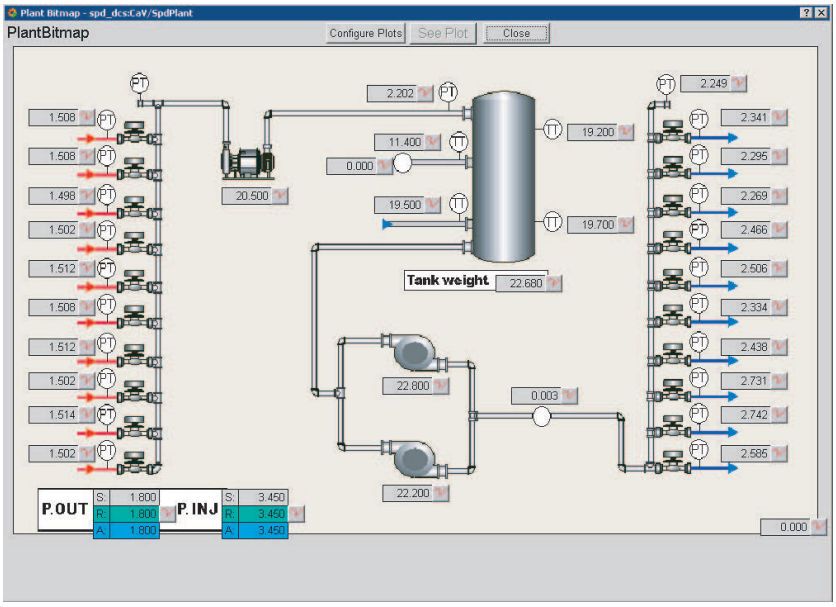

Figure 3.21: A synoptic cooling system view.

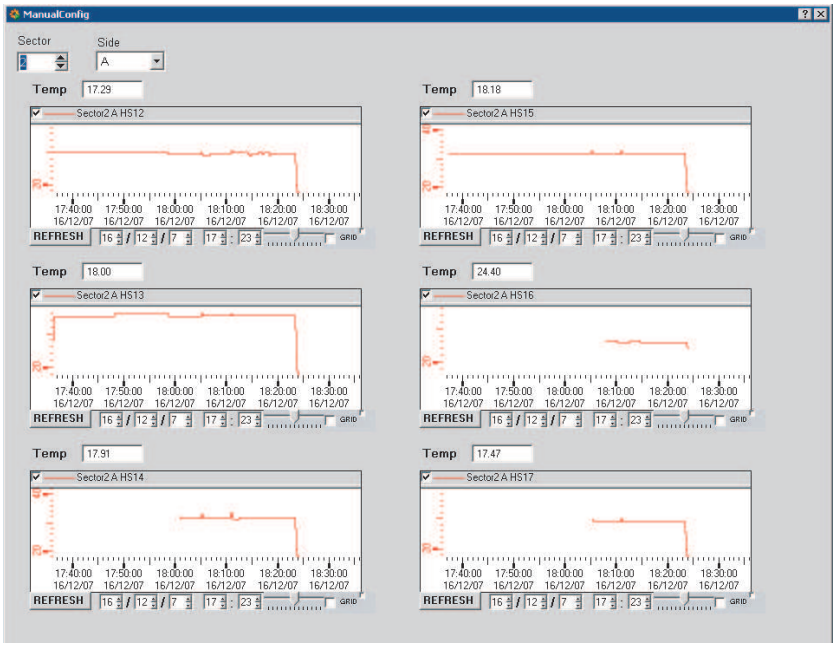

Figure 3.22: The ICS temperatures monitor panel. It displays the temperature of the 6 Half-Sector HSs. The selector on the top of the panel allows the browsing over the Half-Sectors.

latter is designed with redundant components to avoid any kind of failure of the system. The decision of use the DSS come from the strong DSS framework reliability. The DSS manages and controls the system but it forwards to the ICS, via DIP [36], the HSs readout temperatures. These temperatures are stored in a series of ICS DPs. These DPs are archived on change into an ALICE DCS centralized archival Oracle Database. The connection to the Db is performed running a specific PVSS manager. DPs alarms are generated whenever a temperature passes a certain threshold. A background script monitors the communication with DIP and the temperatures readout. In case of either faulty communication or high temperature, the background script switch off automatically the corresponding HSs.
The ICS has a main panel (Fig. 3.22) displaying the temperatures trends of the 6 HSs corresponding to a Half-Sector.

The Services Control System manages the system crates. These devices communicate with the CS via MODBUS. A series of user panels allow to switch on/off the crates and operate their cooling fans.

3.3 The SPD Finite State Machine (FSM)

This section describes the Finite State Machine Layer (Fig. 3.1) general structure. I have been the main designer of this software component that reached a high level of complexity and automation. However due to the elevate number of FSM objects used ($\sim$ 1500) and the corresponding control loops number, the full FSM description would be too long and complicated for this thesis. Hence I decided to recall in this section only the general FSM hierarchy and its main features. More details on the FSM implementation can be found in the SPD literature such as indicated in this thesis references [34].

The FSM is the logical software component that merges the SPD subsystem controls such as front-end electronics CS, power supply CS, cooling CS, detector services CS to form a unique entity. It is responsible for the synchronization and automation of the detector operational phases. The FSM receives the status (i.e. READY, NOT READY, ERROR) of the SPD subsystems, and it performs start-up, shut-down and standard operation procedures as well as emergency routines, e.g. during cooling failures according to pre-defined sequences.
The FSM, trough its top-node, is the interface to the ALICE Detector Con-

trol and Experiment Control systems. Furthermore the FSM is the main user interface to the detector control. Any user should be able to operate the detector using only the FSM interface; the FSM top-node should be the main gateway to the detector operation.
The design of the SPD FSM followed a series of guidelines such as:

Intuitive interface: The user should access easily and quickly the system components control. A not SPD expert should be able to operate the detector.

Errors and Warnings handling: The FSM should be able to spot intuitively, also to a not expert user, an eventual system error or warning condition. The ALICE DCS should be informed in case of critical conditions. Moreover the operator should be provided with an unambiguous list of actions to recover from an error condition.

Automation and Safety: The system should react automatically to unsafe hardware or software conditions. Only self-consistent and armless operation should be allowed to the operator. The detector should be bought automatically to a state ready for data taking or calibration, departing from any not error state.

Partitioning: The FSM should allow operating a detector subset (or many) independently by the rest of the detector.

Performances: Any action should be propagated from the hierarchy top-node to any device in less than 1s. The top-node state update should be performed in less than 1s from any state transition in the hierarchy.

In order to fulfill these requirements I decided to give to the SPD FSM a detector oriented hierarchy. This structure divides the system in modules corresponding to the actual detector and systems components. It allows partitioning the detector up to the Half-Sector level. Furthermore a detector oriented hierarchy allows merging in logical entity elements belonging to different subsystems. The SPD to operate needs indeed to connect the cooling, power and front-end electronics systems. Moreover the overall FSM performances are enhanced by the use of this structure. This structural choice allows having a simple user interface accessible also to a not SPD expert

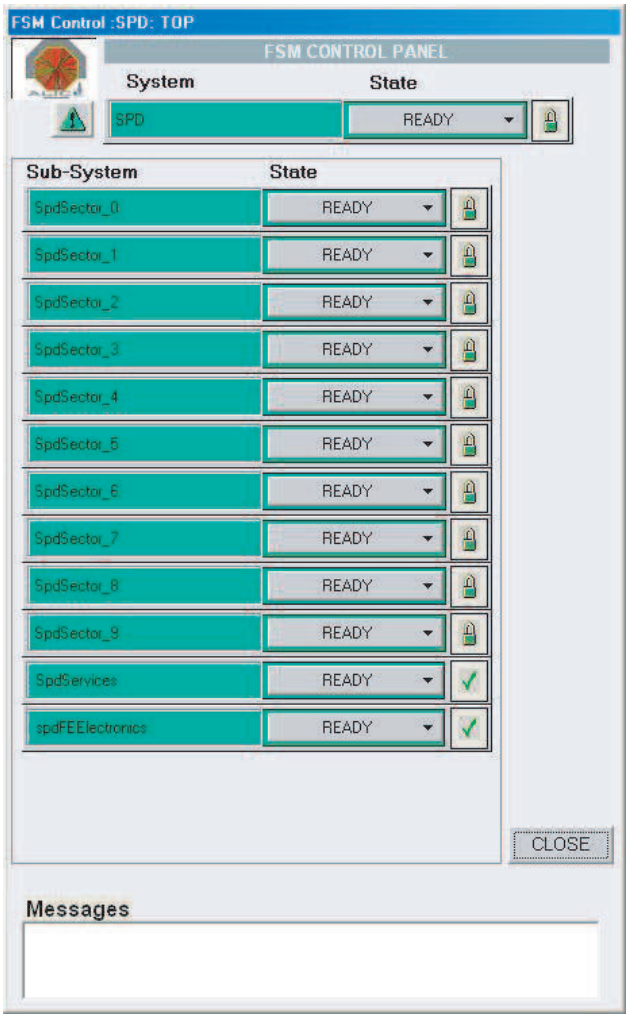

Figure 3.23: The FSM top-node panel. The global detector and its components states are displayed by the states indicator (all READY in this example). Clicking on a component name, the corresponding FSM panel is opened. This system allows browsing the FSM hierarchy.

users (e.g. the FSM top-node panel displayed in Fig. 3.23). The components are indeed logically grouped in services, sectors, Half-Sector, HSs, etc. In the following part of this section it will be shown that the full SPD FSM hierarchy has a four levels depth. Any hardware component can be reached, monitored and operated departing from the top-node and just browsing these four hierarchy levels. The drawback of use a detector oriented FSM hierarchy is the increase of complexity in the FSM design. A series of hidden logical components are required to perform the system components connection and synchronization. Fig. 3.24 displays a simplified version of the SPD FSM; only the main components and structures are reported in this schema.

The FSM top-node (*SPD DCS*) has 12 branches: 10 to control the SPD sectors (*Sector0..9*), one dedicated to the SPD services (*Services*) and one to operate the front-end electronics (*FECS*).
The services LU (Fig. 3.24 top right),hosts the powers supply and Router cards crates control. Moreover this object controls the cooling system and it monitors the interlock system status. The *Services* state is READY only when all the required infrastructure services are fully operative. Whenever the *Services* LU is in an error state, the FSM top-node switches off all the power channels. The detector can be powered only when all the services are ready.

The *FECS* DU is designed to communicate with the front-end electronics control system (FECS) described in section 3.2.1. This DU receives commands such as CONFIGURE, CALIBRATE, DOWNLOAD, etc. and, using the required FECS Control Libraries, it forwards the appropriate command sequences to the FED Servers. The *FECS* DU states are corresponding to the on-detector and off-detector electronics configuration status, e.g. NOT_CONFIGURED, CONFIGURED, CALIBRATION, etc. Moreover the DU publishes the version number used for the system configuration.

The ten *Sector0..9* CUs (Fig. 3.24 top left) represent the SPD sectors and each of them is partitioned in two Half-Sectors by two *HSectorA-C* CUs. The structure of the sector and Half-Sector CUs is identical in term of states, actions and operation. They have three stable states such as MCM_ONLY, BEAM_TUNING and READY. Two temporary but not intermediate states are CALIBRATING and CONFIGURING.
MCM_ONLY is a state in which only the MCM is powered and the MCM can be operated in stand-alone mode. This is a debug and standby state.
BEAM_TUNING is a state applied when the accelerator beam is not clean. In this state the HSs are powered but the sensor voltage is set at 2V.

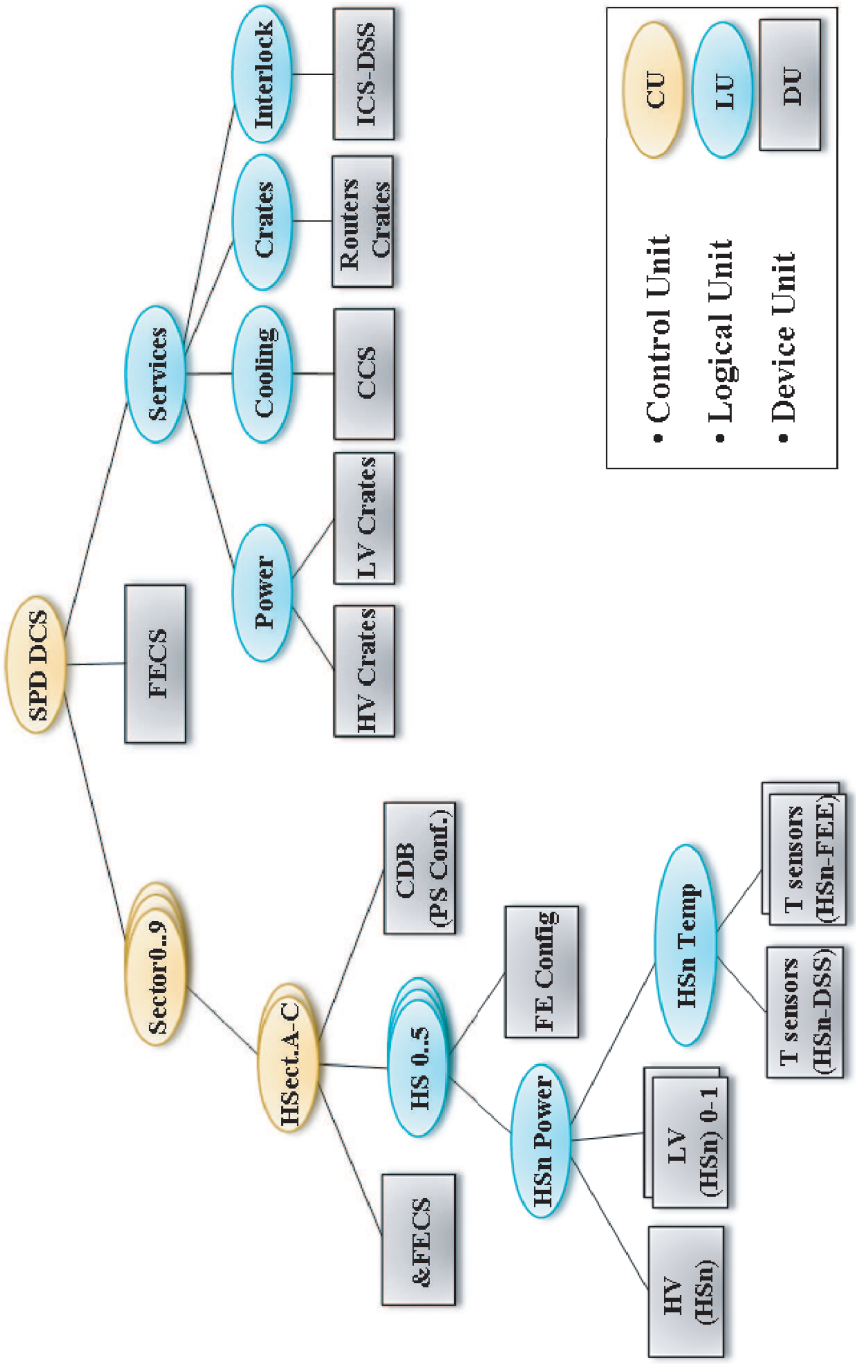

Figure 3.24: A simplified version of the SPD FSM hierarchy.

The READYstate is the state in which the detector is fully powered and configured. The data taking and the calibration procedures can be initiated in this state.
The CALIBRATING state is temporary and it is applied during the detector calibration. The CUs leave automatically this state when the calibration finishes. The CONFIGURING state behaves as the CALIBRATING state but it is applied during a detector configuration procedure.
The use of CUs also for the Half-Sector control allows the hierarchy partitioning up to this level, hence, the Half-Sectors and all their components can be operated autonomously.

Each Half-Sector CU includes six Half-Staves (*HS0..5*) LUs, one Configuration Database (*CDB*) DU and a reference to the *FECS* DU. This latter allows operating the front-end electronics when the Half-Sector is used in stand-alone mode. Otherwise, this DU is disabled. The *CDB* DU connects with the CDB to download the power supply channels configuration. The *HS0..5* LUs operate the six Half-Sector HSs in term of power, configuration and calibration.

Each *HS* DU has children of type *FE Configuration* and *HSnPower*. The former informs the FECS on how the HS should be treated in respect to the configuration and calibration procedures. The HS indeed can be part of these procedures or excluded.
The HV and LV channels are linked together via the *HSnPower* providing the proper HS power-up/down sequences. Moreover this LU hosts a series of safety control loops switching off either completely or partially the HS in case of anomalies. The *HSnPower* also decides whether the HS can be powered or it should be switched off as function of the detector temperature. A *HSnTemperature* LU provides the *HSnPower* LU with a state corresponding to the HS temperature. The *HSnTemperature* LU receives information on the HS temperature distributions via the 11 sensors (Pt1000 and NPT) placed on the HS and it compute the global module state.
The idea of adding the temperature monitoring at this level of the hierarchy is very powerful because it allows switching off only the affected HS. Moreover it guarantee a fast FSM response to critical conditions, indeed, only the hierarchy bottom components are involved in the control loop.
The HV and LV channels are controlled by corresponding DUs. The HV DU has three stable and four transient states. The stable states are: OFF, INTERMEDIATE and READY whereas the transients states are the corresponding RUMP_UP_X and RUMP_DOWN_X; X is the corresponding final stable state. The OFF and READY states names are self-explaining whereas

the INTERMEDIATE is a stable state in which the voltage is reduced respect the nominal operation. The SPD used a voltage of 2 V. This DU allows changing configuration whenever the channel enters in a state. The channel recipes (see section 3.2.2 for details) are indeed reloaded whenever the FSM change state. This mechanism has been used for the first time by the SPD[3] and now it is a standard ALICE mechanism.
The LV DU is equivalent to the HV DU but the INTERMEDIATE state is missing.

The SPD FSM hierarchy comprises 31 CUs , 600 LUs (120 hidden) and 900 DUs (140 hidden). The complexity of the structure and the intensive computing load required impose the FSM scattering over 3 Worker Nodes . A series of performance tests have been carried out in laboratory and in the ALICE environment during the detector commissioning. The specifications described above have been fulfilled.

3.3.1 FSM Top-node

The FSM top-node is the main entering point to the detector control. It allows connecting with the ALICE DCS and Experiment Control System (ECS). In normal operation the user should rely on this component to have information on the overall status of the detector and services. Additionally the top-node commands are forwarded to all the FSM hierarchy. The top-node provides a simple and intuitive list of commands able to bring the full system in any operative stable state. During the ALICE operation the operator is replaced by the ALICE DCS/ECS using only the top-node to operate the detector. In order to integrate the detector control with these systems is mandatory that each detector top-node accepts and recognizes the ECS commands. Viceversa all the detector states should be recognized by the ECS. The SPD top-node list of commands and its state diagram is displayed in Fig. 3.25 whereas Tab. 3.2 describes the states.

[3]This mechanism has been developed in collaboration with the ALICE HMPID group.

State	Description
OFF	Devices are switched off.
STANDBY	Services ON but detector channels OFF.
DOWNLOADING	All configurations are being downloaded from CDB, according to Run Mode.
STBY_CONFIGURED	Only the MCMs are powered and configured
CALIBRATING	The system is performing a calibration procedure.
MOVING_BEAM_TUN	The system is changing its configuration to reach the state BEAM_TUNING.
MOVING_STBY_CONF	The system is changing its configuration to reach the state STBY_CONFIGURED.
MOVING_READY	The system is changing its configuration to reach the state READY.
BUSY	The CDB is being updated
BEAM_TUNING	The HSs are powered and configured but the detector HV is set at 2V.
READY	The system is suitable for physics data taking.
READY_LOCKED	Like READY, but no further configuration or calibration possible.
PWS_FAILURE	Power Supply problem.
INTERLOCK	Any relevant interlock.
INTERLOCK_WENT	The interlocks automatically recovered; waiting for acknowledge.
MIXED	Units of the same kind are not all in the same stable state.
ERROR	General fatal error.
NO_CONTROL	Control is lost. After control is back, it should automatically go to the most appropriate state.

Table 3.2: The SPD FSM top-node states description.

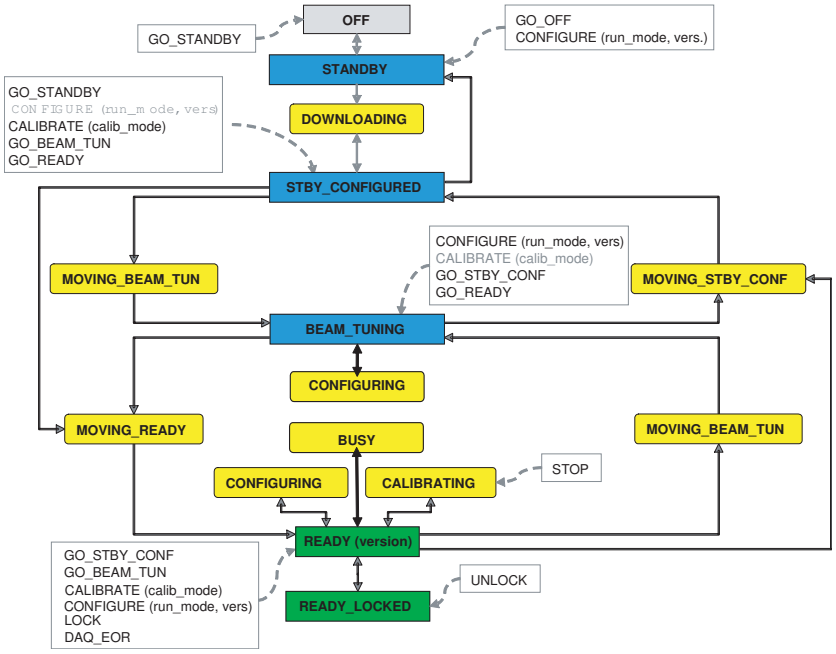

Figure 3.25: The SPD FSM top-node state diagram and action list.

3.4 Configuration Database (CDB)

The systems configuration is stored in an Oracle based Database named Configuration Database (CDB). The ALICE DCS group provides the infrastructure and the Db maintenance but it is the detectors responsibility the Db data management.
The SPD uses the CDB to store the off-detector electronics, on-detector electronics and the power system configuration. Hence the CDB is divided in two independent parts: the FERO CDB and the Power System CDB.
This section gives a general introduction to the CDB structure as well as a description of the FERO CDB client. This latter is a software component designed to manage the FERO DCB. It is introduced in this section because it is a general application used in various DCS components as described below.
My activity was designing and planning the general SPD CDB structure keeping in mind the specific SPD DCS needs.

3.4.1 The FERO CDB

The FERO Configuration Database stores the Router cards, LinkRx cards and HSs configurations. The database access policy described in section 3.2.1

foresees that the electronics configuration is performed via the FED Servers downloading the required information from the CDB. Each time a new configuration is required, the CDB should be updated and a new configuration version generated. Further the configure command specifying the version number is sent to the FED Servers. Hence, the Db has been designed to have a powerful versions schema and the minimum amount of data duplication over versions.

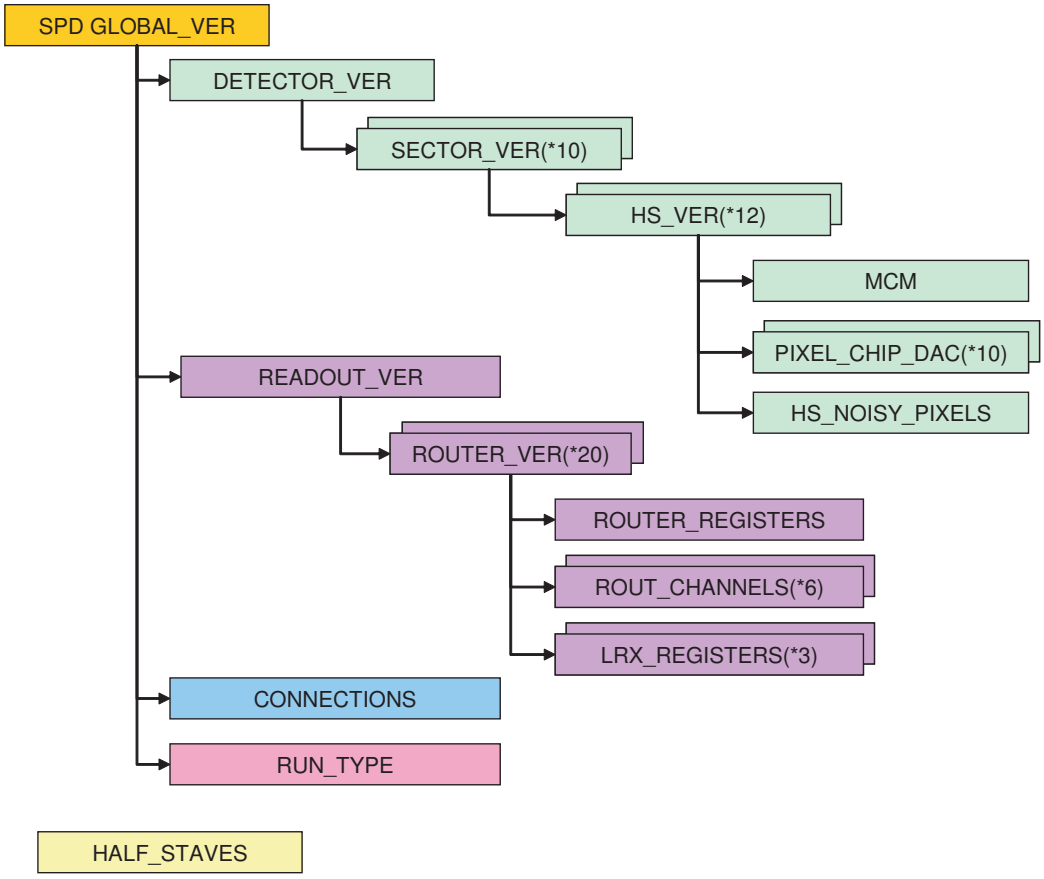

Figure 3.26: The FERO CDB table diagram.

The CDB hosts two families of tables: the data tables storing the actual configuration parameters and the version tables linking the data tables. Designing the Db has been used the intermediate version tables mechanisms that reduces the data duplication when only few parameters are changed and speed up the Db data query operations. This mechanism foresees to split the global version tables in a series of small sub-tables organized in a hierarchy. Using this structure the update of a data table propagates only to

the version tables of the corresponding hierarchy branch. The intermediate table mechanism drawback is the increase of the Db tables number, hence, the Db management and maintenances are more complex. However a series of studies have been carried out to optimize the FERO CDB structure in term of performances and complexity.
The FERO CDB schema has a detector oriented structure such as displayed in the CDB table diagram of Fig. 3.26. The FERO CDB hosts 1798 tables of which 157 version tables and 1641 data tables.

The top level configuration table, named SPD GLOBAL_VER, stores the global version number that is an integer incremented anytime a new version is generated. This table points to the detector version table (DETECTOR_VER), to the off-detector electronics version table (READOUT_VER), to the hardware connection table (CONNECTIONS) and to the RUN_TYPE table.
The CDB schema indeed has two main branches, respectively for the detector configuration and for the off-detector electronics configuration. This structure allows separating the two electronics blocks and accessing the data separately. Moreover the number of version tables to be either updated or read back during the Db I/O procedure is limited to the corresponding branch.

The DETECTOR_VER table points to the ten sector version (SECTOR_VER) tables. Each of these is pointing to twelve HS version (HS_VER) tables. The HS_VER table links to the actual HS configuration information organized in 32 tables. The MCM table stores the configuration to be loaded into the Digital Pilot, the Analog Pilot and the GOL. Ten Pixel Chips DAC (PIXEL_CHIP_DAC) tables contain information on the DAC to be downloaded on each HS Pixel Chip. In total 4400 DACs are stored in these tables. A HS_NOISY_PIXELS table has information on the noisy pixels identified on the HS. These parameters are used to mask the corresponding pixels during the detector run.
Each time an actual configuration table is updated the corresponding version tables at the upper level generate a new configuration version. The version generation is propagated up to the SPD GLOBAL_VER table.

The READOUT_VER table points to twenty Router cards version tables. Each of these are pointing to ten data tables where the actual configuration to be downloaded in the hardware is stored. The global Router cards reg-

isters parameters are hosted in the ROUTER_REGISTERS table whereas the information related to the Router card channels is stored in the six ROUT_CHANNELS tables. The three LRX_REGISTERS tables contains the LinkRx cards configurations.

The FED Server configures the components using their logical name such as described in section 4.3.6. If a hardware components connection swap occurs, the FED Server should be informed to redirect the configuration to the appropriate devices. The CONNECTIONS table establishes the link between actual hardware position and logical name associated to the component.
The table HALF_STAVES is a static table linking the HS position inside the detector (sector, side, HS number) and the HS production number. This information is not needed for the detector configuration however it is used as reference to link the SPD construction Db[4] and the CDB.

The FERO configurations are tagged in the CDB with a global version number. To any global version is associated also a tag defining the run type to which the configuration should be applied. The run type can be of e.g. p-p, Pb-Pb, CALIBRATION, etc. The RUN_TYPE table associates to each configuration version the mentioned tag.

The CDB client performing the Db update is responsible of the data and version management. In order to reduce the Db update time, the data tables are updated adding a new configuration line for each request in which the data are different by the last configuration. This procedure can generate a data duplication if the new version produced is equivalent to an old one. In order to avoid this problem a cleaning script can be initiated by the operator. This script checks for data duplication and delete them updating the version tables. Due to the CBD structure, the cleaning operation is very efficient and easy to be performed.
The CDB dimension is self-controlled and the only table that is never adjusted is the SPD GLOBAL_VER.
Two main tools have been designed to manage the FERO CDB: the CDB Interface (see section 4.3.7) and the FERO CDB client described in the next session.

[4]The construction Db stores the HSs history before integration on the detector. Moreover it keeps track of the HSs performance test results and the configuration files (see section 4.3.7 for more details on their use) produced during the modules assembly phases.

OM value	Operation to be applied in the CDB
0	The changes are applied to the version type associated to Version.
1	The information to be changed is retrieved by Version. The output is a new type defined by Run_Type.
2	The DAC update is applied to the old version tagged with Run_Types.
3	The changes are applied to all the type with the same Version tag.
Version: If >= 0 it is the global version number in the Db. If < 0 the HEAD version is taken.	
Run_Type: If >= 0 it is the value specified. If < 0 they are all Run_Types.	

Table 3.3: The CDB client operational parameters. The Operation_Mode define the operation to be accomplished whereas Version and Run_Type are used as additional parameters. Not all the parameters are used in all the modes.

3.4.2 The FERO CDB Client

The FERO CDB client is an application designed to connect and manage the FERO Configuration Db. It receives as input a series of files of type Configuration Data containing the parameters to be stored in the Db and it performs automatically the Db data update.
The application is built up of two main blocks: the Configuration Data file decoder and the CDB Interface (see section 4.3.7 for more details). The first block reads from a specific configuration file the list of the Configuration Data files to be used for the Db update. These files have the structure of .ini files. They contain the list of parameters to be updated in the Db and a series of command to the client. The CDB client, indeed, modifies the Db tables as function of three integer parameters: Operation_Mode (OM), Version and Run_Type. The Operation_Mode defines the actual operation to be developed whereas the Version and Run_Type are used as parameters. Tab. 3.3 describes the use of the three parameters.
The Configuration Data file decoder, using the files information, builds in memory objects of type *ActualConfiguration* (see section 4.3.2 for more details) and send them to the CDB Interface that performs the actual CDB update.

During the update procedure the new data are compared with the already stored in the Db. If changes are detected, a new configuration version is generated. If the tables specified do not exist, the client creates them inside the CDB. The CDB client has been also used to build up the Db structure. Moreover this client manages automatically the Db versions.
The Configuration Data file decoder appears as a static library as well as the CDB Interface. The application has been divided in two blocks to simplify the code maintenance and to re-use the same functions in different applications. For example, the CDB Interface is also used by the FED Server.
Another advantage of this two blocks structure is to maintain static interfaces; an upgrade of the CDB structure, requires only the upgrade of the CDB Interface and not of the full client. The same can be applied to the Configuration Data files structure change.
The CDB client can be used as independent application and it is already used by the FECS and by the FXS-CDB Connector (see section 5.2.1.2 for more details).

3.4.3 The Power Supply System CDB

The Power System stores in the CDB the power channels configuration such as voltages, currents limits, rump-up/dowm times, etc. This information is connected to the PSCS DPs of type CAEN channel.
The JCOP Framework group provides a package managing automatically the connection between PVSS DPs ad the CDB. This tool allows to groups DPs together in tables named recipes. Moreover this tool generate the corresponding table inside the CDB and it manages the recipes upload/download.
The PSCS uses two main recipes type: one for the LV channels and one for the HV channels as described in section 3.2.2. In total 360 recipes are stored in the CDB.

Chapter 4

Front-End Device (FED) Server

The on-detector and off-detector electronics require the control and monitoring online of $\sim$ 2000 parameters and $\sim$ 50000 DACs. Roughly $\sim$ 20 M should be configured and the detector performance are evaluated by means of $\sim$ 10 k calibration parameters. The electronics configuration and the detector calibration are two Front-End and Read Out Electronics Control System (FECS) fundamental tasks. Critical parameters such as detector temperature, cooling pressure, trigger data rates, etc. must be monitored online. Timing and data management ($\sim$ 6 GB of raw data for each calibration) are critical issues.

The communication between the control PCs and the front-end electronics is via VME. Hardware control drivers should be integrated in the control software. PVSS is designed for slow control applications therefore it is slow in controlling high speed electronics such as Router cards and the SPD front-end electronics. The FECS required functionality development would be too complex in PVSS and the application would not suit for the required tasks. The solution I proposed is based on an intermediate software layer acting as a bridge between the hardware and the PVSS interface. This application is named Front-End Device Server (FED Server). It is a C++ based stand-alone application able to run as service on a PC. The FED Server is platform independent and can be used either on a Windows or a Linux machine.
The FED Server is a fundamental component in the SPD DCS. Due to the strong interconnection between front-end electronics and services, without this software component the SPD would not be able to take reliable data. I entirely designed and developed the FED Server. After defining a series of requirements I proposed a highly modular and easy to upgrade server structure. For convenience I will explain the server specifications describing its structure and functionalities.

The FED Server has two global operation modes allowing hot-swap between each other: Manual Mode and Automatic Mode. The server decides automatically in which mode it should operate as function of the incoming instruction.
The Manual Mode transforms the FED Server in a driver. The clients, using this mode can access any hardware component sending specific access requests. The server manages the communication with the hardware and it returns the list of the requested parameters.
The Automatic Mode allows the clients to send to the FED Server only high level macro-instruction and the server itself manage the operation needed. The Automatic Mode hosts the detector calibration functions. Due to the operation complexity during calibration, it is not possible to perform them manually.
In the next sections more details on the FED Server internal structure and functionalities are reported.

4.1 FED Server Internal Structure

The FED Server is built up of three main software layers as shown in Fig. 4.1(a). The server top layer is a Communication Layer responsible of the communication between the FED Server and the clients such as the FECS PVSS and the DCS Online Data Analysis Tool (CDT) (see section 5.2.2 for more details).
The FED Server intermediate layer is an Application Layer hosting the logical server functions. It retrieves the commands received by Communication Layer , checks the hardware status, pulls or stores the data from/to the database and communicates with the Driver Layer to perform the required operations on the hardware. The FED Server state machine is hosted in the Application Layer.
The bottom server layer is the Driver Layer designed for the off-detector electronics VME access.
A communication example between the server layers is displayed in Fig. 4.1(b). In this case a client is sending a command directed to the hardware. The Communication Layer receives the commands and it checks the server status. When the server is free the command is forwarded to the Application Layer that communicates with the Driver Layer. The status reports are forwarded to the FED Server standard output and to the Communication Layer. This one produces the appropriate services to be sent to the clients. At the end of the commands the FED Server checks if there are automatic operation

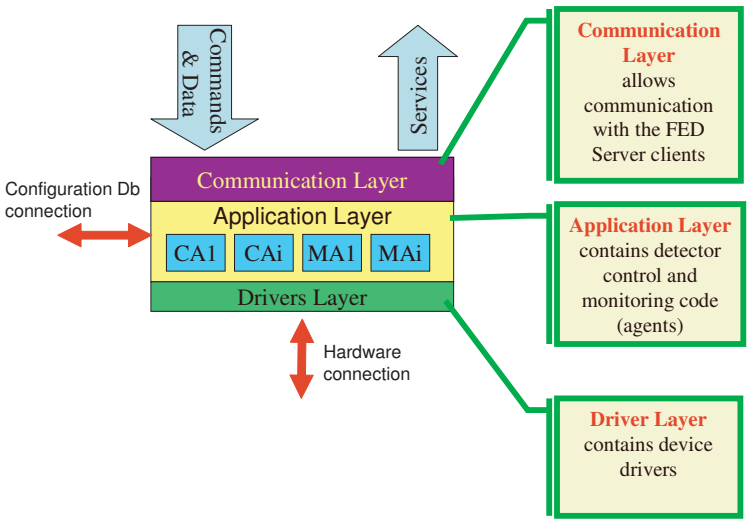

(a)

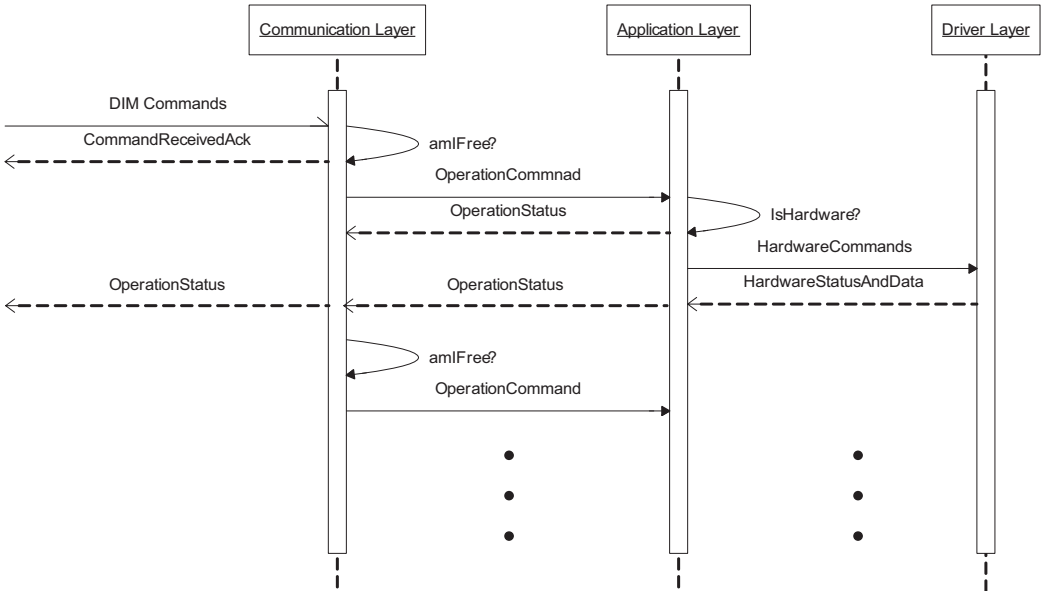

(b)

Figure 4.1: (a) The FED Server internal structure block diagram. (b) A sequence diagram showing a communication example between the FED Server layers. The Communication Layer receives a command and it controls if other procedures are already initiated. if not, it sends the command to the Application Layer . This latter decompose the instruction and forwards the commands to the hardware if needed. The status reports are forwarded either to the standard output or to the clients requesting the command. The cycle starts again.

to be developed and, in case of positive answer, it produces the appropriate Application Layer commands.
In Fig. 4.2 a detailed FED Server internal structure block diagram is shown; the main server subcomponents and their interactions are displayed.
The system structure allows fast remote operator intervention and it is highly modular.
In the next sections a wide description of the FED Server subcomponents will be given detailing the software subblocks functionalities. Due to time and space reasons, this chapter is not intended to describe all the FED Server functionality but it aims to give an overview on the server tasks and their actual development.

4.2 Communication Layer

The Communication Layer is the interface between the FED Server and the other DCS software components.
The FED Server is the only gateway to the detectors electronics and it must be able to accept multiple clients based on different operative system (i.e. Windows, Linux). The FED Server high RAM memory consumption during the calibration operations impose the limitation of having only the server running on a PC. An ethernet based TCP/IP protocol is required to communicate with the server host PCs. A Distributed Information Management (DIM)(see section 4.2.1 for more details) has been chosen as over IP server-client protocol. ALICE adopted DIM as standard communication protocol between FED Servers and CS clients. This communication protocol has been developed at CERN and it is widely used in many HEP experiments. DIM is light TCP/IP protocol and it has easy to implement interface. It has been chosen DIM because suits well with the system specification and allows many users to monitor the communications.
The Communication Layer is based on a DIM Server connected to a decoding class to convert the incoming commands to FED Server Application Layer instructions. The DIM Server accepts two command channels and issues three services. The synchronization between these five elements is performed inside the Communication Layer itself.

4.2.1 The Distributed Information Management (DIM) protocol

DIM is a communication system for distributed/mixed environments, it provides a network transparent inter-process communication layer.

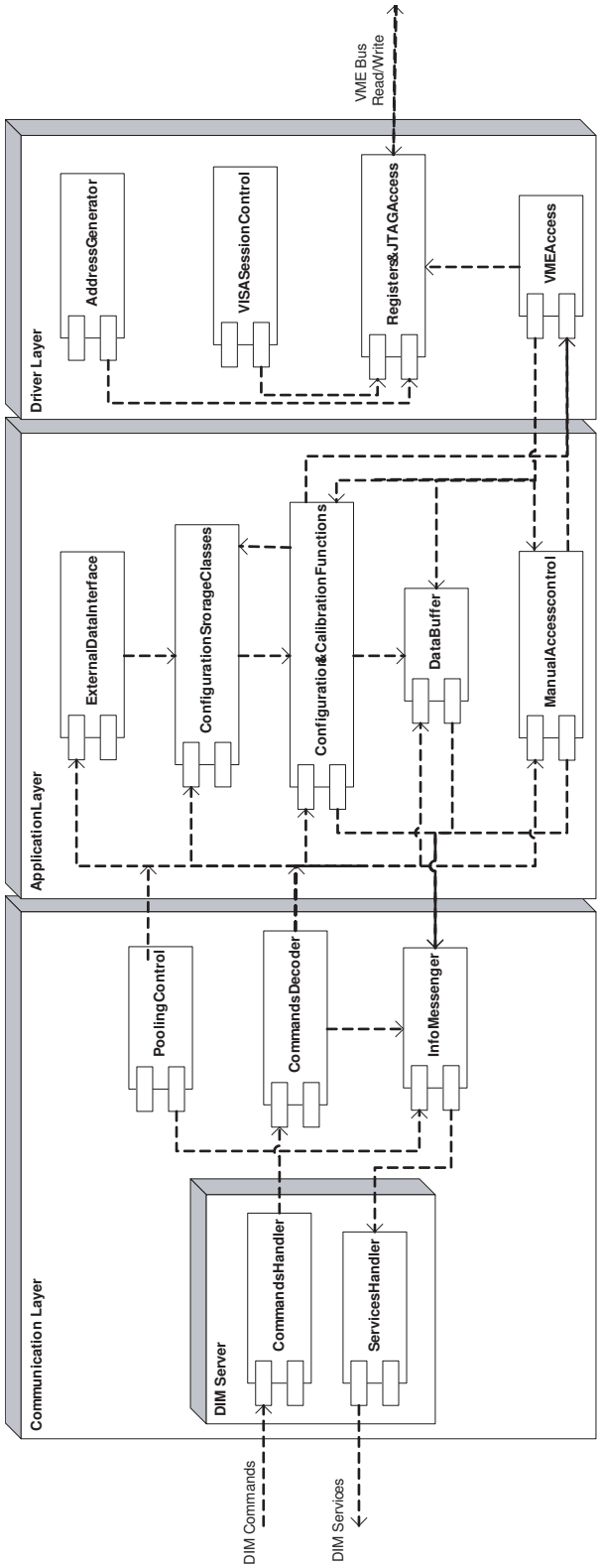

Figure 4.2: The FED Server structure block diagram.

DIM is based on the client/server paradigm. The basic concept in the DIM approach is the concept of "service". Servers provide services to clients. A service is normally a set of data (of any type or size) and it is recognized by a name (named services). Services are normally requested by the client only once (at startup) and they are subsequently automatically updated by the server either at regular time intervals or whenever the conditions change (according to the type of service requested by the client).
The client updating mechanism can be of two types, either by executing a callback routine or by updating a client buffer with the new set of data, or both. In fact this last type works as if the clients maintain a copy of the server data in cache, the cache coherence being assured by the server.
In order to allow for transparency (i.e. a client does not need to know where a server is running) as well as to allow for easy recovery from crashes and migration of servers, a DIM Name Server (DNS) was introduced.
Servers "publish" their services by registering them with the name server (normally once, at startup).
Clients "subscribe" to services by asking the name server which server provides the service and then contacting the server directly, providing the type of service and the type of update as parameters.
The name server keeps an up-to-date directory of all the servers and services available in the system. The Fig. 4.3 shows how DIM components (Servers, Clients and the Name Server) interact.

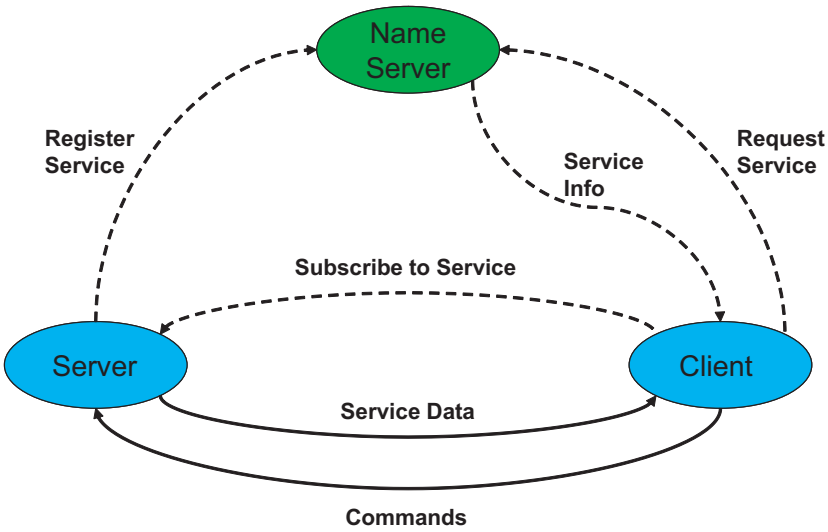

Figure 4.3: DIM elements communication diagram. The dashed lines are present only at startup or after a server/client restart.

Whenever one of the processes (a server or even the name server) in the system crashes or dies all processes connected to it will be notified and will reconnect as soon as it comes back to life. This feature not only allows for an easy recovery, it also allows for the easy migration of a server from one machine to another (by stopping it in the first machine and starting it in the second one), and so for the possibility of balancing the machine load of the different workstations.
The DIM system is currently available for mixed platform environments comprising the operating systems : VMS, UNIX, Linux, and Windows NT. It uses as network support TCP/IP.
The differences in data representation (e.g. byte ordering, floating point format, data alignment and data type sizes) over different machines are automatically (transparently) negotiated between the server, the client and the name server. All DIM functionality is available as server and client libraries providing C++ callable interfaces.

4.2.2 FED Server - clients communication schema

The FED Server-clients communication is an asymmetric handshake. In the following sections the command and services structure will be described in more detail whereas in this section is reported the basic FED Server- clients communication structure.
In order to understand the needs of the communication schema developed is important to bear in mind that the FED Server develops in parallel on-demand and automatic detector control/monitoring functions (more details in section 4.3). The FED Server clients can either send simple commands triggering the start of an operation or send complex commands with embedded data for the FED Server and detector. Moreover the command received and command execution status acknowledge is needed by the clients to define concluded the requested operation. In many cases the FED Server sends status information without a prior request by the clients. Commands have different execution priorities (e.g. Temperature monitor has higher priority than the Pixel Chip DAC settings) and the FED Server manages automatically the sequence. Moreover the FED Server published information is desynchronized respect to the clients requests.
The reasons explained up to now brought to the need of a communication schema such as shown in Fig. 4.4. Few FED Server-clients communication examples are displayed in this sequence diagram.

The various operative scenarios described above are implemented sending FED Server commands with a fixed structure in which is contained also a

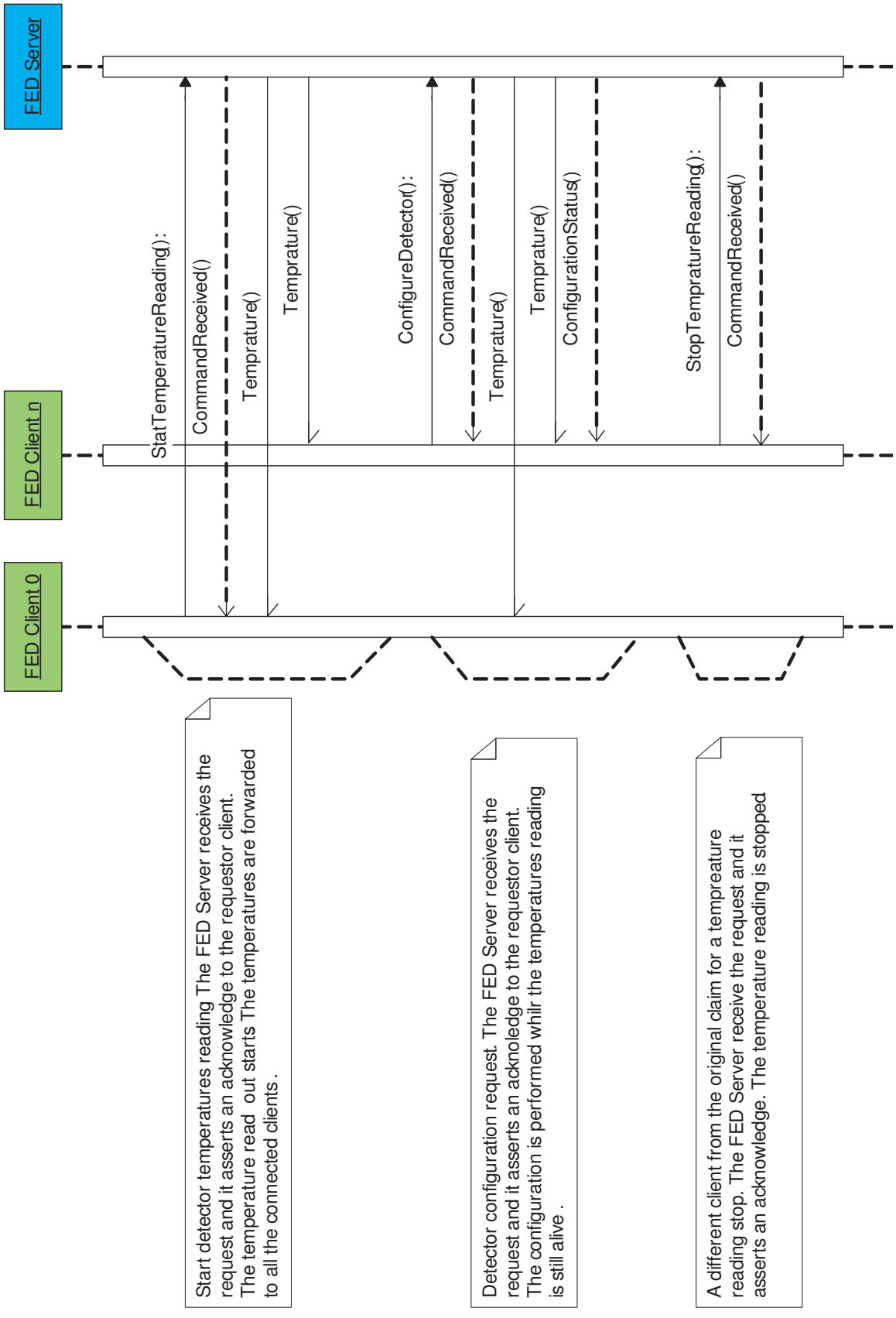

Figure 4.4: Few FED Server-clients communication examples.

command ID. The command ID is stored inside the FED Server and it is returned with a command execution status acknowledge. The data produced by the FED Server executing a command have the same incoming ID. The ID is 32 bits long, and bit 31 is reserved to the FED Server. When the ID bit 31 is 1 (negative integer) the information returned by the FED Server is the result of an automatic server procedure.
The FED Server locates the on-detector electronics and the off-detector electronics components using a channel number schema described in section 4.3.6. However, in order to understand the following sections, is important to bear in mind that the channel number is the Half-Stave number ($0 \div 119$). All instructions with a channel number higher that 119 are considered oriented to all the active detector components. The FED Server computes automatically,using the channel number, the address of the hardware components with different modularity than channel (e.g. Router cards and LinkRx cards).
Many clients can send in parallel commands to the FED Server and the servers answers publishing services in parallel.
In the next paragraphs the commands and services structures are described.

4.2.3 FED Server (DIM) Commands

The FED Server receives two command channels: one for the PVSS clients whereas the other for the DCS Online Data Analysis Tool clients (see section 5.2.2 for more details). The command structure is identical between the two channels. The separation has been applied to avoid the overload of detector calibration data on the control channel. The DCS Online Data Analysis Tool communication channel has less priority than the PVSS channel.

A FED Server commands structure is defined such as displayed in Tab. 4.1. The first element is the size of the entire command block while the second element is a unique ID following the rules described in the previous section. The command block has a variable length depending by the data transfer required.

32 bit word n	Content
0	Block Size
1	ID
2	Channel
3 - 23	Command
24 - End	DATA

Table 4.1: The FED Server commands structure.

Degeneration			Full Command
Main level	First level	Second level	
HSCNF_	API_	SETDAC	HSCNF_API_SETDAC
	PXDAC_	DEFAULT	HSCNF_PXDAC_DEFAULT
		ALL	HSCNF_PXDAC_ALL
		CH	HSCNF_PXDAC_CH

Table 4.2: An example of FED Server commands. HSCNF_ is the root for the Half-Stave configuration commands. API_ means that the command is oriented to the Analog Pilot while PXDAC_ refers to the Pixel Chip DACs. The second degeneration level is the actual operation to be developed, e.g. SETDAC requests the server to load in the DAC the parameters sent in the instruction DATA block.

A string of 20 characters is sent as Command. The sting is user friendly and intuitive respect to the instruction required. It is composed up to three main instruction parts with degeneration levels. Tab. 4.2 shows an example of command whereas at [34] the full list of commands with a detailed operation description and DATA structure is reported.

The last FED Server instruction block is the DATA. This field has dynamic length and varies its structure depending by the Command required. This dynamic structure allows a reduced network and communication bandwidth because only the needed information is transmitted. In instructions in which data are not required, this field is omitted.
The FED Server keeps in memory the DATA block that is overwritten only when a next instruction with DATA block is issued. This operation mode allows the clients sending only once the DATA block in case of repeated commands with the same DATA information.

4.2.4 FED Server (DIM) Services

Four DIM services are produced by the FED Server and they are sent in parallel to all the clients subscribed to them. One service returns the instruction data and execution status to the PVSS clients whereas a second service communicates with the DCS Online Data Analysis Tool clients. A third service is used to transfer the detector readout data the DCS Online Data Analysis Tool. The data block transferred in this last case requires high bandwidth and a dedicated service has been issued for it. The last service sends a flipping bit every 5 seconds and it is used by the clients to monitor whether the server is alive.
The services have the structure described in Tab. 4.3. The first element is

32 bit word n	Content
0	Block Size
1	ID
2	Status
3	Channel
4 - 24	Command
25 - End	DATA

Table 4.3: The FED Server services structure.

the service block size while the second element is the command ID. It corresponds to the ID of the command performing the operation request. In case of automatic FED Server operation the ID is a negative integer.

The Status is a code defining the command execution status. In normal execution it is 0. At [34] the full errors list is reported.
Channel has the same definition described in the previous section. In the services a 20 characters string, Command, is present and it describes the operation executed. It is equivalent to the Command issued to the FED Server. This characteristic allows the clients to have an easy command coding, decoding structure.
The last information block in the services is the DATA. It has dynamic length and the information structure is depending by the Command. The services have a structure very close to the commands one. This characteristic has been kept for simplify the communication and the information coding/decoding.

4.2.5 The Communication Layer structure

The FED Server Communication Layer is a static library composed of 4 main objects. The Fig. 4.5 diagrams show the Communication Layer elements and their basic interaction.

A DIM Server is instantiated as singleton containing a *CommandsHandler* to retrieve the incoming data and a *ServicesHandler* to publish the services. The received commands are pushed to a *CommandsDecoder* that uses the Command field to address the required function in the FED Server Application Layer. Whenever an automatic server function is required, the *CommandsDecoder* forwards the appropriate request to the *PoolingControl* block. A singleton *InfoMessenger* is the FED Server operation status logger. It is accessible from all the internal server functions and it is used to publish status report, operation executions and data. The *InfoMessenger* forwards the information either to the standard output or to the *ServicesHandler* (or

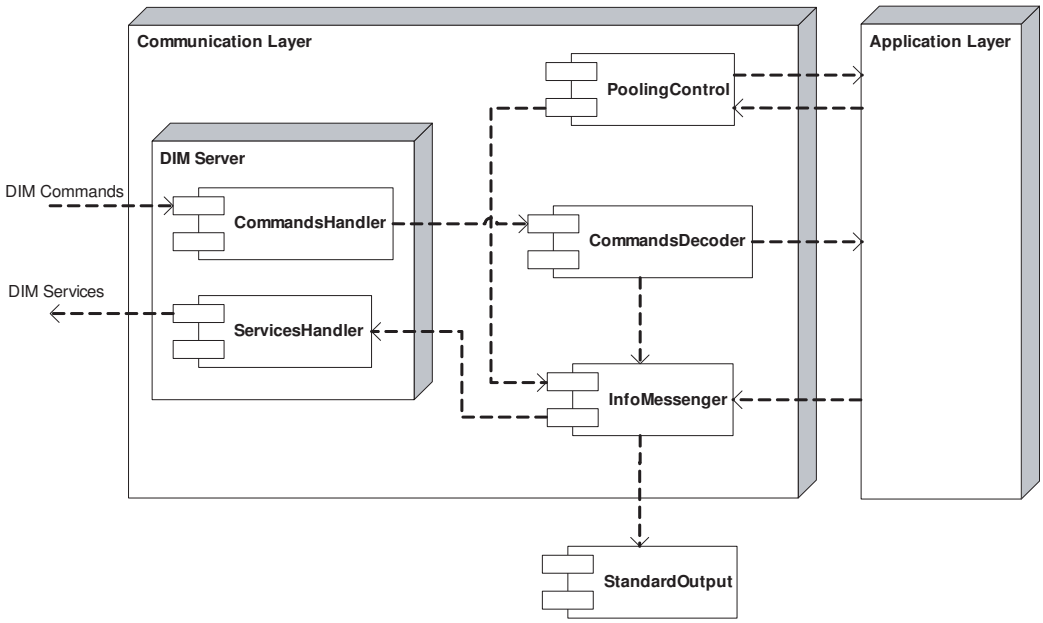

(a) The FED Server Communication Layer component diagram.

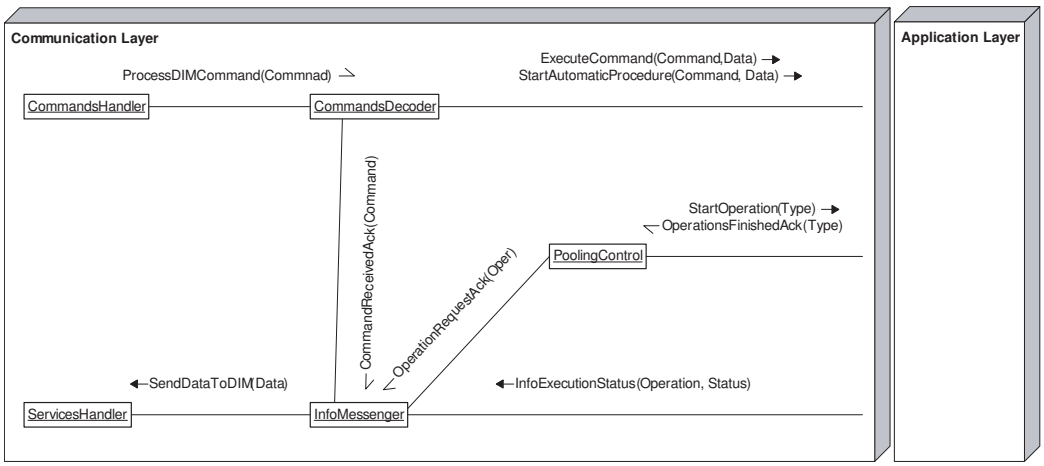

(b) The FED Server Communication Layer collaboration diagram.

Figure 4.5: The component diagram (a) shows the internal Communication Layer blocks whereas the collaboration diagram (b) displays the main communication between the components.

both) as function of the information type.
The Communication Layer hosts a *PoolingControl* object managing automatic and cyclical operations such as temperature reading, Router cards memory reading, calibration routines, etc. The automatic FED Server functions control is shared between the Communication Layer and the Application Layer. Complex FED Server operations are divided in steps inside the Application Layer. At the end of each operation step, the control is returned to the *PoolingControl*. It loops through the various requests and it decides whether to execute a further step in the initiated complex operation or to execute other operations before re-establish the complex operation normal flux. This structure allows the FED Server to be multitasking and to react quickly avoiding the waiting time of long operation return.
The Communication Layer design concept allows also simplifying the Application Layer code structure. In this second layer indeed are hosted smaller functions called cyclically by the Communication Layer. Moreover the main concept idea in the Communication Layer design is to substitute the operator. The *PoolingControl* and the *CommandsDecoder* act as an operator calling sequentially Application Layer functions to perform the required task. The Communication Layer only calls Application Layer functions and process their returns. The full FED design allows replacing easily the Communication Layer with another interface without modifing the Application Layer and the Driver Layer structure.

4.3 Application Layer

The Application Layer is the FED Server logical core where the control, monitoring and calibration functions are performed. The component design requires high modularity in order to simplify the FED Server maintenances and updates. The performance of this layer such as speed and memory occupancy are critical issues in the full architecture design. Moreover the Application Layer is the first level of FE electronics smart control. Low performances of this component have drawback on the full Front-End CS.

A simplified Application Layer component diagram is displayed in Fig. 4.6. This diagram represents only the main logical blocks hosted in the layer.
An Application Layer collaboration diagram is displayed in Fig. 4.7. The diagram entry point is the Communication Layer whereas the exit point is the Driver Layer. The communication with the hardware is performed via VME bus allowing only sequential access. This constraint brings the Application Layer logical structure to be diamond shaped and timed by the Communi-

cation Layer using the *PoolingControl* and the *CommandsDecoder*.
The Communication Layer sends operation request messages to the Application Layer components and they are responding asynchronously with the operation execution status and eventually with data. At the end of each Application Layer operation the control is returned to the Communication Layer.
The next sections are reporting a more detailed Application Layer blocks description and they give information about the various elements interaction.

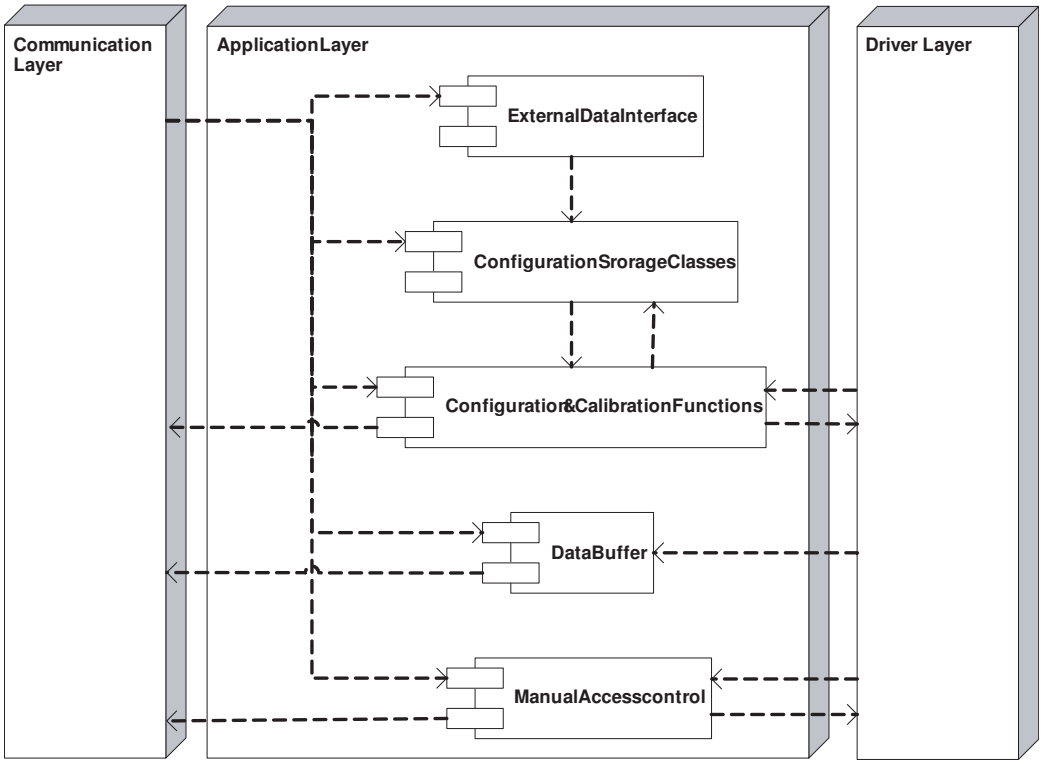

Figure 4.6: The Application Layer component diagram. This is a simplified version representing only the main logical blocks.

4.3.1 *ManualAccessControl* and *AutomaticConfFunctions*

The FED Server can be operated in two global modes: Automatic and Manual. In the Automatic Mode the Application Layer develops automatically complex functions and it computes the required steps to satisfy global requests. In the Manual Mode the FED Server behaves as a driver and the

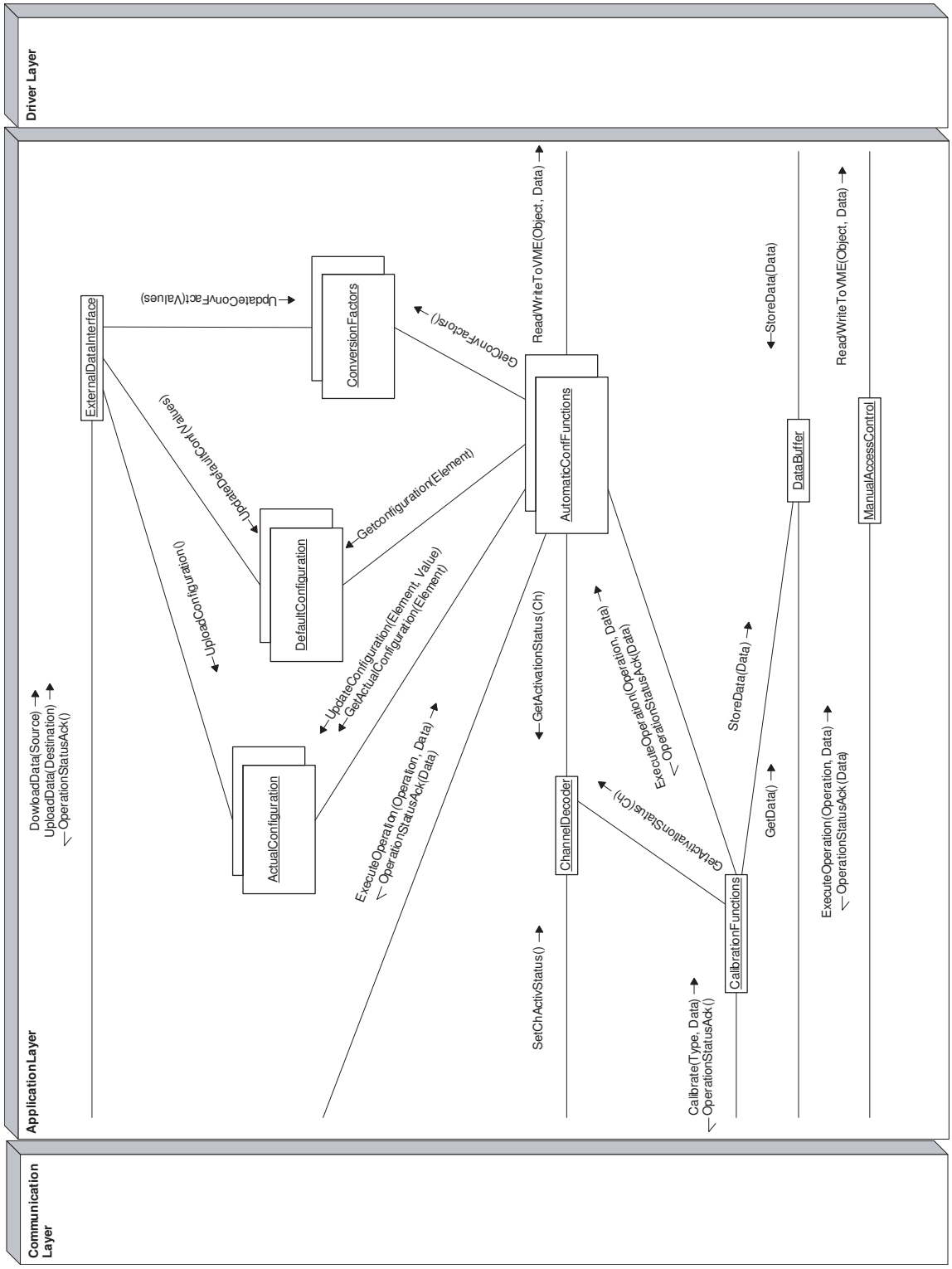

Figure 4.7: The Application Layer collaboration diagram.

Application Layer acts as a translator between the DIM Server commands and the Driver Layer commands.

The *ManualAccessControl* decodes the information coming from the Communication Layer and it calls the appropriate Driver Layer functions. In Manual Mode the FED Server clients produce the JTAG streams and the configuration parameters to be loaded inside the off-detector electronics registers. This information is sent to the FED Server as data field of the commands (see section 4.2.3). The server Communication Layer forwards directly the commands to the *ManualAccessControl* that extract the appropriate parameters to be sent to the Driver Layer.
The Manual operation mode is useful during debug phases and to extend functionality not implemented in the FED Server. The drawback is the speed of operation execution. In this case the operation load, normally taken by the FED Server, is forwarded to the clients. The communication between server and clients add a strong contribution to the operational time. Moreover the *ManualAccessControl* does not update the storage classes containing the actual configuration (see section 4.3.2). The management of these elements relapses on the FED Server clients.

The *AutomaticConfFunctions* are logically represented in Fig. 4.7 as a unique element but their functions are actually scattered over various implementation classes. They contain high level methods capable of retrieving automatically the configuration information and to perform the required Driver Layer function calls to configure and monitor the hardware. The *AutomaticConfFunctions* elements can be divided in four main groups:

The on-detector electronics configuration methods are designed to configure the detector using JTAG. The detector elements to be configured are the Pixel Chip DACs, the Analog Pilot, the Digital Pilot and GOL configuration registers. Moreover these methods allow the test pulse setting and the pixel masking along the pixel matrices. A specific method has been designed for each element described above. They are able to retrieve automatically the configuration parameters, define the hardware structure (the JTAG chain can be modified as described in section 2.1) and compute the JTAG streams to be forwarded to the Driver Layer. It is possible to perform the configuration either of all the Pixel Chip of a HS or only a selective subset of them.
The configuration methods check also the HS activation status (see section 4.3.6 for more details) before operate and they embed also a read back function to verify the configuration consistency after the proce-

dure. An error report is issued to the Communication Layer when any of the above condition is not respected. The methods, in normal conditions, return the actual read back configuration values that are stored in the *ActualConfiguration* classes.
The configuration methods can operate in three modes as function of the configuration parameters source. Tab. 4.4 establish the link between operation mode and configuration parameters sources. Fig. 4.8 on page 108 displays a communication example between the *AutomaticConfFunctions* and the *ActualConfiguration* / *DefaultConfiguration*.
The methods described up to now are designed to configure a HS component. The *AutomaticConfFunctions* host also global methods to configure either the full detector or the full HS at once. This last methods family calls recursively the primitive methods described above.

Operation Mode	Configuration Parameters Source
Refresh	*ActualConfiguration*
Default	*DefaultConfiguration*
Command	Incoming commands DATA field

Table 4.4: The configuration methods operation modes.

The off-detector electronics configuration methods operate as the on-detector electronics configuration methods. In this case they are producing configuration registers values to be written inside the Router cards and LinkRx cards.

The monitoring methods are designed to monitor the on-detector electronics and off-detector electronics status. This set of methods reads the Router cards and LinkRx cards status registers and it identifies the operational status. The detector temperature monitoring is also carried out by this set of methods. The *AutomaticConfFunctions* allow sending out the temperatures either as ADC digital value (see section 2.1) or as already converted temperature. A third operation mode is the sending of the temperature only when a threshold is passed. The information for the temperature conversion and the thresholds to be applied is automatically retrieved by the *ConversionFactors*.
A monitoring method is able to identify if the HS JTAG chain has been modified due to a malfunctioning HS chip.
The monitoring methods are designed to apply only once the specified

request. In case of continuous monitoring, these methods should be called by an external component. In the FED Server case the synchronization is performed by the Communication Layer.
The methods described are designed to operate on a single hardware component. The *AutomaticConfFunctions* host also global methods to monitor at once the full FE hardware system. These methods check the channel activation status and call recursively the basic functions described above.

The detector triggering methods are designed to forward a triggering sequence to the electronics. They are mainly used during the calibration procedures and when the DCS emulates the trigger system.

The *AutomaticConfFunctions* retrieve from the *ChannelDecoder* the list of electronics components on which they should operate (see section 4.3.6 for more details).

4.3.2 *DefaultConfiguration* , *ActualConfiguration* and *ConversionFactors*

The hardware configuration and calibration can be performed automatically by the FED Server that needs to know the configuration parameters to be downloaded in the electronics and the actual electronics status. These configuration parameters are stored in a series of classes grouped in two main logical groups: *DefaultConfiguration* and *ActualConfiguration*. The two groups have the same structure containing 120 objects of type *HSConfiguration*, 20 objects of type *RouterConfiguration* and 60 objects of type *LinkRxConfiguration*.
The *HSConfiguration* class contains the DACs setting for the 10 Pixel Chips, the Analog Pilot and the configuration registers of Digital Pilot and GOL. In this class it is also stored the masking and test pulse configuration associated to a HS pixel matrices. The *HSConfiguration* keeps track of the HS chips included in the JTAG chain (*ChipsInChain*). This information is fundamental to compute the JTAG stream generated for the detector configuration and monitoring. The *DefaultConfiguration ChipsInChain* list is used as starting list for the computing operation. The *AutomaticConfFunctions* are updating *ChipsInChain* online.
RouterConfiguration and *LinkRxConfiguration* contain the Router cards and LinkRx cards configuration registers values needed for the detector operation (see section 2.2 for more details).

The *DefaultConfiguration* stores the configuration parameters downloaded from either the database or the configurations files. This element remains in memory and it is modified only by the *ExternalDataInterface*. When the FED Server Communication Layer performs the update requests, the *ExternalDataInterface* loads in the *DefaultConfiguration* the appropriate configuration parameters.
The *ActualConfiguration* stores the actual on-detector electronics and off-detector electronics configuration. It is modified when either a configuration or a structural change is applied to the electronics. *ActualConfiguration* is updated every time an *AutomaticConfFunctions* readout operation is performed and concluded positively (the readout procedure is also embedded in each configuration procedures). However when a reset is applied to the electronics using the *AutomaticConfFunctions*, the *ActualConfiguration* loads the default electronics settings (not the *DefaultConfiguration* values but the real electronics defaults values).
The FED Server can sore in the Configuration Database a snapshot of the actual detector configuration. When the request is performed by the Communication Layer, the *ExternalDataInterface* forwards to the Db the information stored in the *ActualConfiguration*.
The communication between the *DefaultConfiguration* and the *ActualConfiguration* is performed only via the detector.
The sequence diagram of Fig. 4.8 shows few operational examples in which the storage classes are involved.

As described in section 4.3.1, the FED Server can monitor online the detector temperatures and voltages reading dedicated Router cards registers (see section 2.2 for more details). The information retrieved has the format of Analog Pilot ADC values (see section 2.1 for more details). A series of studies performed in the Analog Pilot test bench demonstrated that different Analog Pilots can have different ADC value-temperature and ADC value-voltage conversion factors (few mV from one Analog Pilot to another). During the detector commissioning has been compiled a conversion table for each Analog Pilot. The *ConversionFactors* contain 120 lookup tables with the conversion parameters and the alarming thresholds to be set inside the Router cards and FED Server. The *ConversionFactors* are static objects updated only by the *ExternalDataInterface* when the Communication Layer performs the request.

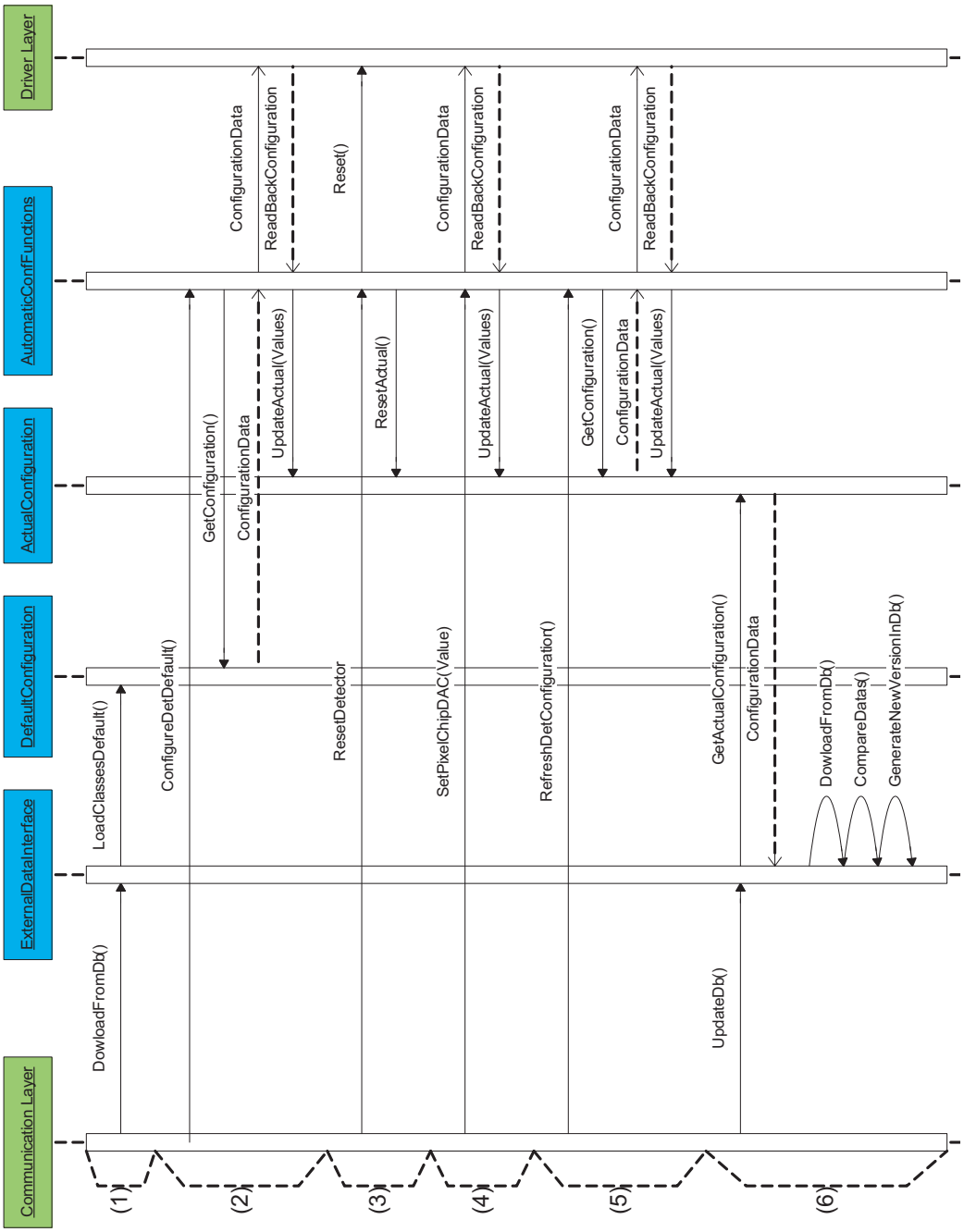

Figure 4.8: The sequence diagram displays few examples in which the storage classes are involved. (1) is a downloading from the database request of the electronics configuration parameters. (2) is a electronics configuration request using the default configuration parameters stored either in the Db or in the configuration files. (3) is a reset electronics request. In this case the electronics default parameters are loaded in the *DefaultConfiguration*. (4) is an example of Pixel Chip DAC configuration where the parameters to be set are specified by the users. (5) is a refresh of the detector configuration. In this case the *ActualConfiguration* parameters are loaded into the electronics. (6) an electronics configuration snapshot is saved to the Db.

4.3.3 *DataBuffer*

The SPD data produced during readout phases are gathered by the Router cards. The Router cards allow forwarding the data collected to the ALICE DAQ, to VME bus or to both of them (see section 2.2 for more details). The Router card operational mode used to forward the data to the VME bus is named data spy mode. This mode is useful during the detector debug and calibration phases.
In data spy mode the data are temporary stored in a 2 MB Router cards Dual Port Memory (DPM) ($\sim$ 100 readout events with 2 % occupancy). The FED Server is liable to read back the data stored and clean the Router card memory. These operations require high performances in term of reading speed and computer memory. The data indeed should be removed by the Router cards memory as fast as possible in order to prevent the memory full condition. This state triggers the busy of the electronics with the consequent stop of the full triggering and readout system. Hence, the trigger rate would be strongly strongly affected. One of the main issues during this operation mode is to assure the detector control also during the data fetch. The achievement of this goal requires a tight synchronization of the various FED Server internal blocks.

The *DataBuffer* is a software data buffer explicitly designed for high speed data push and low memory occupancy. Its core is a concatenate list of memory location pointers generated inside the FED Driver Layer. The Driver Layer reads the Router cards DPMs event by event and attach at the beginning of each event a header, named *Data Header*, with a structure described in Tab. 4.5. The data block formed by merging the DPM data block and the *Data Header* is named *Data Stream*. The *Data Stream* pointer is stored inside the *DataBuffer* as a single element of the concatenate list. The *Data Header* avoids the needs of a random access to the data blocks and it allows the use a light First Input First Output (FIFO) interface. The *DataBuffer* interface accepts and returns only *Data Stream* pointers and a specific configuration flag in the interface set the automatic *Data Stream* deletion after readout.

The implementation described avoids the computing overhead added by data copy and the memory consumption of a more complex structure than a FIFO (average memory overhead = 0.1% event size). The *Data Header* moreover releases the FED Server from the event building capability such the data merging of different Router cards produced during a unique event. The data clients indeed receive in the *Data Stream* the required information

32 bit word n	Content
0	Block Size
1	Router card number
2	DataType (0 = normal data, 1 = DAC Scan, 2 = TP Scan, 3 = Matrix)
3 - 18	at 0, reserved for *Calibration Header*

Table 4.5: The *Data Header* structure.

to perform the event building offline. The FED Server, in this condition, can read DPMs data as function of the various DPMs occupations and not respecting a sequential router schema. This structure increases the FED Server performance delegating to the client the data reconstruction functions.

The *DataBuffer* dimension is limited only by the operative system memory space reserved to the application and by a setting (max number of events in the buffer) inside the FED Server. Performance tests showed that the FED Server can run with a *DataBuffer* of 1.5 Gb on a WindowsXP PC with 2 Gb of RAM installed.

4.3.4 FED Server blocks synchronization during data acquisition and calibration

The synchronization between the Application Layer blocks involved in the FED Server data acquisition is a critical issue, indeed, the FED Server should be able to perform data readout without loosing its monitoring and control functionality.
In Fig. 4.9 a sequence diagram shows the synchronization. The Communication Layer issues a data readout start command and it retrieves, synchronously, the data from the buffer when a client performs a request. The *PoolingControl* allocates a time slot for the Router cards data fetch procedure and issue the correspondent command. When the Driver Layer returns, the *PoolingControl* checks whether other operation are required. When the *PoolingControl* is free again, it sends again the data fetch command. This operation is repeated cyclically up to when a data readout stop is asserted by any clients.

The FED Server can perform the detector calibrations emulating the DAQ system (see 5.2.2 for more details on the calibration procedure). During this operation mode a specific readout data management is required; it is mandatory the synchronization between the data retrieved and the specific detector

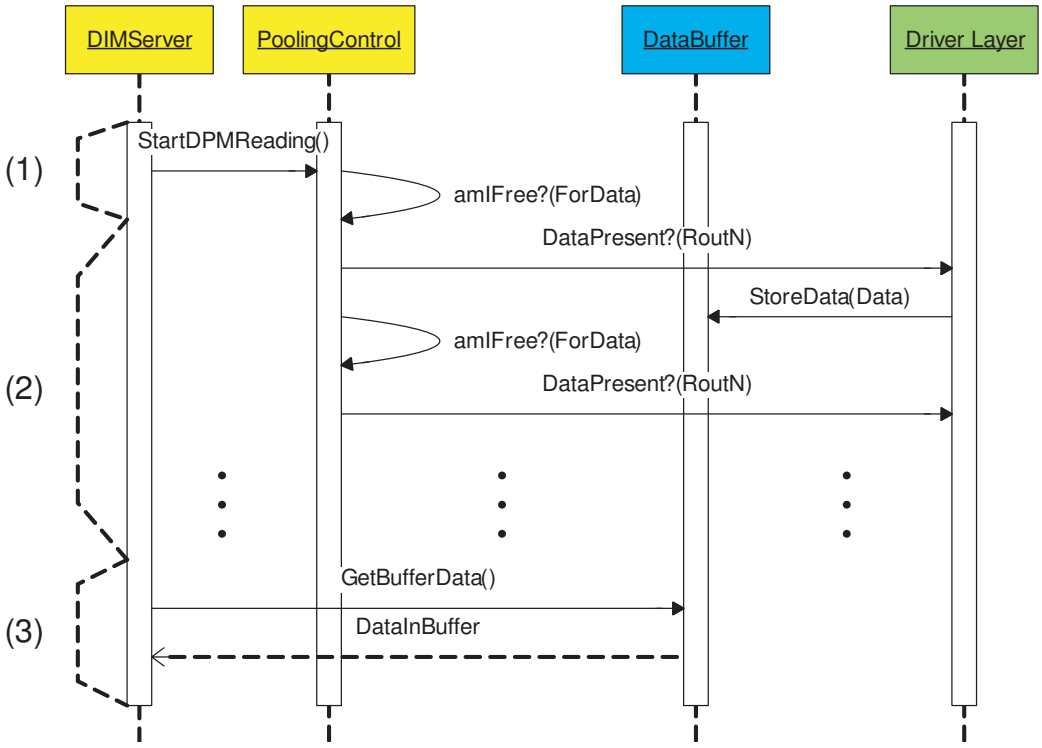

Figure 4.9: Sequence diagram showing the data readout procedure from the Router cards . In this diagram the Communication Layer is considered composed of only 2 elements (yellow): the DIM Server and the *PoolingControl*. The command of start data fetch is forwarded to the *PoolingControl* (1). The data fetch sequence (2) is repeated cyclically. The data readout (from buffer) command (3) can be asserted asynchronously anytime.

configuration.

In Fig. 4.10 a schematic sequence diagram displays the Application Layer blocks synchronization during the calibration procedures. The DIM server sends the calibration start command specifying the type of calibration and the calibration parameters. The *PoolingControl*, when free, gives an operative time slot to the *CalibrationFunctions*. These functions, using also the *AutomaticConfFunctions*, perform the detector configuration, send detector triggers and fetch the data from the Router cards when any are present. The *Data Stream* pointer produced by the Driver Layer is returned to the *CalibrationFunctions* that are adding the detector configuration information needed for the data analysis. The *Data Header* contains indeed free cells to be filled by the *CalibrationFunctions*. The *CalibrationFunctions* are then pushing the *Data Stream* inside the *DataBuffer*.

As it has been described in the previous sections, the *PoolingControl* is the main actor in the synchronization procedure. It decide when allocate time slots to the data readout and to the calibration procedures.

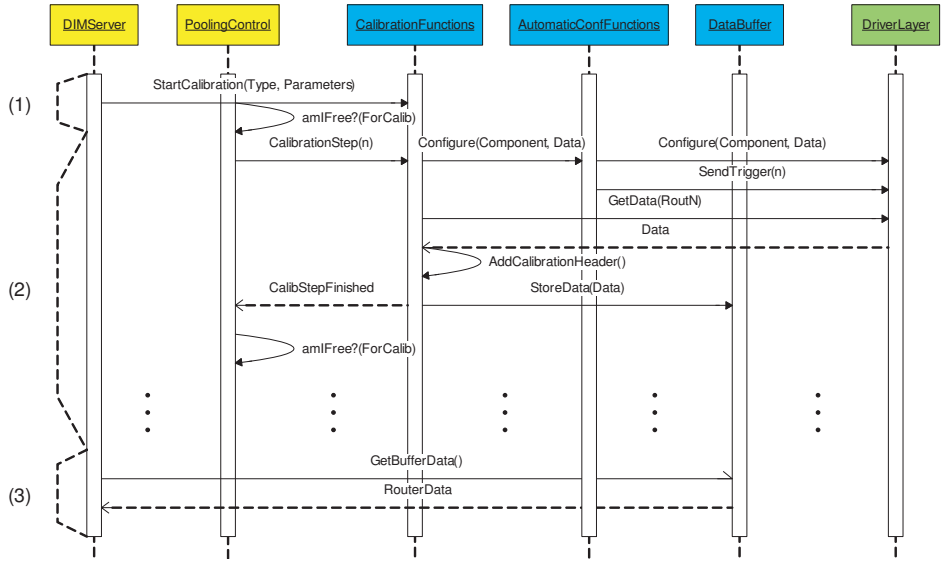

Figure 4.10: A simplified sequence diagram of the Application Layer blocks synchronization during the calibration procedure. The FED Server emulates the DAQ. In this diagram the Communication Layer is considered composed of only 2 elements (yellow): the DIM Server and the *PoolingControl*. The Application Layer is composed of 3 elements (blue): *CalibrationFunctions*, *AutomaticConfFunctions* and*DataBuffer*. The start calibration command is forwarded to the *CalibrationFunctions* (1). The calibration steps (2) are repeated up to the end of the procedure. The data readout (from buffer) command (3) can be asserted asynchronously anytime.

4.3.5 *CalibrationFunctions*

The FED Server is able to perform automatically the detector calibration and in chapter 5 the detector calibration procedures are described. The calibrations require the cyclical change of on-detector electronics and off-detector electronics configurations therefore the FED Server is the only system component able to perform the required tasks autonomously and in a short time[1]. The calibration procedures implemented in the FED Server are:

[1]An average calibration time using the FED Server is of $\sim$ 10 minutes. The use of PVSS to perform the same task would multiply of a factor 10 the operation time.

- Pixel Matrix Response Uniformity Scan;
- Mean Threshold Scan;
- Generic DAC Scan;
- Minimum Threshold Scan;
- Noisy and Dead Pixel Identification;
- Delay Scan;
- Fast-OR Characterization;

In order to clarify the *CalibrationFunctions* operation in this section the Pixel Matrix Response Uniformity procedure is taken as example. The FED Server operational concept is equivalent for all the calibration procedures implemented. In this example it is required to load the TP in one of the pixel matrix rows and perform a series of readout sequences. The operation must be repeated for all the 256 pixel matrix rows and for all the 1200 detector Pixel Chips. The full calibration time is of 10 minutes in this case. The FED Server cannot loose its detector monitor functionality for such a long time. The *CalibrationFunctions* divide the full calibration procedure in small steps and in this case the step correspond to configure the TPs in the detector pixel matrices and perform the triggering sequences.
When the start of calibration is requested, a calibration active flag is set inside the *CalibrationFunctions*[2]. The *PoolingControl* calls recursively the *CalibrationFunctions* and if a calibration active flag (or many) is found, the *CalibrationFunctions* perform the appropriate calibration step. The number of calibration steps accomplished is increment and the control is released to the *PoolingControl*. It decides if either continue the calibration procedure or develop other operations in the meantime. The *CalibrationFunctions* reset the appropriate calibration active flag when the number of steps needed for the calibration procedure is reached.
Fig. 4.10 shows a sequence diagram of a generic calibration procedure in which the FED Server emulates the DAQ. The part of the data retrieval and storage in the buffer is missing when the FED Server does not emulate the DAQ. In this FED Server operation mode the Router cards are configured in *Calibration Header* mode as described in section 5.2.1.

[2]The procedure described is equivalent to sending a pilot job on the WLCG in which the pull architecture is implemented. For example the DIRAC middleware.

The structure described above allows modulating the detector calibration time respect to the monitoring time. Moreover the system allows calibrating in parallel various detector partitions with different calibrations procedures (not all the possible combination are allowed due to the DAQ operation mode). The partitions can be specified by the users with granularity of Half-Sector. The procedures implemented have been designed to operate if either the FED Server emulates or not the DAQ system.

4.3.6 *ChannelDecoder*

The FED Server allows defining detector partitions composed of HSs. Each partition can be operated independently. The *ChannelDecoder* is an Application Layer object designed to define the various partitions operations.

The FED Server associates a state, named channel activation status, i.e. OFF, ON, CALIBRATION, to all the HSs; the *ChannelDecoder* keeps this information. The Half-Staves are named "channels" in the FED Server environment. At FED Server startup all channels are defined as OFF but the FED Server clients can change online the channels state using FED Server commands. State OFF means that the channel should not be taken in account during the FED Server operation neither in automatic nor in manual mode.
The channels in state ON are automatically configured and monitored by the FED Server. The manual access using the *ManualAccessControl* functions is allowed to the channels in this state.
The CALIBRATION state gives to the HSs the same privileges of the state ON and marks the channels as part of the calibration procedures. A calibration request is applied only to the HSs in CALIBRATION state while the HSs monitoring and configuration is performed to all the channels not in state OFF.
The FED Server allows setting the channel activation status also at the level of Pixel Chips and in Tab. 4.6 is reported the allowed configurations for Half-Staves and Pixel Chips.

A Pixel Chip in CALIBRATION imposes the CALIBRATION state to the corresponding HSs but the calibration is performed only to the specified chips.
The *CalibrationFunctions* retrieve from the *ChannelDecoder* the list of chips to calibrate. The FED Server calculate automatically the actions to apply to the Half-Staves and to the off-detector electronics as function of the channels state.

HSs state	Pixel Chips states allowed	FED Server operations		
		Manual	Automatic	Calibration
OFF	OFF			
ON	OFF, ON	 X	 X	
CALIBRATION	OFF, ON, CALIBRATION	 X X	 X X	 X

Table 4.6: The internal FED Server channel state and operational modes. A channel defined to a global state "HSs State" allows only a subset of Pixel Chips states.

The *ChannelDecoder* and the FED Server associate a number to the electronics components following the schema described below. This strategy was adopted in order to have a logical name corresponding to a device. The *ChannelDecoder* embeds also a lookup table storing information on the interconnections between the various devices such as Router cards, LinkRx cards and HSs.
The HSs are identified by a unique number between 0 and 119 named channel number. It is the logical HS name and it is correlated with the HS physical position on the detector. The channel number is calculated as:

Channel Number (0..119) = Sector number (0..9) $*$ Half-Stave position inside the Sector (0..5) + SideIncrement

where SideIncrement = 0 for the detector side A and SideIncrement = 60 for the detector side C.
The Router cards are numbered between 0 and 19. The cards between 0 and 9 are connected to the to the Half-Sectors 0..9 in the detector side A whereas the Router cards between 10 and 19 are connected to Half-Sectors 0..9 in the detector side C.
The LinkRx cards are numbered between 0 and 59. Their number is dependent by the Router card number and by the relative Router card position in which they are plugged.

LinkRx cards number (0..59) = Router card number (0..19) * 3 + Router card slot (0..2).

4.3.7 *ExternalDataInterface*

The *External Data Interface* is designed to download/upload the FERO configuration parameters stored either in the Configuration Database (CDB, see section 3.4.1 for more details) or in a series of configuration files. The on-detector electronics and off-detector electronics is configured automatically by the FED Server using the information obtained via this software component. The main data source during the experiment operation is the Configuration Database but, in case of Db unavailability, the FED Server can operate using a series of configuration files. These files have been widely used during the detector commissioning because the Db connection was not yet established. The configuration files have been produced during the detector modules construction phases.
The *ExternalDataInterface* is a global interface hosting the CDB Interface and the Configuration Files Interface.

The Configuration Files Interface receives as input a list of files and stores their content inside the *DefaultConfiguration* classes. Viceversa the *ActualConfiguration* classes are stored to files when the appropriate command is issued. The Configuration Files Interface is a static library containing two main classes: the command decoder and an I/O to file class.

The CDB Interface is contained in a static library and its internal structure is displayed in the component diagram of Fig. 4.11. It has two main interface objects: the DbConnector and the CommandDecoder. The former, instantiated as singleton, manages the CDB connection. It contains information on the Db communication parameters and it is able to either retrieve or sore data in the Db tables. It is the gateway between the FED Server and the CDB and it is designed to optimize the Db accesses.
The CommandDecoder manages the communication with the FED Server components. It needs, as input, a Version number, a Run_Type, the pointers to objects of type either *ActualConfiguration* or *DefaultConfiguration* and the operation to be executed. Indeed, the main CDB Interface concept design is to release the user from the knowledge of the CDB structure having a very simple and intuitive interface.
During the data upload toward the CDB procedure, the CDB Interface downloads from the CDB the configuration parameters tagged with the specified Version number and Run_Type. These parameters are stored in the StorageClasses objects. The VersionManager comparing the content of the *ActualConfiguration* and of the StorageClasses decides whether a new CDB

configuration version is required. The appropriate commands are sent to the DbConnector to apply the corresponding Db updates. Only the Db tables in which an update is required are modified. The managing of the Db versions tables is performed automatically by this object. A new configuration version is generated anytime the Db is updated (see section 3.4.1 for more details on the version schema). Moreover if Db tables are not existing in the CDB, the CDB Interface generate them in the Db.
In the download from the CDB procedure, the CDB Interface retrieves the configuration parameters tagged with Verion number and Run_Type and store them in the *DefaultConfiguration* objects.
The procedures described above are designed to be applied either to the full detector configuration or to only a configuration subset. This selection is done using the component ID as described in section 4.3.6. Moreover, if the Version number and the Run_type are not specified, the CDB Interface uses the HEAD version.

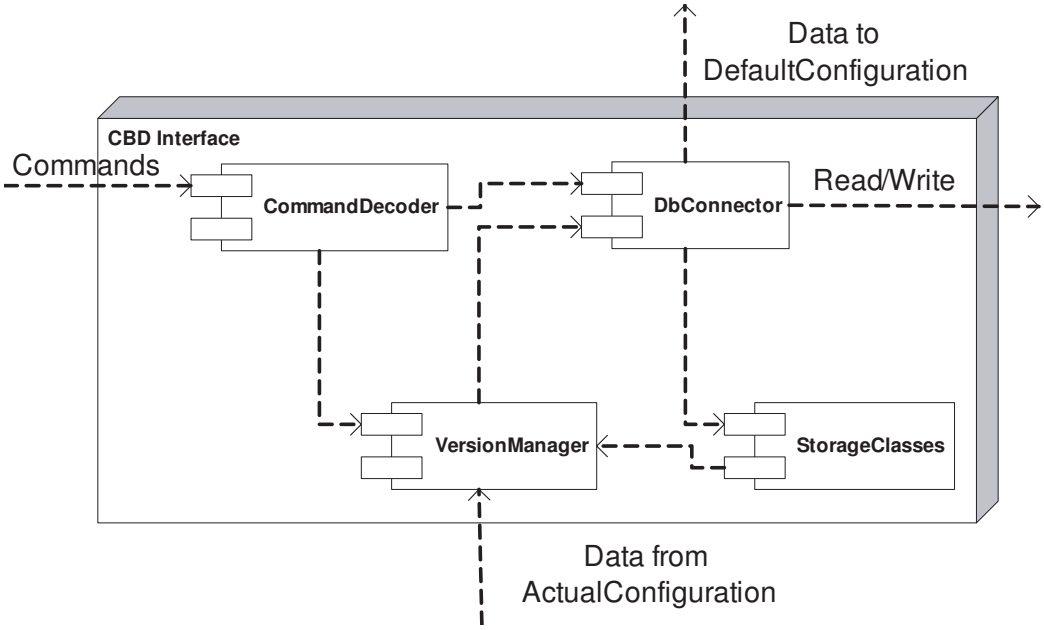

Figure 4.11: The CDB Interface internal structure component diagram.

4.4 Driver Layer

The Driver Layer is the FED Server bottom software layer designed to communicate with the hardware. The PCs running the FED Servers are connected to the Router cards VME crates using a commercial National Instruments (NI) VXI/VME system (more details on section 2.2). National Instruments provides the user with a library to communicate with the devices: NI-VISA library [35]. This library contains primitive and high level functions to access the VME bus. The Driver Layer is based on the NI-VISA library using the primitive functions provided. This choice has been made to optimize the VME access performance. Laboratory tests showed that two sequential accesses are performed in $80\mu s$ using the low level NI-VISA library functions whereas few hundreds μs are needed using the high level NI-VISA library functions. This difference in time comes from the different number of operations performed during the VME access mechanisms. The high level NI-VISA library functions perform always the 5 steps:

1. Open a VISA session;
2. Map the specified hardware address(es);
3. Perform the access;
4. Un-map the hardware address(es);
5. Close the VISA session

The low level functions allow selecting which step should be executed. The Router cards control requires the consecutive access of a limited number of hardware addresses therefore only step 3 should be repeated. The FED Server Driver Layer is designed to optimize this mechanism.
All the Router cards in a crate are seen by the Driver Layer as one device containing all the registers of the cards plugged. It is indeed possible to map sequentially hardware addresses on the same VISA session only if they are part of the same device. Treating the Router cards as separate devices implies repeating the steps 1..5 for each VME access.

The Driver Layer is based on few main blocks displayed in the collaboration diagram of Fig. 4.12. The *VMEAccess* is the Driver Layer interface and it forwards the incoming messages to the appropriate hardware access blocks. The Router cards require two main access types: JTAG controller and Registers. The JTAG controller needs a series of VME accesses [23],

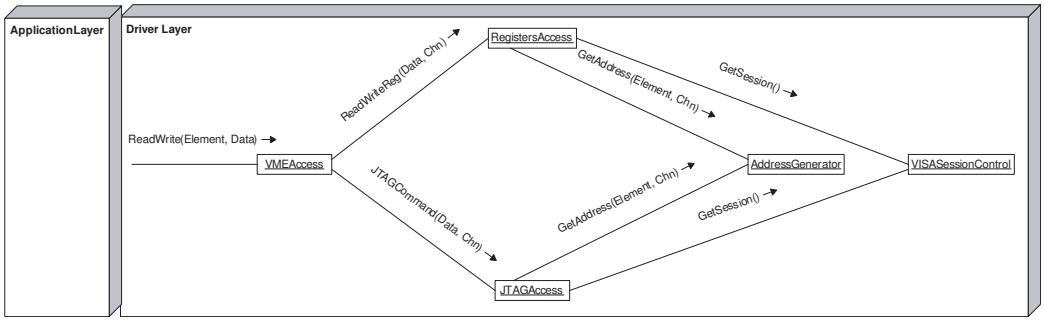

Figure 4.12: FED Server Driver Layer collaboration diagram.

whereas the block Registers gives I/O access to a 32 bit location either inside the Router card FPGAs or inside the memory banks, with a unique VME access.
The Driver Layer is contained in a static library and designed as stand-alone driver element. It can be recalled in any applications and consistently it can drive the hardware using the method implemented.

4.4.1 *JTAGAccess* and *RegistersAccess*

These two Driver Layer blocks are performing the hardware VME access. They have high level functions such as JTAG and registers read/write. The *JTAGAccess* functions require as input the channel number and the JTAG configuration stream in 32 bit words format. These functions are returning the readout JTAG stream and an execution status.
The *RegistersAccess* block contains high level functions to read/write either registers or memory cells. They have as input the channel number, either the register or memory name and the data stream to be written in 32 bit words format. In the case of memory access also an offset is required. These functions are returning the readout data and an execution status.

4.4.2 *AddressGenerator*

The FED Server is the bridge between the software and the detector electronics. The *AddressGenerator* is a software component translating the logical name associated to the hardware components into their hardware addresses. The *AddressGenerator* receives as input the channel number and it returns the VME address for the specified hardware. The addressing of Router cards and LinkRx cards is also performed using the channel number; the *AddressGenerator* extracts from the channel number the hardware component to

which the Half-Stave is connected. The *AddressGenerator* keeps in memory the map of connections between Half-Staves, LinkRx cards and Router cards. This map can be modified online using FED Server commands. This structure allows hot-swap hardware connection without interfere with the FED Server and detector operations.
The physical Router cards number is corresponding to their VME base addresses whereas the logical Router cards number can be modified inside the FED Server.

4.4.3 *VISASessionControl*

The *VISASessionControl* block manages the VME access sessions to optimize the system performance. In section 4.4 on page 118 has been reported the steps needed for a full VME access. The synchronization of these operations is controlled by the *VISASessionControl* that act as cash memory.
When a off-detector electronics location is accessed the Driver Layer components perform a session request to the *VISASessionControl* and this block returns the logical identifier to the session itself. *VISASessionControl* decides either to generate a new session or to use an already opened one. The mechanism used to make this decision consists in defining lists of the actual opened sessions. It checks weather between them the sessions are either used or in standby. In the standby list it is given a priority to each session and it is checked if the required address is already mapped. These parameters are used by the *VISASessionControl* to return a session number.
The interface of this elements is very light, indeed, it requires only a session request and information on the session future usage e.g. if the session will be used recursively. Moreover it is important to bear in mind that this block has a fundamental role in the full system operation. A low performance sessions management can reduce drastically the system efficiency and it can also be very resource consuming.

Chapter 5

Detector Calibration

The SPD electronics has been designed providing the users with a series of parameters to be adjusted to tune the electronics and the detector performance. The aim of the SPD calibration is to adjust these parameters in order to obtain the highest efficiency and response uniformity of the pixels matrices. It evaluates also the sensor and electronics behavior given a certain configuration.
The SPD calibration is an essential phase for the detector operation. Without the appropriate configuration evaluated during the detector calibration, the SPD electronics cannot produce reliable data.

This chapter deals with the SPD calibration and it is divided in three parts. The first recalls the main electronics features in order to introduce the detector calibration parameters as well as the general strategies adopted to evaluate them.
The second part gives an overview on the SPD calibration system. The complexity of the detector calibration, the high number of parameters to be evaluated (~ 10000) and the limited time available for the calibration (< 70 minutes, corresponding to the LHC filling time) impose the development of a high automated SPD calibration system. Moreover this system should be operated directly by ALICE, hence, it is mandatory the system integration in the ALICE framework.
Due to these requirements the SPD calibration system is a fundamental component for the SPD operation. I have been the main system designer in term of general architecture and integration with the SPD DCS and ALICE systems. These latter have been developed considering also the SPD calibration needs and I have been the main interface between the SPD and the ALICE developers.

In order to satisfy the requirements and provide the user with a simple and versatile interface, I foresaw two SPD calibration scenarios. A calibration scenario named DAQ_ACTIVE allows the fast full detector calibration. A second calibration scenario, named DCS_ONLY, is used to calibrate a detector partition without interference with the normal operation of the other SPD partitions.
The third part of this chapter reports some calibration and control systems application examples as well as a brief overview of the detector performance evaluated during the detector commissioning phases.

5.1 The SPD calibration specifications, parameters and strategies

The detector calibration evaluates a series of parameters defining the detector and electronics performances. These parameters are function of the HSs ASICs configuration and power supply. The calibration sequences are iterated adjusting the electronics configuration until the optimum parameters settings is determined.
Chapter 2 and [45] describe in detail the electronics elements to be adjusted during the detector calibration and their influence on the detector performance whereas, in this section, the main SPD electronics features are recalled. Further the calibration parameters are listed and the methods used to evaluate them are described.

Each Pixel Chip has 44 internal DACs to be configured and they influence the behavior of the FE chip analog and digital parts. Acting on these DACs the detector operation e.g. the chip timing, efficiency and uniformity of response of the pixel matrices, the global chip threshold, etc. can be adjusted. It is important to bear in mind that detector performances are defined by the DACs produced voltages. The conversion between the DACs digital values and their produced voltages should therefore be calibrated. This descends from the fact that the Pixel Chip DACs slope and linearity are controlled by two external reference voltages produced by the Analog Pilot. Furthermore the Pixel Chip DACs are also sensitive to the supply voltage (Vdd). Hence each set of references and power voltages define a specific correspondence between DACs digital values and their produced voltages. The details on the Vdd and references effects on the Pixel Chip are not reported in thesis but a wide SPD literature treats these topics [45]. However in order to understand this chapter it should be borne in mind that a variation of either

the Vdd ($>$ 50 mV) or the Analog Pilot references ($>$ 10 mV) impose a new detector calibration. The Pixel Chips DACs digital values should be indeed recalculated.
Due to the SPD material budget limitations the Pixel Bus powering and grounding layers are very thin ($\sim 50\mu m$) aluminum foils. The high HS current on these thin layers generate a loss of $\sim 20mV$ along the powering and grounding layers. Hence, the chips along the HS have slightly different supply power and ground. This condition impose to have a well determined DACs setting for each HS chip.
The radiation effects and the detector aging influence the overall detector efficiency [44] and sensitivity uniformity. Hence, the uniformity of the pixel matrices response should be evaluated regularly (once a week) during the detector lifetime. In addition this parameter gives information on the detector status and on the Pixel Chips configuration.
The dead and noisy pixel identification gives important information on the general detector status. Moreover the list of noisy pixels is used by the DCS to automatically mask these channels. The list of noisy and dead pixels is also used by the offline particle tracks reconstruction algorithms when defining the actual position in which the particle passed.
The SPD has the capability to provide a prompt multiplicity trigger through its Fast-OR pulse (FO). It is generated in each pixel chip when a particle hit is detected. The Fast-OR efficiency is influenced by the settings of various Pixel Chip internal DACs. Hence, the Fast-OR characterization is an important step in the calibration phases.
Summarizing, the operation of the SPD requires a tight control of many parameters such as timing, the Pixel Bus power supply voltage (Vdd), the reference voltages provided by Analog Pilot, and the settings of the various DACs in each Pixel Chip.

Calibration is performed using either particles or Test Pulses (TPs) generated in each FE chips. The pulses can be sent independently to each single pixel; the amplitude is programmable and it is controlled by the Analog Pilot. The SPD calibration will be performed regularly either during the data taking (calibrations with particles) or during the beam breaks (calibrations with TP). The LHC filling time is roughly 70 minutes, hence, this is the only time available for the SPD calibration with TP dung the LHC operation. This is a strict constraint imposing a high automation and performance to the calibration system. Indeed, as it will be described in the next sections, in this short time a series of high time consuming detector reconfigurations and data acquisitions should be repeated.

Following the detector calibration requirements described up to now, a series of calibration parameters have been defined to evaluate the SPD status and performances. I have been strongly involved in the definition of these parameters and in the conceptual design of the method used to evaluate them. In the next sections the calibration parameters are listed and the strategies used to evaluate them are described.

5.1.1 Minimum Threshold

Each pixel has a digital readout obtained converting the charge deposited on the detector in a voltage and comparing it with a threshold. The discriminator inside each pixel cell is a single threshold discriminator and the threshold is proportional to a global Pixel Chip DAC named *pre_VTH*. The *pre_VTH* DAC has a reversed behavior, indeed the threshold is increased when the DAC value is reduced and viceversa. All the pixel cells of a Pixel Chip have the same discrimination threshold. The DAC can move the threshold up to $\sim 3000e^-$ equivalent.
The Minimum Threshold (*minTH*) is defined as the minimum global threshold value in which the noise effects induced by the system noise are suppressed.
The strategy utilized to evaluate the *minTH* consists in reading out the pixel matrices, without passing particles, at various thresholds. When the threshold is low the Pixel Chips are producing fake hits due to the system electric noise. The threshold is increased up to when the matrices are completely silent apart for the noisy pixels. The noisy pixels indeed have a noise level much higher than the threshold limit and they can not be removed by acting on the threshold.
The Minimum Threshold is calculated for each Pixel Chip and it is expressed in *pre_VTH* DAC units. The correspondence between DAC units and electrons equivalent depends on the DAC slopes and it can vary as function of the Analog Pilot and Vdd settings. The Mean Threshold (described below) establishes precisely the conversion factor. A rough conversion can be anyway performed considering that $pre\_VTH = 200$ (average Minimum Threshold value) corresponds to $\sim 2500e^-$ and that a DAC unit corresponds to a variation of $\sim 120e^-$.

5.1.2 Pixel Matrix Response Uniformity

This calibration procedure, also called Uniformity Scan, evaluates the distribution of pixel efficiency over the pixel matrices. The uniformity is studied

applying TPs to each pixel cell and determining the efficiency of response as ratio of hits recorded over the number of pulses applied. The matrices efficiency histograms are plotted and they give already visually a feeling on the uniformity of response. In order to evaluate automatically the matrices responses, three parameters are calculated using the efficiency histograms:

Mean efficiency (M_{EL}): This parameter gives information on the global efficiency over a pixel matrix. It is calculated as:

$$M_{EL} = 1 - \sqrt{(N_{TP} - M)^2/{N_{TP}}^2}$$

where N_{TP} is the number of TPs sent and M is the mean of hits recorded per pixel. $M_{EL} = 1$ in case of full uniformity with the pixels efficiency = 1. In any other case $M_{EL} < 1$.

Efficiency deviation (σ_{EL}): This parameter evaluates the spread of pixel efficiency in the efficiency distribution. It is calculated as:

$$\sigma_{EL} = (N_{TP} - \sigma)/N_{TP}$$

where σ is the standard deviation of the hits per pixel distribution. $\sigma_{EL} = 1$ in case of full uniformity.

Efficiency loss fraction (D): This parameter defines the fraction of pixels with efficiency loss. It is calculated as:

$$D = (N_P - N_{NE})/N_P$$

where N_P is the number of pixels in the pixel matrix being evaluated and N_{NE} is the number of pixels with efficiency < 1. D = 1 in case of full uniformity.

These three parameters are multiplied to give a Uniformity Factor (UF) in the range $0 \div 1$; the full uniformity of response is defined by UF = 1. A uniformity factor is calculated for each Pixel Chip.

In order to speed up the Uniformity Scan procedure the TP is not applied individually to each pixel but in parallel to four full Pixel Chip matrix rows. I decided to limit to 128 the number of pixels activated at a time (4 rows) in order to verify the uniformity of response in multiplicity conditions

equivalent to the ALICE runs (average occupancy 2%). The TP is applied in rows and not in columns in order to reduce the noise introduced by the TP injection system. The TP, indeed, is distributed by column and many pixels activated in the same column generate a TP overload on the specified line. This operational mode is also close to the physical response of the pixel matrices crossed by interaction particles. The event topology indeed foresees hits distributed on the matrices surfaces and not concentrated on a defined column.
Concluding this section is important to remember that the pixel efficiency is also function of the TP amplitude when the pulses are smaller than twice the threshold set. The stand-alone Uniformity Scan is in general performed with TP amplitude bigger than three times the global threshold ($\sim 100mV$). The region of TP amplitude less than twice the threshold is in general studied with the Mean Threshold scan.

5.1.3 Mean Threshold

The Mean Threshold (*meanTH*) is a parameter establishing the conversion factor between the charge deposited on the detector volume and the corresponding threshold DAC value. Indeed, as seen in the previous sections, the Pixel Chip DACs linearity is dependent on the Vdd and on the external reference voltages provided by the Analog Pilot. Different sets of these parameters require a new evaluation of the conversion factor. Moreover the change over time of the *meanTH* indicates detector and electronics aging effects. The method used to calculate the *meanTH* gives also information on the electronics noise associated to each pixel cell.
The Mean Threshold is evaluated applying to each pixel a series of Test Pulses with various amplitudes. The TP amplitude corresponds to the difference between the two voltages ANALOG_TEST_HI and ANALOG_TEST_LOW provided by the Analog Pilot. For each pixel an efficiency curve (named S-curve from its typical shape) function of the TP amplitude is plotted.
It is defined as Mean Threshold for each pixel the amplitude of TP to which the pixel has an efficiency of 50%. The Pixel Chip *meanTH* is the mean value of the pixels *meanTH* distribution.
This TP scan evaluates also the RMS of the Gaussian noise associated to each pixel. The difference of TP amplitude between the efficiency of 98% and 2% corresponds to 4σ.
The RMS noise associated to a Pixel Chip is the mean value of the pixel noise distribution.
The *meanTH* is evaluated repeating a series of Uniformity Scans with vari-

ous TP amplitudes[1].
The *meanTH* is expressed in mV but a series of studies performed on Pixel Chips demonstrated that the conversion between TP amplitude and deposited charge on the pixel pad is $\sim 66e^-/mV$ [32].

5.1.4 Noise and Dead pixels identification

The detector ladders have been tested before assembly and they have been considered operative if the percentage of defecting channels was less than 1%. The aging, the radiation effects and the mechanical stress can increment the number of not functioning channels [44]. The survey and identification of noise and dead channels is a detector calibration procedure.
Noise pixels can be consequence of either malfunctioning pixel cells in the FE chips or bad sensor diodes. There are several classes of noise pixels such as maskable, un-maskable and partially noisy. The maskable can be masked directly in the FE electronics whereas the un-maskable cannot be removed from the detector data. Both categories can have always-noisy and partially-noisy pixels. The always-noisy pixels are firing respecting a Poisson distribution whereas the partially-noisy have a completely random behavior. Moreover the un-maskable noisy pixels contribute to the Fast-OR signal generation, hence, reducing the detector trigger efficiency.
Dead pixels are in general either consequence of missing bump-bonding between the sensors and the FE electronics or defects in the FE chip readout channels. New dead pixels can appear due to mechanical stress or by radiation effects.
The survey of the evolution of noisy and dead pixels gives important information on the detector status. Moreover the identification of malfunctioning pixel is useful information for the offline track reconstruction algorithms.
The noisy pixel identification is performed during the various calibration procedures as well as during dedicated procedures. In the specific noise scan few millions of triggers are sent to the detectors without any stimulation (neither particles nor TPs). The pixels producing hits are defined noisy.
The dead pixels are identified using particles produced by the interactions during the experiment data taking. The data are collected until the average multiplicity is above a certain value defined by the operator. The pixels with either low ($< 20\%$) or null efficiency are defined as dead.

[1]The TP amplitude is varied for each row activated and not at the end of each Uniformity Scan. This method allows saving time in the scan without changing the results.

5.1.5 Delay Scan

The pixel readout electronics has a programmable delay line (see chapter 2 for more details) to adjust the L1 latency respect to the particle arrival. This delay can be operated acting on two Pixel Chip internal DACs: delay_control and misc_control. The former increases the delay of 200 ns for DAC unit whereas misc_control can delays the incoming L1 of 100 ns. The L1 latency is guaranteed to be $\sim 6\mu s$ at the Router card level depending on the ALICE trigger partition used. However the effective arrival to the Pixel Chips depends on the command serialization/de-serialization time and to the optical fibers length. One clock cycle (100 ns) L1 jitter can also be introduced during the off-detector electronics reset phase. The swap between beam, radioactive source and TP requires the adjustment of the delay lines. A calibration procedure has been designed to find the appropriate delay: Delay Scan. This scan modifies the values on the two DACs involved while a series of triggers is sent to the detector. Using the collected data, a multiplicity plot shows the multiplicity distribution as function of the delay set. This plot spots the right delay as a pick of multiplicity above the background.

5.1.6 Fast-OR Efficiency and Uniformity

The SPD has the trigger detector capability trough its Fast-OR signal (more details can be found in chapter 2). The understanding of this section needs only to bear in mind that the Fast-OR signal is generated, asynchronously, by each Pixel Chip, whenever a pixel is fired on the matrix.
The Fast-OR circuitry operation is controlled by four Pixel Chip internal DACs influencing the Fast-OR response in term of uniformity along the pixel matrices and the Fast-OR efficiency. The Fast-OR calibration studies these parameters and it defines the best DACs settings to obtain the higher efficiency and uniformity.
Studies performed to the FE chips demonstrated that the Pixel Chip Fast-OR response is equivalent whether the circuitry is stimulated by a particle crossing the detector or using TPs. I foresee to calibrate the Fast-OR using TPs in order to reduce the calibration time.
The off-detector electronics hosts 1200 Fast-OR counters recording the number of produced Fast-OR for each Pixel Chip in a given time.
The Fast-OR uniformity and efficiency are studied applying to a pixel at a time a given number of TPs and reading back the number or Fast-OR produced. Efficiency maps are produced associating to each pixel the corresponding number of Fast-OR counted. The histograms produced have the

same structure of the Uniformity Scan histograms. Hence, the same method are used to evaluate Fast-OR uniformity and efficiency.
The operations described are repeated several times modifying the DACs values in order to reach the full uniformity of response and efficiency.

5.1.7 Generic DAC Scan

The generic DAC scan is used to study the FE electronics and detector performances as function of a Pixel Chips DACs. The methods described in the previous sections are focalized to extract a defined set of operational parameters whereas the DAC scan is completely generic; it is used to evaluate the system performance and tightly adjust the detector operation point.
The DAC scan is performed applying a sequence of trigger to the detector under test, using either TPs or particles (radioactive sources during the integration phase and the particles produced by the interactions during the experiment data taking), while varying the references generated by the Analog Pilot and/or a specific DAC in the Pixel Chips. The readout data are used to produce average multiplicity and efficiency histograms function of the DAC values.
The DAC scan can be performed sequentially on various DACs defining an operational region in which the system archives the best performance. At present it is implemented an automatic procedure to perform a unique DAC scan but it is foreseen to extend this functionality to apply changes on a series of DACs in parallel.

5.2 Calibration procedures

The SPD calibration requires a series of complex and time consuming operations such as those described in the previous section. Moreover the calibration requires various system capabilities such as configuration, triggering, data acquisition and analysis. As already mentioned, the time available for the calibration is less than 70 minutes corresponding to the LHC filling time. Hence, the calibration time has strict constraints in the system design. Indeed, the detector pixel matrices reconfiguration is a very time consuming operation requiring the download of more than 15 Mb of data in the on-detector electronics. More than 10000 calibration parameters should be evaluated online during the detector calibration.
Due to the constraint mentioned above, the SPD calibration automation is vital for the detector operation. These constraints increase the complexity of the SPD DCS and DAQ systems and they brings the SPD online software

to be one of the most complex in the ALICE experiment.
The calibration system is designed to allow fast and automated calibration procedures in witch the updated configuration settings are calculated automatically.

I foresaw two independent calibration procedures: DCS_ONLY and DAQ_ACTIVE. They provide the same results but they use different strategies to collect and analyze the calibration data.
The DCS_ONLY procedure foresees the DCS emulation of the ALICE DAQ and trigger systems. This procedure is much slower than the DAQ_ACTIVE during the data acquisition but it allows calibrating and debugging a detector subset without interfering with the data acquisition of the other detector partitions. Moreover this procedure allows to calibrate automatically the detector in stand-alone without the ALICE systems such as DAQ, trigger, ECS and DCS.
The DAQ_ACTIVE procedure uses the DAQ system to collect and analyze the calibration data. Hence, this procedure allows the fast calibration of the full detector using the DAQ parallel data readout functionality. The DAQ_ACTIVE is the procedure generally used during the detector operation.
The calibration procedures are initiated by the Experiment Control System (ECS) forwarding the calibration request to the SPD DCS. In the case of DAQ_ACTIVE procedure, the ECS configures also the DAQ and the trigger systems according to the specific calibration requirements.
The two calibration procedures have been developed and testes in the system test facility at CERN. They have been used for the sector characterization and during the first ALICE cosmic run of December 2007.

Next sections describe the two procedures in details trying to focalize on the global system functionality without entering in technical details. However, it is important to bear in mind that to protect the ALICE subsystems from network attacks, they operate in private networks. The communication between the systems is allowed only trough a series of gateways and file exchange servers. This safety strategy strongly influences the calibration system design in which the interaction between DCS, ECS and DAQ is vital. However I found a series of innovative solutions (widely described in the next sections) using the SPD framework to overcome this problem and now these solutions are widely used in the ALICE experiment.

5.2.1 DAQ_ACTIVE scenario

The DAQ_ACTIVE calibration scenario allows the fast detector calibration and it requires the DCS, DAQ and Trigger systems. This scenario allows calibrating the detector either in dedicated calibration runs or during physics data taking. Many calibration parameters must be evaluated in specific run because the TP is used and particles passing trough the detector would prevent the calibration. Another reason to have specific calibration runs come from the fact that during physics data taking, the DAQ system does not allow to collect all the data online (see below for more details) while the majority of the SPD calibration procedures needs to retrieve all the data produced. Hence, during the specific calibration runs, all the data collected are stored and analyzed online. However during the physics run a series of monitor functions are used to sample the incoming data and they are used to define the map of dead pixels.
The requirements mentioned above strongly influence the calibration system design and strongly increase the system complexity.
This section describes the calibration scenario during dedicated calibration runs whereas section 5.2.1.1 contains more details on the calibration during physics runs.
This description will focus on the system block interconnections and it tries to avoid the technical details. They would not be useful at this stage, while possibly confusing the understanding of this already complex mechanism.

A block diagram of the DAQ_ACTIVE scenario is displayed in Fig. 5.1 whereas Fig. 5.2 shows a scenario sequence diagram in which the Router cards are emulating the trigger system.
In the DAQ_ACTIVE scenario the Experiment Control System (ECS) synchronizes the operation of the subsystems involved in the calibration procedures. The former operation consists in configuring the DAQ and the trigger systems for the calibration data taking as function of the calibration type required. During physics data taking the SPD DAQ Local Data Concentrators (LDCs) are used only as temporary data buffers. The events collected by the LDCs are immediately forwarded to the DAQ Global Data Collectors (GDCs) in order to be merged (built) to form a unique super event [64]. This procedure is called event building. The built events are automatically forwarded to the permanent data storage (CASTOR). This configuration cannot be applied during the SPD calibration because the new parameters to be used to configure the electronics should be calculated online and before the start of a new physics run. Moreover, the calibration procedures

automation would be very complex if the data should be retrieved from the permanent data storage, analyzed offline and then used to update the CDB. Furthermore, in many calibrations methods, the triggers are generated by the off-detector electronics hence the required trigger information needed for the event building is missing.

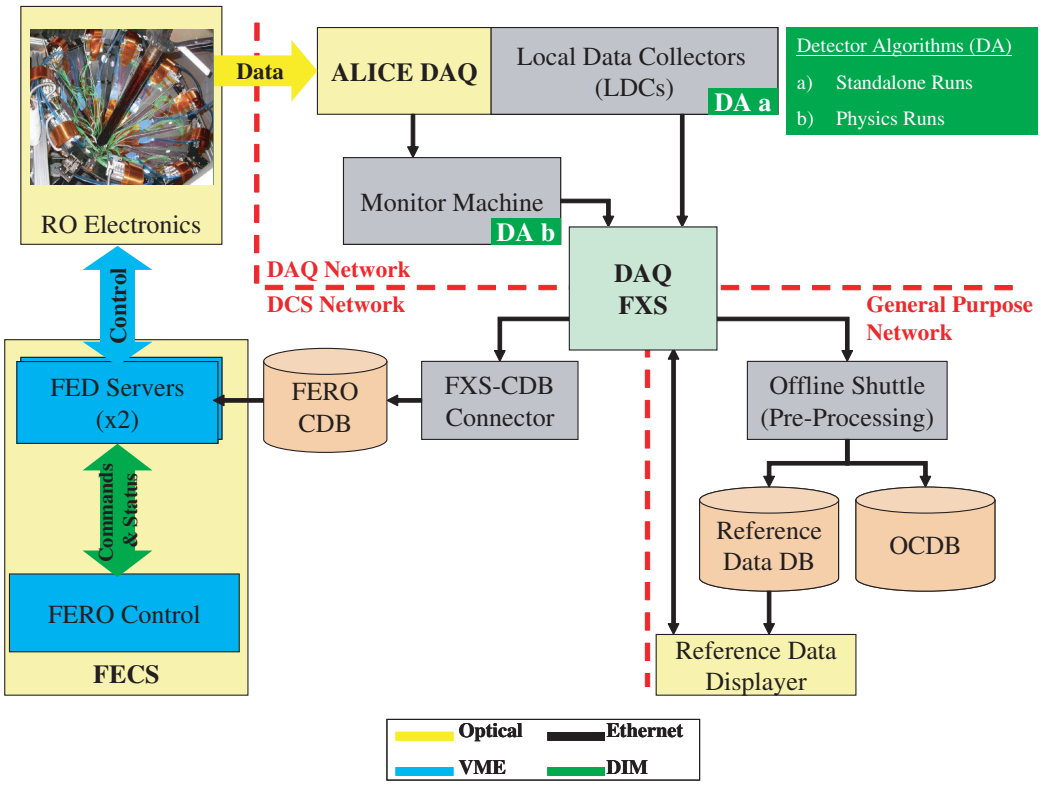

Figure 5.1: A DAQ_ACTIVE calibration scenario block diagram.

In order to cope with these specifications I foresaw that, during the SPD calibration, the produced calibration raw data are stored locally in the SPD LDCs and they are analyzed online at the end of each run. The event building is as well suppressed during the SPD calibration. The DAQ configuration swap between the physics data taking mode and the calibration mode is performed, if needed, automatically by the ECS at the beginning of each run.

When the DAQ is ready for calibration data taking, the ECS sends to the SPD FSM top-node the start calibration command. Using the command information, the top-node decides if the calibration to be performed is ei-

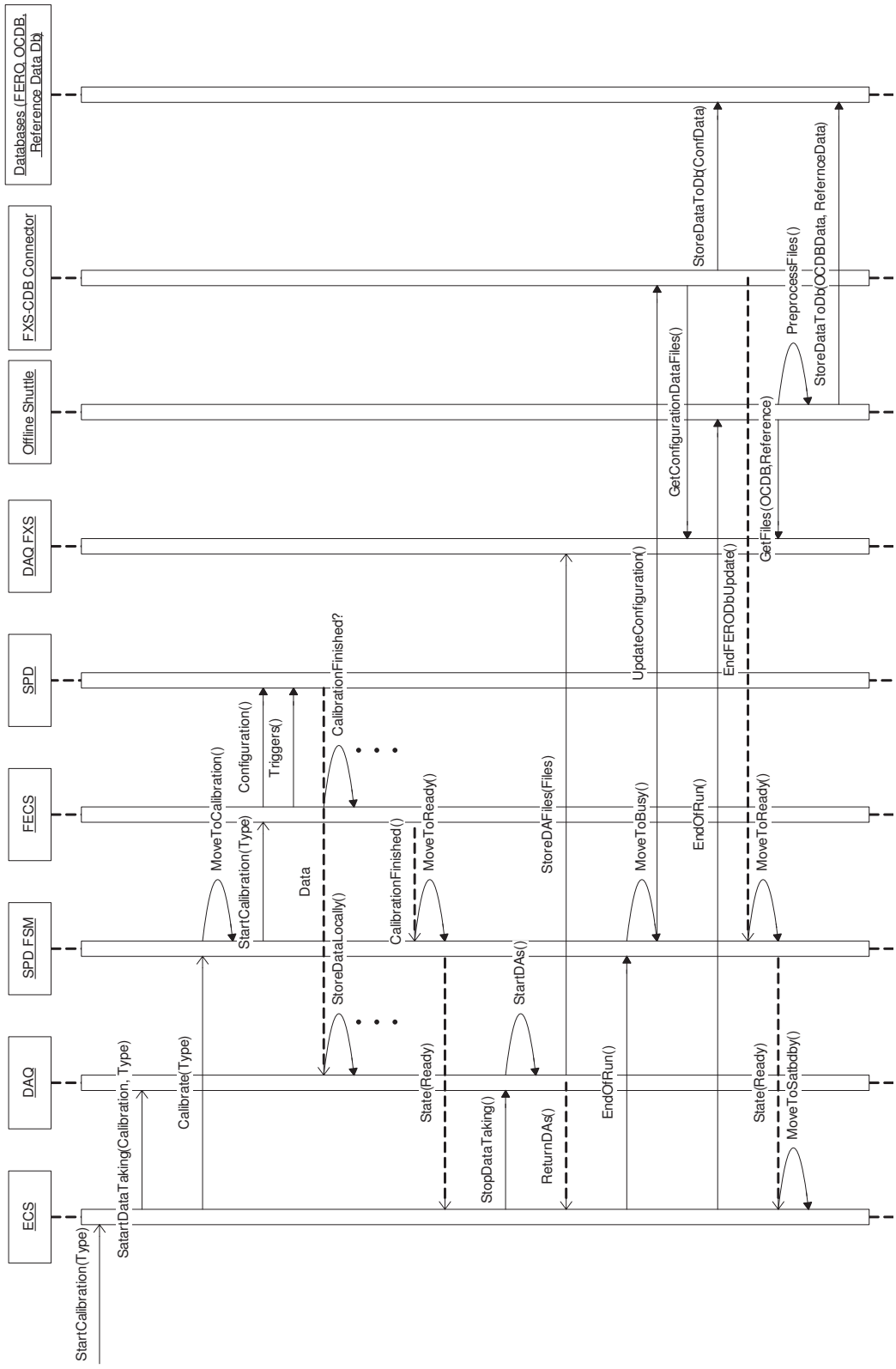

Figure 5.2: A DAQ_ACTIVE calibration scenario sequence diagram example. In this example triggers are generated by the Router cards.

ther in scenario DAQ_ACTIVE or DCS_ONLY. The FECS is informed that a calibration is required and it gets the calibration parameters to be applied from its internal DPs and the CDB. Moreover the FSM top-node moves to the CALIBRATING state.
The FED Servers are receiving a command containing the list of elements (HSs and Pixel Chips) involved in the calibration procedure, the calibration type and the calibration parameters (i.e. number of rows to which apply TPs, number of triggers, etc.). The FED Servers perform the detector configuration. Further, depending on the required calibration type, the FED Servers are performing triggers request either to the trigger system (using DIM) or to the Router cards. Once the trigger sequence has finished the FED Servers start a new configuration phase if needed. This loop continue up to the end of the calibration phase. The FED Servers are then downloading, in the detector, the old configuration and issuing a calibration end flag. On receiving this flag the FSM get released from the CALIBRATING state and it moves to the appropriate operational state (usually it is the READY state).

When the FSM leaves the CALIBRATING state, the ECS starts a set of LDCs analysis scripts called Detector Algorithms (DAs). Section 5.2.1.1 describes in more details these scripts operation whereas here only the main features are reported.
The DAs analyze the raw data files and they generate two files for each Router card involved in the calibration process. One of the two is named Reference Data file and it has a ROOT [33] compatible format. It contains the hits distributions on the pixel matrices (hit-maps) divided per calibration steps and the calibration parameters (see section 5.2.1.1 for more details). The Reference Data are pre-processed data to be stored in a specific reference Db in the offline environment. These references will be used in the future to survey the evolution of the detector status. The ALICE policy indeed foresees that raw data, after being processed, will be deleted.
The second type of files produced by the DAs are named Configuration Data file (see section 3.4.2 for more details). They are text files containing the new detector configuration setting calculated by the DAs. These file contains the information to update the CDB.
When the DAs return, the ECS is informed and the produced files are moved automatically to the DAQ File Exchange Server (FXS).

When the DAs files moving has finished the ECS closes the DAQ run and it informs the FSM top-node and the offline systems.
The offline, upon arrival of the end of run message, lunches a process called Offline Shuttle [39] that moves the Reference Data files stored in the DAQ

FXS to the Offline Reference Data Db[2]. The shuttle contains also a preprocessing script (Shuttle pre-processor), produced by the SPD group, extracting from the reference files, the list of noisy and dead pixels to be stored into the Offline Condition Database (OCDB)[40]. This Db is actually the AliEn[40] file catalogue and it contains information used from the offline tracks reconstruction algorithms.
The FSM top-node, upon arrival of the end of run message, moves to state BUSY and trough the DU *SpdDbConnector* lunches the FXS-CDB Connector described in section 5.2.1.2. This application reads the Configuration Data files in the DAQ FXS and it updates correspondingly the DCS Configuration Database (CDB).
When the FXS-CDB Connector finishes its operation, the FSM top-node gets released from the BUSY state and it moves to the appropriate operational state. The ECS closes the calibration procedure and eventually a new run can be initiated.
The ECS does not wait for the end of the Shuttle to close the run because this process is completely asynchronous. Anyhow, also the FXS-CDB Connector is an asynchronous process but it has been decided to wait for the CDB update before starting a new run. This strategy allows using immediately the new configuration produced by the calibration process.
During the normal detector operation the procedure described up to now is fully automatic but, during the detector debug and in case of anomalous behavior, it is not advisable to store automatically the new configuration in the CDB. It has been foreseen a lighter procedure that does not perform this last step. A Reference Data displayer described in section 5.2.3 allows the user to inspect the calibration results and, eventually, also to re-analyze the raw data producing new Reference Data and Configuration Data files. The CDB can be update starting manually the FXS-CDB Connector via the corresponding FSM DU.

The DAs, in order to analyze the data, need information on the actual detector configuration, on the calibration parameters and on how to update the CDB. Moreover, the DAs are performing consistency checks on the incoming data to evaluate the calibration procedure quality. In the calibration procedures the detector configuration is modified before each bunch of data, hence, the synchronization between data produced and the detector configuration should be guaranteed.
In order to provide this information to the DAQ system and to guarantee the

[2]It register the files to the AliEn[40] file catalogue.

synchronization I proposed to add a *Calibration Header* (CH) to the raw data stream. I proposed this idea in the SPD framework and it is innovative in the ALICE environment. It allows establishing a communication channel between the DCS and the DAQ system without using the ECS. This channel is fast, easy to implement and it gives high flexibility to the entire system. The synchronization problems between the subsystems are automatically solved using this strategy. The software complexity is strongly reduced because each system element can be completely independent and self-consistent. The FECS needs only to perform the detector (re-)configuration, the trigger operations and add the *Calibration Header*. The DAs (in principle everyone) reading the raw data can understand directly which calibration procedure has been applied, the actual detector configuration, the detector status and the data analysis procedure to be used. The *Calibration Header* contains also commands to the DAs and information on the data source (Router card number). The DAs structure is strongly simplified using the *Calibration Header* because there is no need to open separate communication channels between DCS/ECS/DAQ systems. The DAs become completely independent and stand-alone applications to be used also offline. They require only a series of raw data file to operate.
The *Calibration Header* length and structure is varying as function of the calibration procedure performed and of the number of HSs involved in the calibration procedure. Tab. 5.1 reports the *Calibration Header* content.

In order to generate the *Calibration Header*, each Router card has a 256 x 32 bit FIFO writable via VME. When the *Calibration Header* functionality is activated, the FIFO content is added at the first event forwarded to the DAQ. In order to avoid redundant information, this header is sent only when the detector configuration changes. It is assumed that the calibration information is valid up to when a new *Calibration Header* is sent. Fig. 5.3 (left) displays a series of events generated by a Router card during a calibration procedure. The calibration procedure start at event 0 and a *Calibration Header* is attached. The detector is re-configured after the event n-1, hence, a new *Calibration Header* is inserted. This mechanism is repeated up to the end of the run. In this figure also a Common Data Header (CDH) is visible. It is needed by the DAQ system to separate events and it is generated by each Router card for each event. The SPD uses 4 LDCs reading 5 Router cards each. Inside each LDC the raw data have the structure displayed in Fig. 5.3(right)[3]. This figure shows only event 0.

[3]Each device connected via DDL to the DAQ system in named equipment and it is identified by an equipment ID. It is a sequential number and the SPD uses the range 0..19

Position	Parameter	Note
0	Router Number	
1	bit 0..7: Scan Type, bit 8..16: Data Type	The Data Type defines the data format expected: 0 → normal data; 1 → matrix format;
2	Number of triggers	
3	Chips status HSs 2..0	Present, Masked, Not Active
4	Chips status HSs 5..3	”
5	Calibration information DAC Min, DAC Max, Step, DAC identifier	Used during DAC Scans
6	Calibration information Start Row, End Row, Actual Row, Actual DAC Value	First 3 parameters valid during Uniformity Scan
7..9	Commands FXS-CDB Connector	See section 5.2.1.2 for more details
10..17	misc_control; ANALOG_TEST_HI and ANALOG_TEST_LOW ; Chip Select Fast-OR Counters	During Delay Scan During Mean Threshold During Minimum Threshold The header is extended of 60 values

Scan Type	
0	Minimum Threshold Scan
1	Mean Threshold Scan
2	Generic DAC Scan
3	Uniformity Scan
4	Noisy Scan
5	Delay Scan
6	FO Characterization

Table 5.1: The *Calibration Header* content. The header length and content are changing as function of the calibration method used. Information such as Router Number, Trigger Number, etc. is added for redundancy. The analysis software issues an error if mismatches are found in the data.

Furthermore, inserting the *Calibration Header* inside each Router card allows

with direct correspondence with the Router cards number.

applying different calibration procedures to each Half-Sector[4]. Each Router card can indeed perform a calibration procedure without interfering with the others. The data analysis can be performed following the same strategies because the information associated to the calibration procedures is anyway attached to the raw data stream.

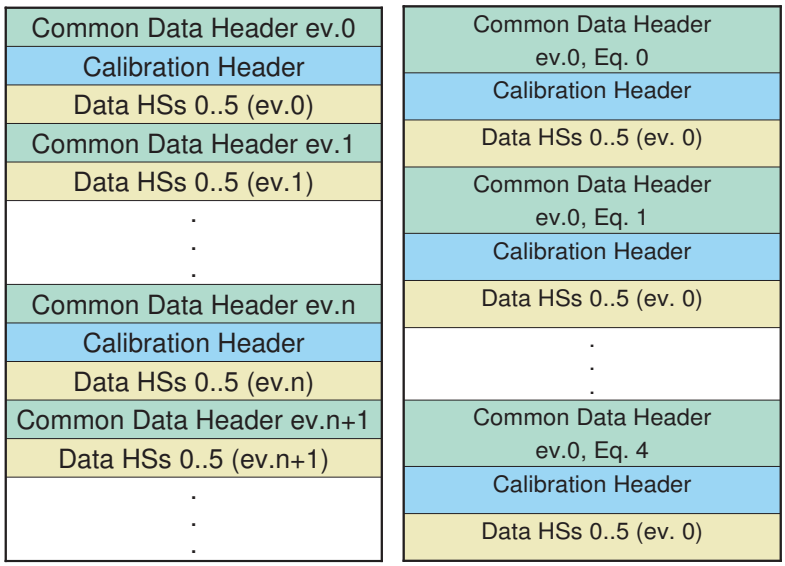

Figure 5.3: (Left) A series of calibration events produced by a Router card. A *Calibration Header* is added at the start of the calibration procedure and when the detector configuration changes. In this example a re-configuration is applied at the event 0 and n. (Right) The structure of an event recorded in a LDC. In this example the first event in which the CH is attached is displayed.

5.2.1.1 Detector Algorithms (DAs)

The Detector Algorithms are a series of detector oriented algorithms used to process data online. They run in the DAQ system during physics and calibration runs. The DAs are designed to run on Linux platform and they are based on C++ and ROOT. The name Detector Algorithms comes from the fact that each ALICE sub-detector has its own set of analysis algorithms. The strategy of performing the calibrations with these tools has been proposed at first by me in the SPD framework and now it is part of the ALICE

[4]Not all the possible combinations is allowed.

calibration structure. The DAs are now embedded in the offline/online ALICE analysis software named AliRoot [40].
The SPD has two DAs types packaged in two different applications. One type is used to find dead pixels and uses physics run data whereas the second type is able to analyze the data produced by specific calibration runs. In this section the former DAs set are called dead pixel finder DAs whereas the second DAs set are called calibration DAs[5].

The dead pixel finder DAs use particles produced during beam interactions to identify the dead pixels. They plug on the data streams using the DATE [64] monitoring libraries. However only a sample of the events produced is retrieved by these libraries. The efficiency depends on the DAQ load and on the DAs analysis speed but tests performed up to now demonstrated the efficiency to be always $> 80\%$. The dead pixel finder DAs are running on dedicated DAQ monitoring PCs.
During data taking the pixel matrices hit-maps are filled up by the DAs. At the end of each run one Reference Data[6] file is produced for each Router card involved in the data taking. The files are stored locally and in the FXS. Further the dead pixel finder DAs analyze the hit-maps and if the required statistic (occupancy) is reached the DAs are producing also another file containing the list of dead pixels. This file is moved to the FXS and further the Offline Shuttle will move it to the OCDB.
If the statistic is not reached the dead pixel finder DAs continue their operation in successive runs using as starting point the former hit-maps calculated. In p-p collisions $\sim$ 50 tracks per event are foreseen, hence, $\sim 3M$ events should be collected by the DAs to reach the appropriate statistics. In Pb - Pb collisions the multiplicity is assumed to be $\sim$ 3000 tracks per event, hence, the DAs should collect $\sim 10K$ events to reach the required statistics[7]. When the list of dead pixels is calculated, the dead pixel finder DAs delete the preceding hit-maps and they start again the data collection. These DAs are running continuously receiving the start and end of physics run information by the ECS. Each time the appropriate statistic is reached the OCDB is updated.

The calibration DAs use data produced by specific calibration runs to

[5]In Fig. 5.1 the calibration DAs are named DAa whereas dead pixel finder DAs are named DAb.

[6]See below for more details and Fig. 5.4 for their internal structure.

[7]Considering the monitor library efficiency = 80%, the number of events collected by the DAQ is: $\sim 3.75M$ for p-p collisions and $\sim 12.5K$ for Pb-Pb collisions.

calculate the calibration parameters. These DAs are running on the four SPD LDCs and they access the locally stored raw data files.
The calibration DAs have two main blocks performing each a processing step. The former foresees the raw data reading and the Reference Data files producing. These files are in ROOT format with the structure described in the block diagram of Fig. 5.4. The Reference Data files contain the integral hit-maps tagged with the actual detector configuration, the calibration procedure parameters, information on the data source and related to the detector status.
The Reference Data files information is accessible by any ROOT based system because they are based on ROOT containers. Moreover they also have a high compression level that allows storing in few Mbs almost the same information of few hundreds Mbs of raw data. However, the hit-maps are integrated over a certain number of events. The single event multiplicity and efficiency are not contained in these files but this information is not important in the calibrations.

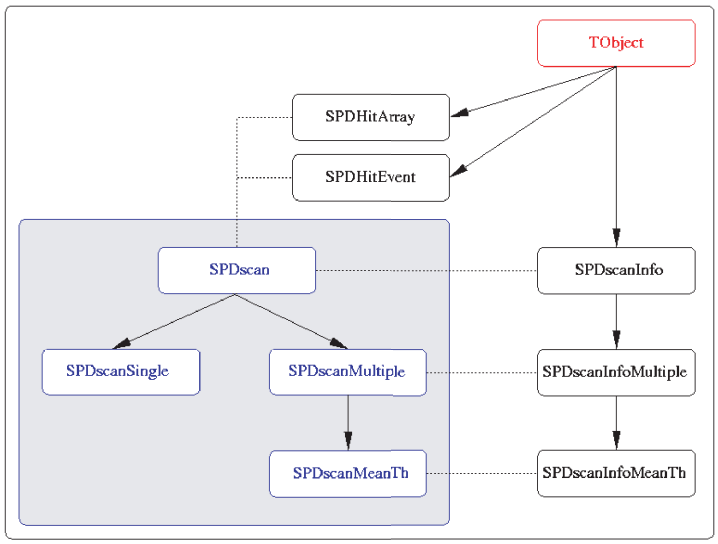

Figure 5.4: The Reference Data container classes structure.

The second calibration DAs analysis phase reads the Reference Data files and calculate the calibration parameters required and it produces Configuration Data files (see section 3.4.2 for more details).
These files have a windows .ini file structure and they contain the list of the

detector configuration elements to be updated in the CDB, e.g. Pixel Chips DACs and noisy pixels to be masked. These files host also instruction to the FXS-CDB Connector (see section 5.2.1.2 for more details). I foresaw the use of text files with an easy structure in order to allow the manipulation of these files by the operator. Furthermore this file structure allows reusing the FXS-CDB Connector also in other context. Indeed for its operation it is enough a text file with the list of parameters to update in the CDB.

The calibration DAs are started by the ECS at the end of each calibration run and they receive as input the run number and the root files name to be analyzed. Automatically the DAs collect the corresponding raw data files and they retrieve from the *Calibration Header* the detector and calibration information required for the analysis. A series of consistency checks on the input files are performed to guarantee the raw data integrity. During the analysis, the quality of the calibration procedure is as well evaluated. For example, if during a Minimum Threshold scan the noise region is not reached, the calibration procedure is rejected. Similar parameters are defined for each type of calibration. The error and status messages produced by the DAs are recorded in the DAQ info logger and they are available online. The info logger is stored into a messaging Db for future reference.

As mentioned before the DAs have been designed with two main blocks corresponding to two processing phases. This structure has been used to achieve high code modularity and easily upgrade the analysis code. The Reference Data generator uses the same offline classes (AliRoot streamer and digitizer) to decode the raw data and it is foreseen to maintain this block structurally unchanged for the full SPD operation time. This DAs block can be also run as stand-alone application on any calibration raw data file to produce Reference Data files. At present it is used in stand-alone inside the Reference Data displayer.
The use of intermediate Reference Data files allows also to repeat the calibration parameters computation and, eventually, to update the methods used.
The second process step has been kept separate by the other DAs block for two main reasons: easy upgrade and use it as stand-alone application. When either an update or a different analysis is required, it is possible to modify or extend only this DAs block. This application can also be used in stand-alone to analyze any reference file. It is planned indeed to use Reference Data analyzer also in the offline reference data analysis. At present the application is used in stand-alone inside the Reference Data displayer (more details can be found in section 5.2.3).

5.2.1.2 FXS-CDB Connector

The FXS-CDB Connector is a process establishing the communication between the DAQ File Exchange Server (FXS) and the DCS Configuration Db (CDB). Its main task is to retrieve the Configuration Data files produced by the DAs and update correspondingly the CDB.
The process is divided in two main blocks as shown in Fig. 5.5. The first

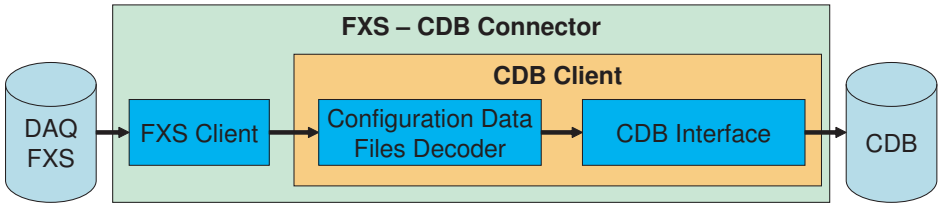

Figure 5.5: The FXS-CDB Connector structure. The two main blocks are FXS Client and CDB client . The CDB client is divided in two blocks: the Configuration Data file decoder and the CDB Interface.

block is the FXS Client whereas the second block is the SPD CDB client already described in section 3.4.2. The process has a two blocks structure allowing an easy code maintenance and to reuse applications.
The FXS Client is a PVSS script able to recognize automatically the Configuration Data files present in the FXS. These files are indeed tagged with a calibration IDs in the FXS files catalog.
The FXS Client operates in three steps. At first it performs a FXS MySQL query to the FXS catalog to retrieve the published Configuration Data files list. The script initiates a secure copy (scp) process that copies the files to a SPD DCS repository; usually it is a local folder on the system running the client. A second FXS MySQL query tags the files in the FXS files catalog as read. The FXS garbage collection system will take care of removing the files from the FXS.
The FXS Client can run in stand-alone mode and it is very useful to retrieve information from the FXS. The client as well as the FXS-CDB Connector can be also started manually by the FSM.

5.2.2 DCS_ONLY scenario

The DCS_ONLY scenario allows the detector calibration using only the DCS. It is a very powerful because does not involve the other SPD subsystems and it can calibrate the detector completely in stand-alone. The drawback of this scenario are the system performance; it is up to a factor 20 slower than the

DAQ_ACTIVE scenario. In general this scenario is used either for system debug or to calibrate a detector partition without interfering with the other detector partitions operation.
The DCS_ONLY scenario block diagram is displayed in Fig. 5.6.

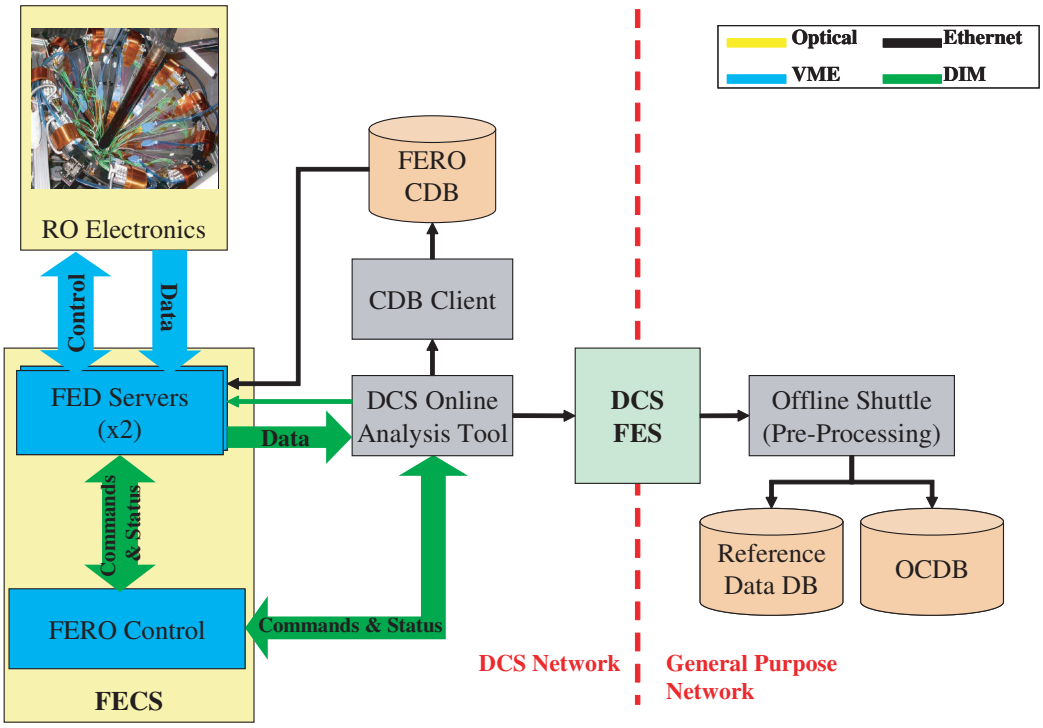

Figure 5.6: A DCS_ONLY calibration scenario block diagram.

The ECS initiate the calibration procedure sending to the SPD FSM top-node a calibration request in DCS_ONLY mode. The FSM moves to CALIBRATING state and it operates the FECS as in the DAQ_ACTIVE scenario; it configures the detector and it sends the triggers requests either to the FED Server or to the trigger system. The main detector data stream is forwarded to an internal Router cards Dual Port Memory (DPM) accessible via the VME bus. The FED Servers readout the data in the DPMs and keep them in memory (see section 4.3.3 for more details). Furthermore, the FECS starts also a ROOT based DCS Online Data Analysis Tool (CDT) (see below) that constantly pools the FED Servers requesting raw data. As soon as the servers receive a data request, the data are forwarded to the CDT that fills the corresponding hit-maps. When the calibration procedure finishes, the FECS informs the FSM that moves to the appropriate operational state. Moreover the FECS requests the CDT to start the raw data analysis process. This process is equivalent to the process used in the DAs. The CDT displays

the calibration results and produces the same DAs output files: a Reference Data file and a Configuration Data file for each Router card.
The Reference Data files are stored in the DCS File Exchange Server (FES). Further the ECS calls the Offline Shuttle to forward these files to the Reference Data Db and to the OCDB.
The FSM starts the CDB client to update the CDB using the Configuration Data files information. The calibration procedure is then finished.

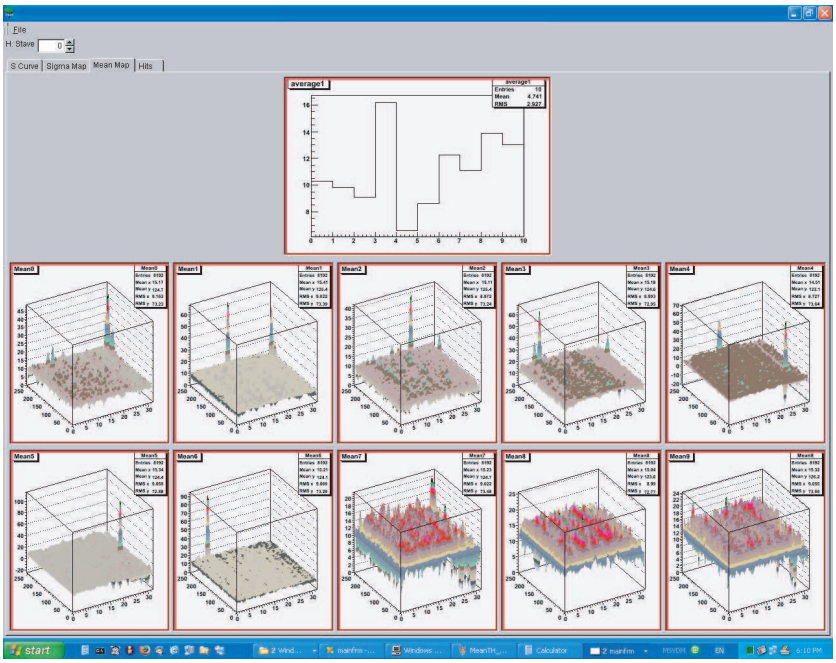

Figure 5.7: A DCS Online Data Analysis Tool screen-shot in which the ten Pixel Chip hit-maps of HS 0 are displayed.

The CDT is not only an analysis tool but it can also be used as data displayer. The DCS_ONLY scenario can be used for physics data taking[8] either emulating the DAQ or spying the data streams inside the Router cards. Moreover, the CDT can produce raw data files[9].
The CDT is controlled and it receives the information needed for the data analysis by the FECS. The communication between the 3 software tools such as CDT, FECS and FED Servers is performed via DIM. Two channels are devoted to the FED Server communication; the former perform the data

[8]In SPD stand-alone run only because the trigger rate is reduced using this tool.
[9]The format of the CDT raw data files is different by the standard DAQ raw data format.

request while the second transmits the data stored in the FED Servers. In this scenario, indeed, the FED Servers act as software data buffers. The data should be read quickly from the Router cards in order to maintain high trigger rate and prevent the busy of the readout electronics. On the other hand the CDT contains data processing routines not fast enough to catch up with the Router cards data production.
The third DIM channel establishes the communication between CDT and FECS. The FECS sends commands (i.e. start pooling, start processing, etc.) and a series of CDT configuration information. On the other hand the CDT returns to the FECS status reports on the ongoing operations.
The CDT is a very powerful tool but in this thesis only a screen-shot is reported to give an idea of how it looks like. However more details on the CDT operation, functionalities and structure can be found in [41]. Fig. 5.7 shows a CDT screen-shot in which the ten Pixel Chips hit-maps of HS 0 are displayed. These have been recorded during a Mean Threshold scan.

5.2.3 Reference Data Displayer (RDD) and SPD MOOD

The Reference Data Displayer (RDD) and the SPD Monitor Of Online Data (MOOD) are two user interfaces. The former displays the calibration results whereas the latter shows the detector data. This section is not intended to describe these complex applications because it would not be interesting in this thesis. However a brief introduction is reported and few screen-shots are displayed. Full references can be found in [43], [42].
The RDD is a ROOT based application designed to display the Reference Data and the Configuration Data with a user friendly interface. This application is not only a displayer but it hosts also the DAs analysis capabilities, indeed, the DAs code has been embedded inside this application. It can read the raw data files and it produces the corresponding Reference Data files. Moreover the RDD can read these files and generate the associated Configuration Data files.
The RDD is running on the DAQ monitor machines and can be used by the user to check the Reference Data files quality. In the debug phases the DAQ_ACTIVE calibration procedures will be stopped at the Reference Data production. The RDD will compute the Configuration Data files under operator request.

Fig. 5.8 displays two RDD screen-shots: the former is related to a Delay Scan whereas the latter to a Minimum Threshold Scan.
In the bottom of the RDD frame two selectors allow to choose from which

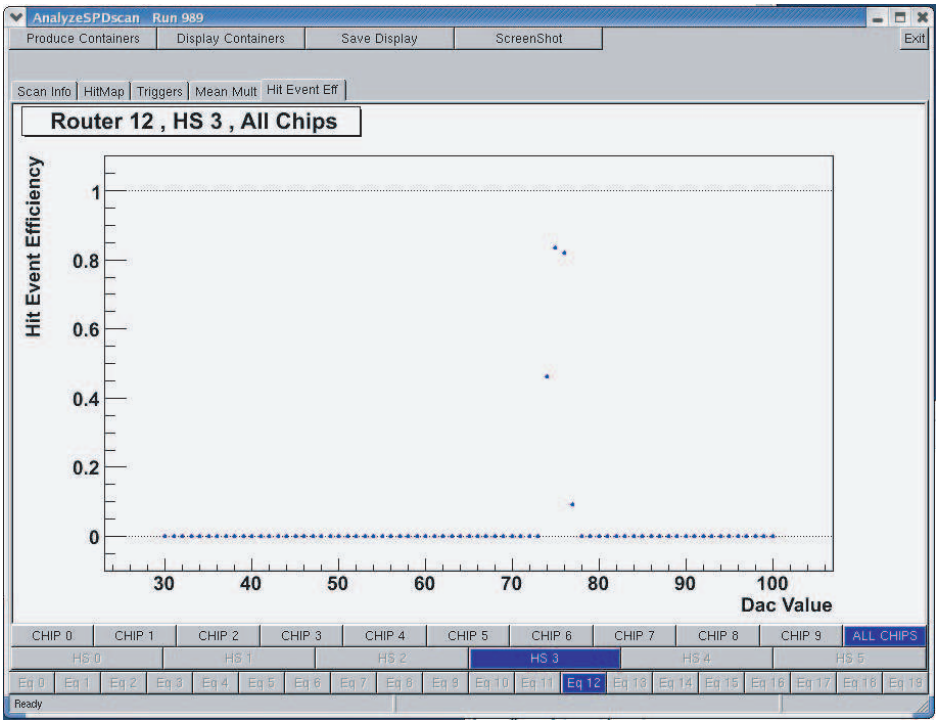

(a)

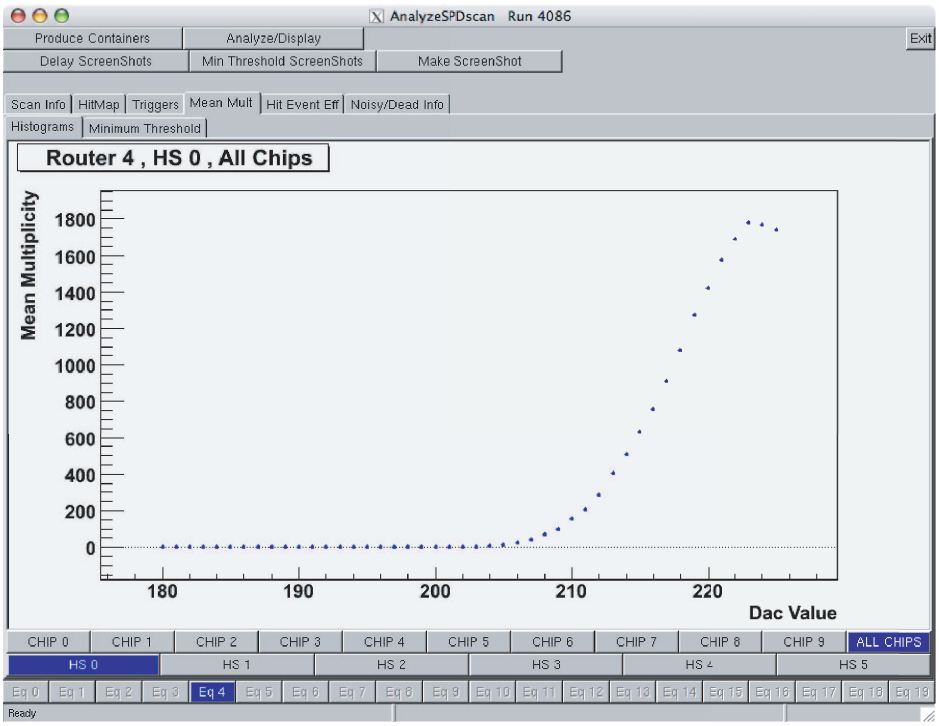

(b)

Figure 5.8: Two Reference Data Displayer schreen-shots. (a) displays an efficiency plot used to evaluate the L1 latency in a Delay Scan. (b) shows a multiplicity plot used to determine the chip Minimum Threshold.

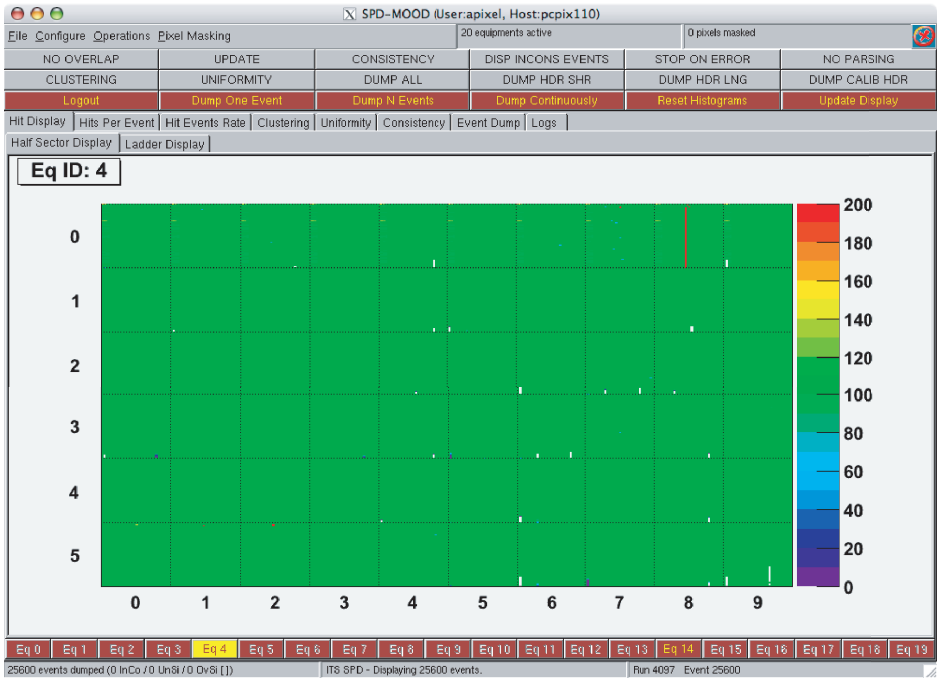

(a)

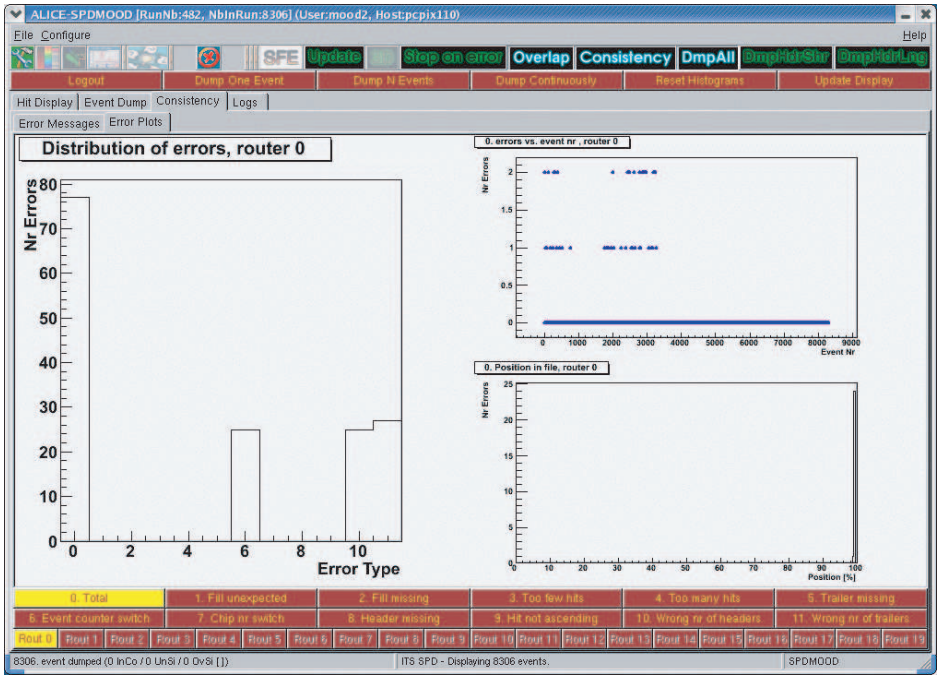

(b)

Figure 5.9: Two MOOD screen-shots. (a) displays all the hit-maps of a Half-Sector . On the bottom part a selector allows moving the view over the activated Half-Sectors . (b) displays the data format consistency check results. On the bottom a selector allows choosing which error to display.

Router card (equipment) and from which HS the data should be displayed. A third selector defines whether to show the histogram corresponding to a Pixel Chip or an integral histogram on all the HS Pixel Chips. The RDD reading the Reference Data defines automatically which selectors should be enabled as function of the hardware structure used during the calibration procedure.
On the top of the RDD frame three tabs allow selecting which histogram to display, choosing between: efficiency, multiplicity and hit-maps. A tab is dedicated to the calibration procedure information.

The SPD MOOD is a ROOT based application designed to display either online or offline the SPD data. MOOD is running on DAQ monitoring PCs and it uses the DATE monitor libraries [64] to retrieve the raw data. This application performs also consistency checks on the incoming data in order to identify data format errors. Moreover, MOOD hosts a clusterer used for online pixel cluster finding.
In this section only two MOOD screen-shots are reported to give an idea of its look.
Fig. 5.9(a) displays the hit-maps of a full Half-Sector. Each square corresponds to a Pixel Chip matrix (32x256 pixels). The screen x-axis is the chip number whereas the y-axis is the HS number. A selector on the MOOD frame bottom allows moving the view over the activated Half-Sectors.
Fig. 5.9(b) displays the raw data format consistency checks histograms. Using a selector on the bottom of the MOOD frame it is possible to choose which error type should be displayed. A global histogram (on the left) reports the number of error for each type. Two histograms (on the right) show at which event and at which percentage of the data file the errors occurred.

5.3 Systems Application and Detector Performances

This section is devoted to the SPD characterization tests performed using the described detector and calibration systems. Without these systems the SPD could not have been commissioned.
The SPD test, integration and commissioning before the installation in ALICE have been carried out within the Departmental Silicon Facility (DSF) clean room area (class 100,000) at CERN. The facility was equipped with the final trigger/DAQ systems, cooling plant, power supply system, readout

electronics and DCS including temperature monitoring and safety interlocks. Two FED Servers were implemented and operational. Three working nodes were used to run the FSM, the DCS SCADA layer and the DCS Online Data Analysis Tool. The DAQ system hosted the DAs, the FXS and the ECS. An external CDB running in the ALICE DCS lab has been used. The two calibration scenarios (DAQ_ACTIVE and DCS_ONLY) have been set up and tested at the DSF.
The main objective was to test and commission the full detector with all the final systems and services before installation in the experimental area. The ten SPD sectors have been characterized at first independently and after integration in the two SPD half-barrels. The configuration parameters retrieved have been stored in the CDB to generate a startup set for the ALICE operation and, in particular, for the first ALICE commissioning run which took place in December 2007.

5.3.1 Sectors and Half-barrels Test overview

During the commissioning phases the performance of the 10 sectors have been evaluated. On each sector, all the Half-Staves have been tested following a well defined procedure for a full functionality check. The operation point of every HS has been verified in terms of minimum threshold, bias voltage and number of working pixels. The results obtained are in agreement with those found in the preceding HS production tests. Pixel matrix uniformity measurements have been performed using TPs. A good response uniformity of all the matrices was found while applying a TP equivalent of $\sim 5000e^-$ and applying a common threshold of $\sim 2500e^-$.
Sector tests were also carried out using a ^{90}Sr radioactive source to unambiguously identify non-working pixels. Few pixels (< 1 %) did not respond correctly due to bump bonding problems and electrically malfunctioning pixels. Bump bonding yield was in agreement with the corresponding measurements on HS.
Combining the results of the electrical test pulse and the source measurements, a mean threshold of $\sim 2400e^-$ with an RMS noise of $\sim 200e^-$ has been found for all the HSs. In Fig. 5.10 the mean threshold distribution for one Half-Sector is displayed.
The mean threshold has been evaluated individually reading single HSs and during the full sector readout. These measurements demonstrate that the system is not sensitive to common noise or cumulative effects. The values of mean threshold and RMS noise remained unchanged for both configurations of readout.

The measured mean threshold for all the HSs tested is in agreement with the operational requirements for ALICE.
No degradation of the minimum threshold compared to the HSs tests was found. The noisy and dead channels have been identified studying the uniformity of response of the pixel matrices and via dedicated noisy runs. The ratio of noisy and dead channels over the total number of pixels is 10^{-5}. All the noisy pixels identified can be masked in the FE chips and they will not influence the offline track reconstruction process.
The mean leakage current is around 1.49 μA with a RMS of 1.65 μA.
The temperature distribution over the HSs has been analyzed and it is stable at 28 ± 2^oC on the HS surface, while the cooling system operates, without load, at 17^oC. This measurement was carried out using a thermal camera and the two independent Pt1000 chains mounted on each HS.
The interlock system reacts in less than 1 s and the full detector configuration is performed in less than 60 s.

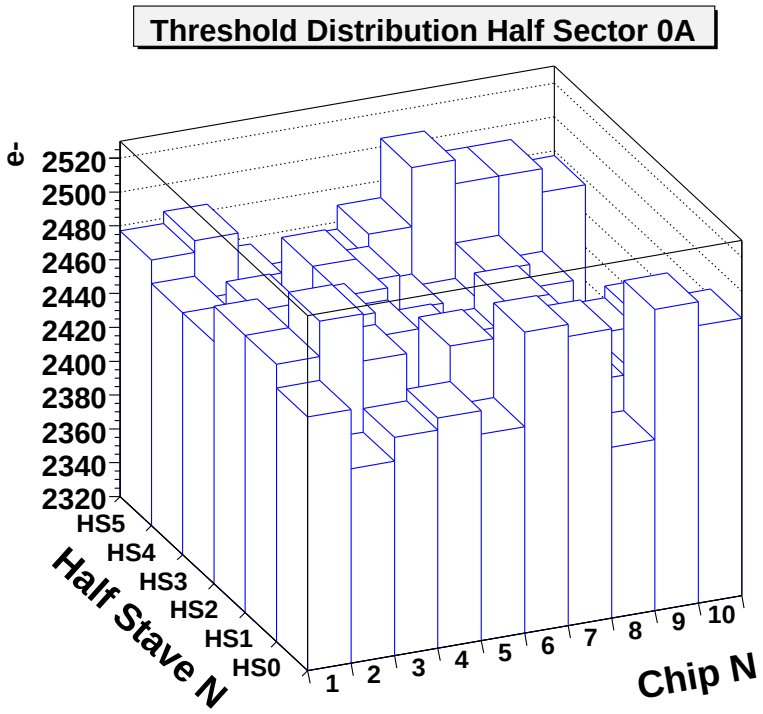

Figure 5.10: A histogram displaying the mean threshold distributions of the Half-Sector 0, side A, FE chips.

The following sections are reporting more details on the detector characterization performed during the detector commissioning.
The SPD sectors have been delivered to the DSF as soon as each of them was produced. During the test phases it has been associated a sector number corresponding to the number of sector delivered. Fig. 5.11 shows the conversion between test sector number (outer numbers) and the official sector numbering in the SPD (inner numbers). The following sections and plots displayed are using the test sector numbering schema.

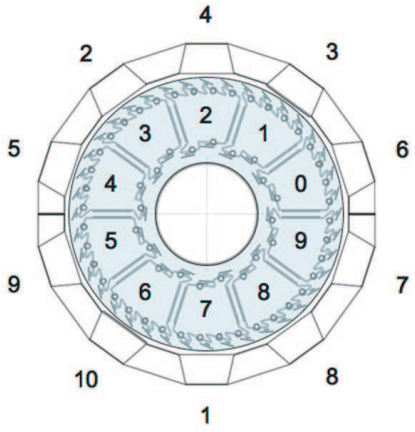

Figure 5.11: Nomenclature conversion between the sector number used during the test phases and the actual sector position in the ALICE SPD.

5.3.2 Leakage Current

The depletion voltage of the ALICE silicon sensor is ≈12 V. The I-V curve of each HSs was recorded between 0 - 50 V. Eleven Half-Stave sensors are not operable at 50 V due to current breakdown, but all can be operated above the depletion voltage. Fig. 5.12 (a) shows the leakage current distribution of all 120 HSs measured on the sectors and normalized to 25 °C at working point. Fig. 5.12 (b) displays the measurements repeated on the HSs once the sectors were integrated in the half-barrels.

Comparing the two distributions it can be seen that in (b) some HSs have higher values whereas most of the other HSs have a shift to smaller leakage current. This is a result of the integration of the sectors; since the outer layer was covered by the Carbon Fiber Support (CFS), therefore not illuminated with light. The inner layer on the other hand was not covered and the leakage current increased due to the sensitiveness to light. During the sector tests the sector was covered with a not transparent cover to reduce the light influence

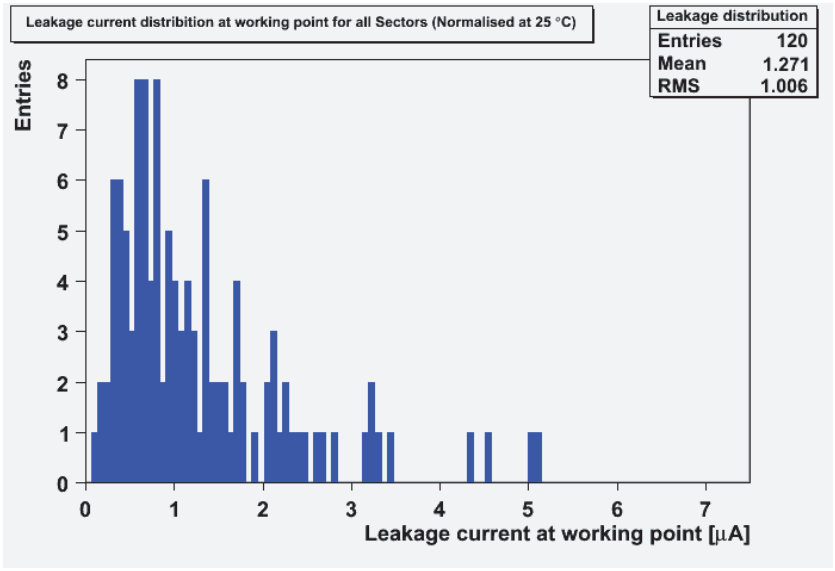

(a)

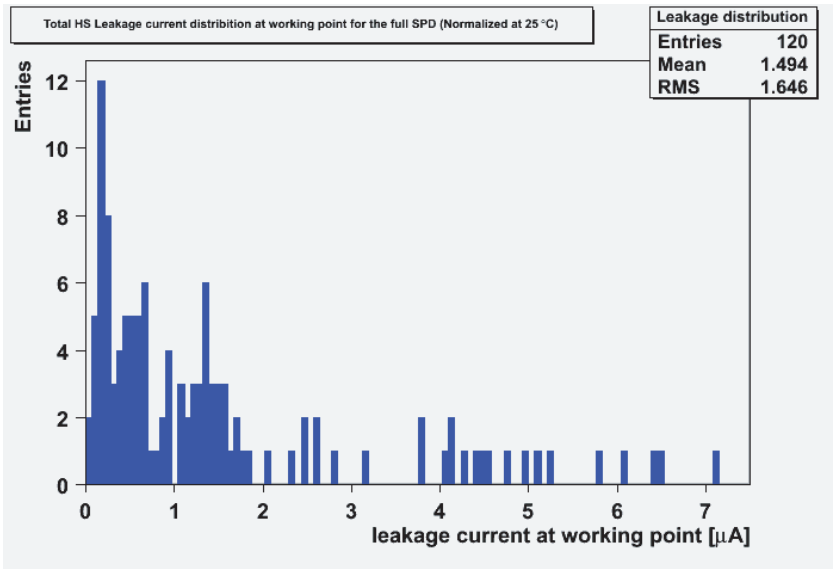

(b)

Figure 5.12: (a) Leakage current of all 120 HSs measured during sectors test at working point. (b) Leakage current of the full SPD after half-barrel integration at working point.

on the sensor. The mean leakage current is 1.27 μA with an RMS of 1.00 μA measured during the sector tests and 1.49 μA with an RMS of 1.65 μA for the half-barrels tests. The large RMS can be explained by the long distribution tail.

5.3.3 Temperature

The Half-Stave temperatures along the Pixel Bus are measured by two independent Pt1000 chains. On each chip a Pt1000 element is mounted. One chain is read by the Router cards whereas the other is directly measured by the PLC of the interlock and temperature monitoring system.

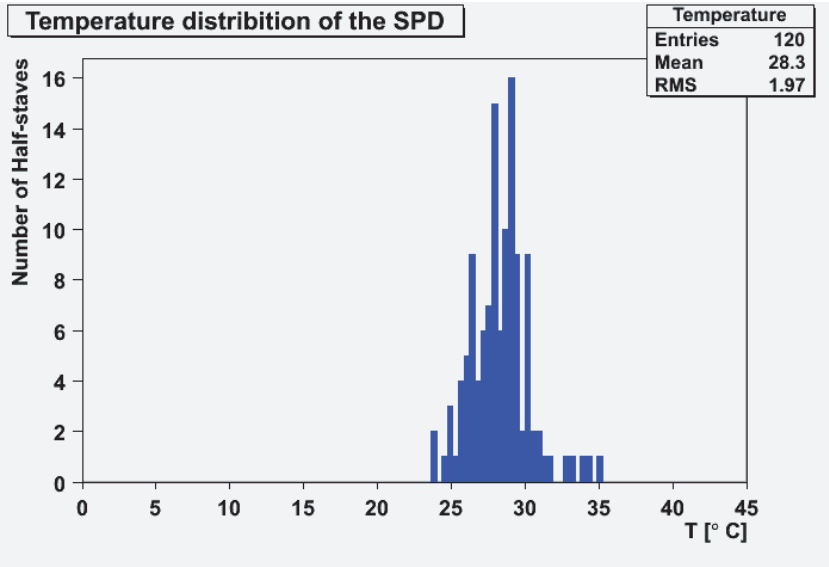

Figure 5.13: Temperature distribution for the complete SPD.

As a reference system a thermal camera was used to double check the reading of the Pt1000 chains.
Three Half-Staves out of 120 showed connection problems in the Pt1000 chain read by the PLC. On those Half-Staves the chip temperature can only be measured using the second Pt1000 chain.
The HSs temperature distribution measured on the half-barrels is displayed in Fig. 5.13. The mean temperature is 28.3 $\pm$ 2.0 °C. The temperature distribution measured during the sectors test is correspondent to the distribution measured during the half-barrels test.

5.3.4 Minimum Threshold

The Minimum Threshold was measured (see section 5.1.1 for more details) varying the global Pixel Chip threshold acting on the Pixel Chips internal *pre_VTH* DAC. The Pixel Chip noise level was measured for each DAC value. It is important to recall that high *pre_VTH* means low threshold and vicev-

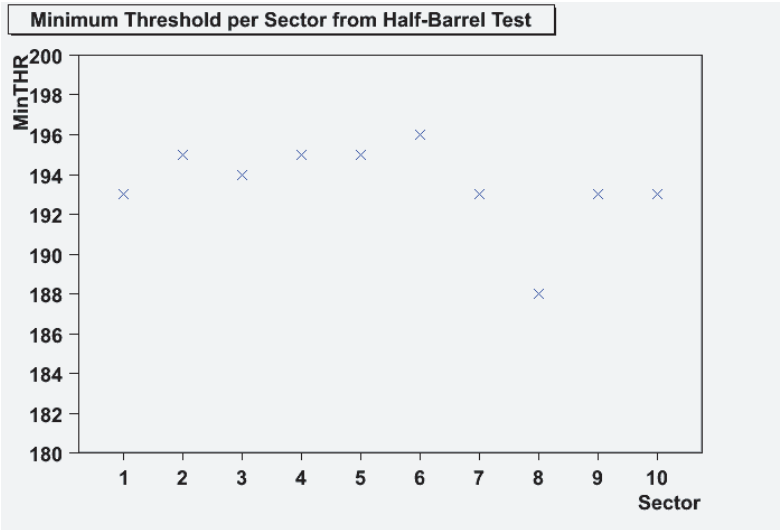

(a)

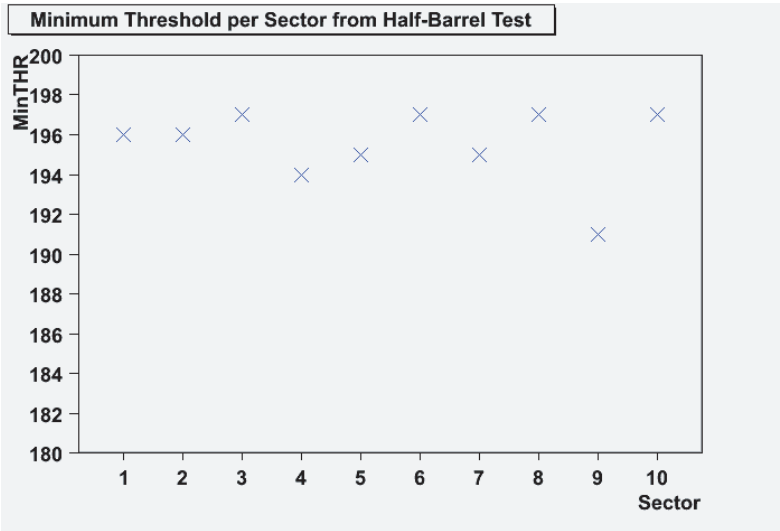

(b)

Figure 5.14: (a) Sectors Minimum Threshold measured during the sector test. (b) Sectors Minimum Threshold after half-barrel integration.

ersa. The sector Minimum Threshold is the highest Minimum Threshold DAC value measured over all Pixel Chips of the sector. Fig. 5.14(a) displays the sector Minimum Threshold distribution evaluated during the sectors test whereas Fig. 5.14 (b) shows the same distribution measured after the sectors integration into the half-barrels.
The Minimum Threshold values do not change appreciably between sectors and half-barrels tests. The Minimum Threshold for the sectors test is 193.5 $\pm$ 2.1 and for the half-barrels test 195.5 $\pm$ 1.8.

5.3.5 Noisy Pixel

During the DSF tests the noisy pixels have been identified setting a global threshold of $\sim 3000e^-$ (much higher than the Minimum Threshold evaluated). A pixel was counted as noisy if it was responding at this high threshold. Fig. 5.15 shows the noisy pixels distributions on the sectors before integration whereas Fig. 5.16 shows the same distribution on the half-barrels. The

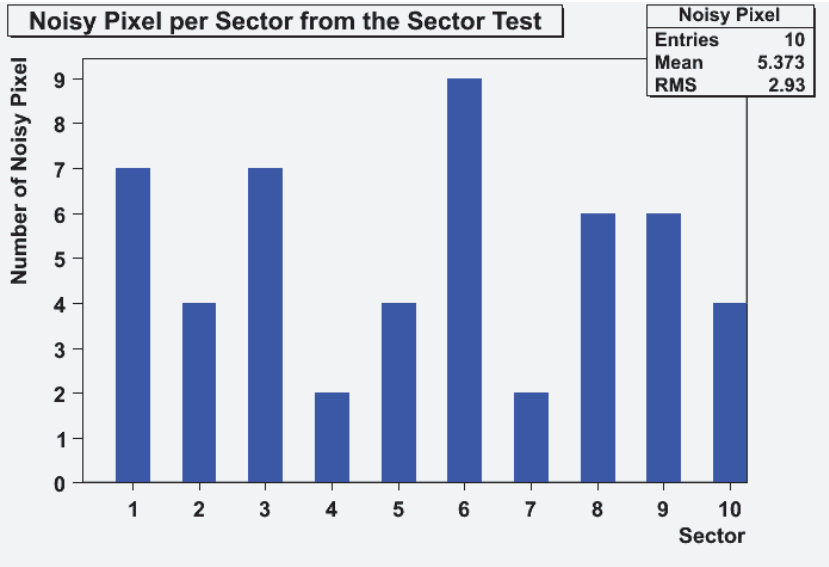

Figure 5.15: Noisy pixels found during the sector test.

total amount of noisy pixels evaluated from the sector test is 51 which is 0.0005 % of all SPD pixels (9830400) whereas in the half-barrels test have been found 39 noisy pixels which is 0.0004 % of all pixels. The reduction of the number of noisy pixels can be explained considering that the 5 sectors connected together form a stronger grounding plane with respect to the single sector. Pixels close to the noisy region, in this case, are less affected by the chip electronics noise.

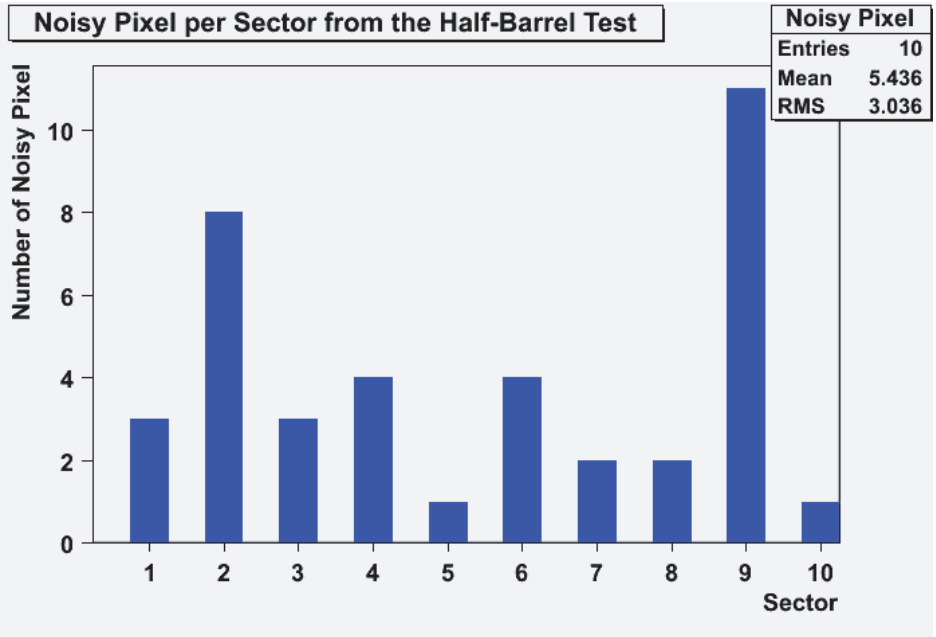

Figure 5.16: Noisy pixels found on the half-barrels.

5.3.6 Cosmic Rays Runs at DSF

On a subset of Half-Staves mounted on a sector the Fast-OR trigger setting was adjusted to carry out dedicated runs with cosmic rays. For this purpose the sector was oriented for maximum vertical acceptance in both the inner and the outer layer. A similar test was later carried out on part of one half-barrel. In a 6 hours continuous run, in which the trigger was based on the coincidence of the Fast-OR of the inner and outer layer, approximately 7000 events were collected. The data have been analyzed using the DAs (see section 5.2.1.1 for more details) and using the offline ALICE analysis framework, AliRoot. The results obtained are equivalent. This test verified also the DAs functionalities. The observed distribution of clusters in the two layers and the clusters correlation along the sector axis were compatible with the expectations, considering that the limited test time available did not allow the optimization of uniformity response and Fast-OR DACs settings required for maximum efficiency.

A plot of the number of clusters on layer 2 (outer) vs the corresponding number on layer 1 (inner) is shown in Fig. 5.17(a). The correlation along the z-axis between clusters fired in the two layers is also shown in Fig. 5.17(b). Fig. 5.18 shows an example of the offline event display (AliEve of AliRoot).

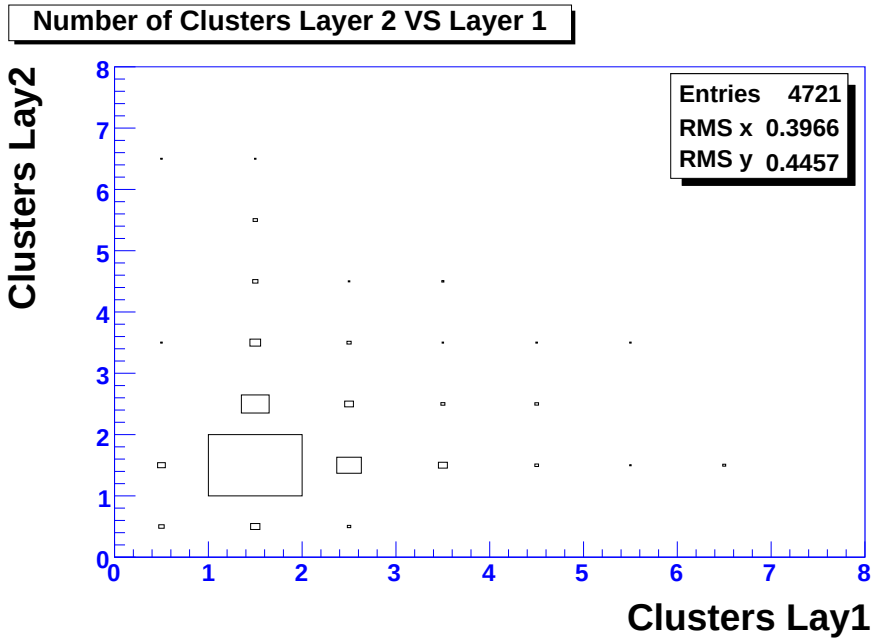

(a)

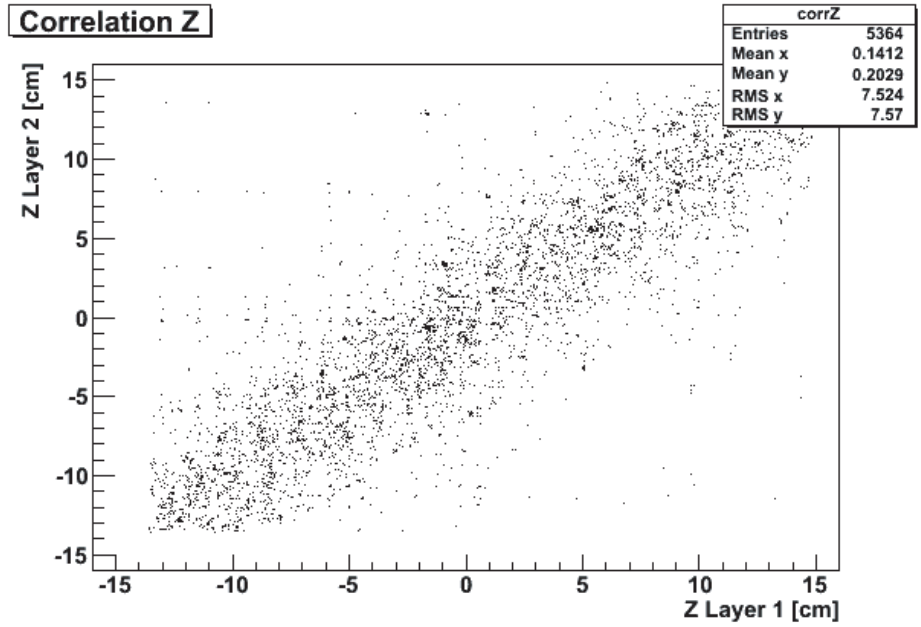

(b)

Figure 5.17: Results of the sector commissioning run triggering using the coincidence of Fast-ORs in the inner and outer sector layers. (a) Number of cluster in the sector inner and outer layers.(b) Clusters correlation plots along the z-axis.

In this figure the cosmic ray hits have been detected on two sectors. The plot integrate over 1000 events.

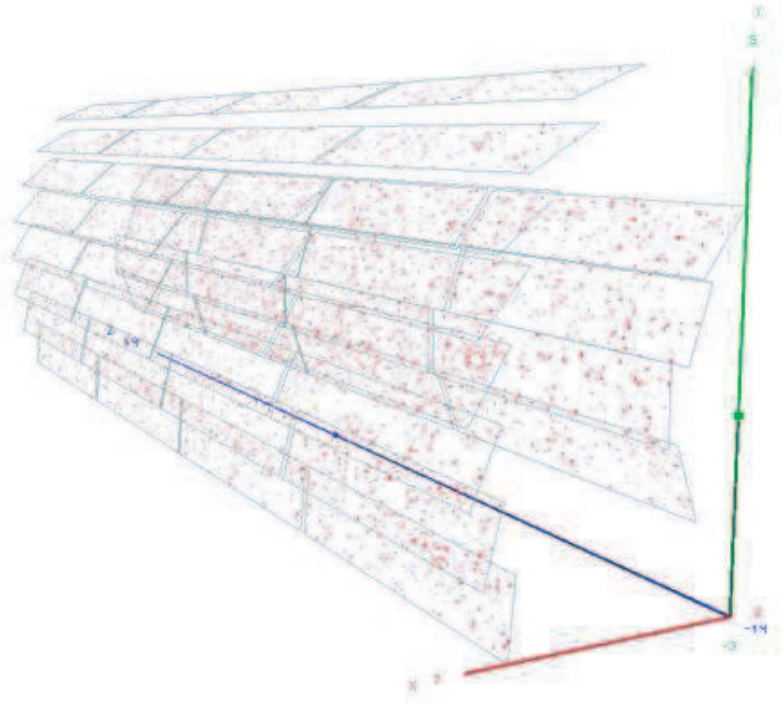

Figure 5.18: An offline ALICE event display (AliEve) picture. Two half-barrel sectors are traversed by cosmic rays and the hits are displayed in both inner and outer layer. The plots integrate over 1000 events.

After the integration tests were completed the detector was moved to the ALICE experiment and installed around the beampipe. First tests were carried out on the electronic readout system and showed full functionality. A complete detector test was carried out during the December 2007 ALICE commissioning run. The detector, the DCS, the DAQ, the trigger and the ECS run stably; and a series of cosmic data runs were performed. The data analysis is ongoing at the time of writing of this thesis.
The calibration procedures have been tested in the ALICE environment and the performance fulfilled the requirements (more details in the conclusions of this thesis).

Conclusions

This manuscript gives a general overview on the SPD online software. It focuses on the control and calibration systems.
I started this project from scratch and now a stable version of the systems is operative and installed in the ALICE experiment. The work described in this thesis is the result of my work and of a small team of collaborators who I coordinated.

The SPD control and calibration systems are complex software designed to operate, monitor and evaluate the performance of the SPD hardware such as front-end electronics and services. Fundamental characteristics of these systems are automation and their fast reactivity. These systems are essential for the SPD operation, indeed the SPD subsystems synchronization, the complex configuration and the calibration procedures could not be performed without. Moreover, critical conditions such as cooling system failure or power supply errors could damage irreversibly the detector. In these conditions corrective actions should be taken in few seconds. Furthermore, the detector data quality and the corresponding rates are fundamental parameters to be evaluated online. Only the systems with high level of automation can cope with the requirements described above.
In the control and calibration systems design I gave a special care to the systems integration with the ALICE systems (DAQ, DCS, ECS and Offline framework), to their performance and to the user interface. Moreover, one of the main goals in the systems design was allowing any operator, also not SPD expert, to operate the detector easily and intuitively.
These strict requirements brought to a complex system structure divided in two main software layers. A FSM layer is on top of a SCADA layer. The FSM layer has a detector oriented hierarchy and it hosts $\sim$ 1500 FSM elements interlinked. With a four levels depth, the FSM hierarchy allows reaching any hardware devices with a fast and intuitive hierarchy browsing. This software layer hosts more than 5000 control loops to guarantee a safe and automatic detector operation. The SCADA layer allows the individual SPD subsystems

(front-end electronics, power supply, cooling, interlock, crates, etc.) operation and monitoring. It also provides an expert user interface giving access to the $\sim 20M$ system settings and to the ~ 5000 monitored online parameters. A Configuration Database (CDB) stores the hardware and the software settings needed for the detector, services and control system operation.
Fundamental SCADA layer components are two SPD Front-End Device Servers (FED Servers) able to operate and manage autonomously the complex SPD front-end electronics. They receive macro-instruction from the clients and automatically configure and monitor the electronics status. Moreover, the FED Servers host the automatic calibration procedures. The FED Server is a complex objects built up of three software layers. The top layer is a Communication Layer responsible of the communication between the FED Server and the clients. These applications are the FECS PVSS and the DCS Online Data Analysis Tool (CDT). The FED Server intermediate layer is an Application Layer hosting the logical server functions. It retrieves the commands received by the Communication Layer, checks the hardware status, pulls or stores the data from/to the CDB and communicates with the driver layer to perform the required operations on the hardware. The FED Server state machine is hosted in the Application Layer. The server bottom layer is the Driver Layer designed for the VME access of the off-detector electronics.
The SPD calibrations allow studying the detector performance and adjusting the detector operation parameters to obtain the best detector response. The calibration system autonomously calculates the best detector setting and it correspondingly updates the CDB. Two calibration scenarios have been designed to automatically calibrate the detector. A DAQ_ACTIVE scenario allows fast full detector calibration. It involves the DAQ, trigger and ECS systems. A DCS_ONLY scenario allows the calibration of a detector partition without interference with the normal operation of the other detector partitions.
The calibration and control systems are now operative and running on a small farm of 10 PCs inside the ALICE experiment; they have been crucial for the detector integration and commissioning. The integration of the systems with the ALICE ECS, DAQ and trigger systems has been accomplished. The full system allowed the SPD data taking in stand-alone run and in global run mode during the ALICE commissioning run which took place in December 2007. In this run the SPD was integrated with all the other ALICE subdetectors. The analysis of the collected events is ongoing.
The commissioning run has been also used as system benchmarks and the DCS performance matched the challenging requirements as reported. The calibration procedures have been tested in the ALICE environment and the performance has fulfilled the requirements. The detector has been calibrated

in terms of uniformity of response and delay in less than 30 minutes. The DCS allowed the detector to run for 24 h/day.
With these systems a series of studies on the SPD components were performed. The cooling system was evaluated and the results showed a good general operation stability. Moreover new cooling settings (pressures) were found to enhance the cooling performance. Studies on the data rates demonstrated that the SPD fulfills the trigger requirements, running stably with a rate of $\sim 3.3\ KHz$.
During the commissioning run the detector was also operated by non SPD experts, using the DCS and the calibration systems. The feedback received from the users performing the detector tests will be used to release a new version of the systems.

Main Acronyms

ADC	Analog to Digital Converter
ALICE	A Large Ion Collider Experiment
API	Application Programming Interface
ASIC	Application-Specific Integrated Circuit
ATLAS	A Toroidal LHC ApparatuS
BSC	Boundary Scan Cells
CaV	Cooling and Ventilation
CCS	Cooling Control System
CDB	Configuration Database
CDH	Common Data Header
CDT	DCS Online Data Analysis Tool
CERN	European Organization for Nuclear Research
CFSS	Carbon Fiber Sector Support
CMOS	Complementary MOS technology
CMS	Compact Muon Solenoid
CU	Control Unit
CS	Control System

DAC	Digital to Analog Converter
DAQ	Data Acquisition
DAs	Detector Algorithms
DATE	Data Acquisition Test Environment
DCS	Detector Control System
DDL	Detector Data Link
DIM	Distributed Information Management
DNS	DIM Name Server
DP	DataPoint
DPE	DataPoint Element
DPM	Dual Port Memory
DPT	DataPoint Type
DSF	Divisional Silicon Facility
DSS	Detector Safety System
DU	Device Unit
ECS	Experiment Control System
FE	Front-End
FECS	FERO Control System
FED	Front-End Device
FED Server	Front-End Device Server
FERO	Front-End and Read Out Electronics
FES	File Exchange Server
FIFO	First Input First Output
FO	Fast-OR
FPGA	Field Programmable Gate Array
FXS	FES
FSM	Finite State Machine
GDC	Global Data Collector
GEDI	Graphical Editor
GOL	Gigabit Optical Link
GUI	Graphic User Interface

JCOP	Joint Controls Project
JTAG	Joint Test Action Group
HLT	High Level Trigger
HS	Half-Stave
HV	High Voltage
ICS	Interlock Control System
ITS	Inner Tracking System
L0	Start trigger sequence (latency < 1 μs)
L1	First level of trigger (latency ~ 6 μs)
L2	Second level of trigger (latency ~ 100 μs)
LDC	Local Data Concentrator
LHC	Large Hadron Collider
LU	Logical Unit
LV	Low Voltage
LVDS	Low Voltage Differential Signaling
LVECL	Low Voltage Emitter-Coupled Logic (ECL)
MCM	Multi Chip Module
MOOD	Monitor Of Online Data
OCDB	Offline Condition Database
ON	Operator Node
OO	Object Oriented
OPC	OLE for Process Control
PARA	Parametrization tool
PCA	Partition Control Agent
PIT	Pixel Trigger
PLC	Programmable Logic Controller
PLL	Phase Looked Loop
PS	Power Supply
PSCS	Power Supply Control System
PVSS	in English it means "Process visualization and control system"
QGP	Quark-Gluon Plasma

RAM	Random Access Memory
RDD	Reference Data Displayer
SCADA	Supervisory Control And Data Acquisition
SCS	Support Services Control System
SMD	Surface Mounted Device
SMI	State Management Interface
SPD	Silicon Pixel Detector
SPS	Super Proton Synchrotron
TP	Test Pulse
TTC	Timing, Trigger and Control
WN	Worker Node

List of Figures

List of Tables

Bibliography

[1] The ATLAS Experiment. Website. http://atlas.ch/index.html.

[2] CMS Wiki. Website. http://en.wikipedia.org/wiki/Compact_Muon_Solenoid.

[3] QGP Wiki. Website. http://en.wikipedia.org/wiki/Quark-gluon_plasma.

[4] S Kiselev, W Klempt, Andreas Morsch, G Paic, Jean Pierre Charles Revol, and K Safarik. *Day One Proton-Proton Physics with the ALICE Central Detector*, 2000. ALICE-INT-2000-28. CERN-ALICE-INT-2000-28.

[5] ALICE Web. Website. http://aliceinfo.cern.ch/Collaboration/index.html.

[6] *ALICE Time Projection Chamber (TPC) : Technical Design Report*, 2000. CERN-LHCC-2000-001.

[7] E. Scapparone. The Time of Flight Detector of the ALICE Experiment. *Proceedings of the QM06*, 2006.

[8] *The ALICE Time of Flight (TOF) : Technical Design Report*, 2000. CERN/LHCC 2000-012.

[9] B. Belin. The Construction of the ALICE HMPID RICH Detector. *Proceedings of HCP 2005*, 2005.

[10] A. Gallas. Experience from the Construction and Installation of the HMPID CsI-RICH Detector in ALICE. *Proceedings of the 11th VCI 2007*, 2007.

[11] Tariq Mahmoud. The ALICE Transition Radiation Detector (TDR) : Technical Design Report. *Nucl. Instrum. Methods Phys. Res., A 502 (2003) 127-132*, 2003.

[12] *The ALICE Transition Radiation Detector (TDR) : Technical Design Report*, 2001. CERN-LHCC 2001-021.

[13] *A High Resolution Electromagnetic Calorimeter based on Lead-Tungstate Crystals*, 2005. ALICE-INT-2005-053.

[14] *ALICE Photon Multiplicity Detector (PMD) : Technical Design Report*, 1999. CERN-LHCC-99-032.

[15] *ALICE forward detectors: FMD, T0 and V0 : Technical Design Report*, 2004. CERN-LHCC-2004-025.

[16] R.Arnaldi. The Time of Flight Detector of the ALICE Experiment. *Proposal of abstract for CALOR99, Lisbon*, 1999.

[17] S. Beole et al. The ALICE Silicon Drift detectors: Production and assembly. *Proceedings of VERTEX 2006*, 2006.

[18] J P Coffin. Development and tests of double-sided silicon strip detectors and read-out electronics for the internal tracking system of alice at lhc. *Nucl. Phys. A*, 1999. CERN-ALI-99-01. CERN-ALICE-PUB-99-01.

[19] *ALICE Inner Tracking System (ITS) : Technical Design Report*, 1997. CERN-LHCC-99-012.

[20] G. Aglieri Rinella et al. The level 0 pixel trigger system for the alice experiment. Proceedings of the 12th Workshop on Electronics for LHC and Future Experiments, LECC, September 2006. Valencia, Spain.

[21] Kluge A. *Specifications of the On Detector Pixel Pilot System-OPS*. CERN, June 2000. http://akluge.home.cern.ch/akluge/work/alice/spd/.

[22] A. Kluge, *The ALICE silicon pixel detector front-end and read-out electronics*, *Nucl. Instr. and Meth.*, **A 560** (2006) 67-70.

[23] M. Krivda et al. Alice spd readout electronics. Proceedings of the 12th Workshop on Electronics for LHC and Future Experiments, LECC, September 2006. Valencia, Spain.

[24] A. Kluge et al. The ALICE Silicon Pixel Detector: Electronics System Integration. *Proceedings of IEEE 2005*, 2005.

[25] M. Caselle et al. Assebly Proceduree of the Module (Half-Stave) of the ALICE Silicon Pixel Detector. *Proceedings of 9th Pisa Meeting and Advanced Detectors*, 2003. published in Nuclear Instruments and Methods in Physics Research A, 501 p. 111 - 118.

[26] P. Riedler et al. The ALICE Silicon Pixel Detector: System, Components and Test Procedures. *Proceedings of Waldbadkreuth*, 2005.

[27] Parker K. P. *THE BOUNDARY-SCAN HANDBOOK*. Kluwer Academic Publishers, first edition, 1994.

[28] Fadmar Osmic. The ALICE Silicon Pixel Detector System. PHD Thesis, 2005. Technical University of VIenna.

[29] Specification of the digital control part of the analog pilot chip. *CERN*, April 2002. http://akluge.home.cern.ch/akluge/work/alice/spd/.

[30] ALICE. *The ALICE Pixel Pilot Chip, Users Manual*. CERN, November 2002. http://akluge.home.cern.ch/akluge/work/alice/spd/spd_frame_intro.html.

[31] Moreira P et al. *Gigabit Optical Link Transmitter manual*. CERN. GOL Reference Manual.

[32] Riedler P. et al. First results from the alice silicon pixel detector prototype. *Nucl. Instrum. Methods Phys. Res.*, A(501):111–118, 2003.

[33] Brun R. & Rademakers F. *ROOT, Users Guide 3.10*. CERN, December 2003.

[34] Alice SPD wiki website, https://twiki.cern.ch/twiki/bin/view/AliceSPD/WebHome

[35] National Instruments Visa website,http://www.ni.com/visa/

[36] ITCOBE website,http://www.itcobe.cern.ch/index.html

[37] CAEN Wwbsite, http://www.caen.it

[38] ELMB website, http://elmb.web.cern.ch/ELMB/ELMBhome.html

[39] ALICE Offline Shuttle website, http://aliceinfo.cern.ch/Offline/Activities/Shuttle.html

[40] Allice Offline website, http://aliceinfo.cern.ch/Offline

[41] DCS Online Data Analysis Tool website, https://twiki.cern.ch/twiki/bin/view/AliceSPD/SpdDcsSoftware

[42] Reference Data Displayer website, http://tydes.web.cern.ch/tydes/doc/CalibrationOverview/SPDRefDisp/

[43] MOOD website, http://tydes.web.cern.ch/tydes/doc/SPDMood/

[44] Nucl. Instr. Meth. A360 (1995), 91;
F. Antinori *et al.*, Nucl. Phys. A 590 (1995) 139c;
V. Manzari *et al.*, Nucl. Phys. A 590 (1995) 139c.

[45] K. Wyllie et al., "Front-end pixel chips for tracking in ALICE and particle identification in LHCb", *Proceedings of the Pixel 2002 Conference*, SLAC Electronic Conference Proceedings, Carmel, USA, September 2002.

[46] P. Riedler et al., "Overview and Status of the ALICE Silicon Pixel Detector", *Nuclear Instruments and Methods in Physics Research A* 565, p. 1-5, 2006.

[47] P. Riedler et al., "The ALICE Silicon Pixel Detector (SPD): System, Components and Test Procedures", *Nuclear Instruments and Methods in Physics Research A* 568, p. 284-288, 2006.

[48] F. Faccio *et al.*, Proceedings of the 4th Workshop on Electronics for LHC Experiments, Rome, Sept 21-25, 1998, pp. 105-113.

[49] A. Kluge *et al.*, Proceedings of the 7th Workshop on Electronics for LHC Experiments, Stockholm, Sept 10-14, 2001, pp. 95-100;

[50] A. Kluge *et al.*, Proc. of the PIXEL 2002 Workshop, Carmel, Sept. 2002, published in the SLAC electronics conference archive.

[51] W. Snoeys *et al.*, Pixel readout electronics development for the ALICE pixel vertex and LHCb RICH detector, Proc. of the PIXEL 2000 Workshop, Genova, 5-8 June 2000.

[52] ALICE Central Trigger Processor (CTP) User Requirement Document (URD).

[53] ALICE Collaboration, ALICE Physics Performance Report, CERN-LHCC-2003-049, J. Phys., G 30 (2004) 1517-1763.

[54] P. Riedler et al., Overview and status of the ALICE Silicon Pixel Detector, Proceedings of the Pixel 2005 Conference, Bonn, Germany.

[55] A. Kluge, The ALICE silicon pixel detector front-end and read-out electronics, Nucl. Instr. and Meth. A 560 (2006) 67-70.

[56] Agilent Technologies, Low Cost Gigabit Rate Transmit/Receive Chip Set with TTL I/Os, Technical Data, HDMP-1022/HDMP-1024 data sheet, December 2003.

[57] J. Conrad et al., Minimum Bias Triggers in Proton-Proton Collisions with the VZERO and Silicon Pixel Detectors, ALICE-INT-2005-025.

[58] G. Aglieri Rinella et al., The Level 0 Pixel Trigger system for the ALICE experiment, Journal of Instrumentation JINST 2 P01007, 24 January 2007.

[59] J. Grahl, S. Corum, CMS Collaboration, Acceptance Test Report for NGK 12 channel Opto-Receivers for CMS ECAL data links, CERN Note.

[60] E. Dupont, Electronics cooling with FLOTHERM: the Level 0 Pixel Trigger System for the ALICE Silicon Pixel Detector, CERN TS, CFD-2006-05, June 2006.

[61] Morsch and Pastircak, Radiation levels in the ALICE detectors and electronic racks, ALICE-INT-2002-028.

[62] F. Scarlassara *et al.*, 'Cooling Tests for the Silicon Pixel Detectors', ALICE Internal Note INT-2000-018 (2000).

[63] A. Pepato *et al*, Nuclear Instruments and Methods **A**, 565, 6-12.

[64] ALICE Internal Note/DAQ, ALICE-INT-2002-036

[65] G. Rubin *et al*, The ALICE Detector Data Link, 5th Conference on Electronics for LHC Experiments LEB '99 , Snowmass, CO, USA , 20 - 24 Sep 1999 - pages 493-8

[66] ETM website, http://www.etm.at/

[67] F. Carena *et al*, The ALICE Experiment Control System, Proceedings of Computing High Energy Physics conference 2004, Interlaken, Switzerland

[68] I.A. Cali *et al*, The ALICE Silicon Pixel Detector control system and on-line calibration tools, JINST 2 P04008 (2007).

[69] P. Riedler *et al.*, Proceedings of the $VERTEX$2003 Workshop, Lake Windermere, 2004, to be published on NIM A.

[70] P. Nilsson *et al.*, Proceedings of the 10^{th} Vienna Conference on Instrumentation, Vienna (Austria), February 2004, NIM A 535 (2004) 424-427.

[71] D. Elia *et al.*, ALICE Internal Note, ALICE-INT-2005-007.

[72] D. Elia *et al.*, ALICE Internal Note, ALICE-INT-2005-011.

[73] P. Riedler *et al.*, Proceedings of the 10^{th} International Workshop on Vertex Detectors, Brunnen (Switzerland), September 2001, Nucl. Instrum. Methods Phys. Res. A501 (2003), 111-118.

[74] I.A.Cali et al., *Test, Qualification and Electronics Integraion of The ALICE Silicon Pixel Detector Modules*, World Scientific 2005.

[75] *SMI++ Manual*, http://smi.web.cern.ch/smi/.

[76] The Alice Pixel Team, *Receiver Card*,Alice Notes, Jenuary 2003, CERN, http://alice1.home.cern.ch.

[77] Alice Team, *ALICE Technical Design Report of the Inner Tracking System (ITS)*,CERN /LHCC / 99-12 ALICE TDR 4.

[78] I.A.Cali, *Readout of the Silicon Pixel detector in tha ALICE experiment*, 2003 ICFA Instrumentation School, Itacuruça, Rio de Janeiro, Brazil, Poster.

[79] C. Quigg, *Gauge Theories of the Strong, Weak and Electromagnetic Interactions*, Benjamin-Cummings, Reading (1983).

[80] I. Aitchison and A. Hey, *Gauge Theories in Particle Physics*, Institute of Physics Publishing, 2004.

[81] S. Weinberg, Phys. Rev. Lett. **36** (1976) 294.

[82] T. Hambye and K. Riesselmann, *Matching conditions and Higgs mass upper bounds revisited*, Phys. Rev. D **55** (1997) 7255.

[83] The LEP Collaborations ALEPH, DELPHI, L3, OPAL, the LEP Electroweak Working Group and the SLC Heavy Flavour Group, hep-ex/0312223, (Prepared from contribution of the LEP and SLD Experiments to the 2003 Summer Conferences).

[84] S. Söldner-Rembold, *Standard Model Higgs Searches and Perspectives at the Tevatron*, submitted to proceedings of Les Rencontres de Physique de la Vallee d'Aoste, Italy, 5-11 March 2006.

[85] T. Appelquist and C.W. Bernard, Phys. Rev. **D22** (1980) 2000.

[86] Results presented at the XXXth International Conference on High Energy Physics, Osaka (2000).

[87] G. *t Hooft Recent Developments in Gauge Theories*, ed. G. *t* Hooft et al. (Plenum Press, 1980).

[88] P. Ramond, Phys. Rev. **D3** (1971) 2415.

[89] P. Fayet, S. Ferrara, Phys. Rep. C**32** (1977) 249.

[90] A.P. Heinson (for the CDF and DØ Collaborations), *Top Quark Mass Measurements*, Fermilab-Conf-06/287-E DØ Note 5226 August 2006.

[91] P. Horava, E. Witten, Nucl. Phys. B**460**,569 (1996).

[92] C. Jarlsmog *Phenomenology of CP violation*, eds. J. Bernabeu, A. Ferrer, J. Velasco, World Scientific.

[93] G. Altarelli and M. L. Mangano (editors), *Proceedings of the Workshop on Standard Model Physics (and more) at the LHC* (2000) CERN 2000-004.

[94] The LHC Study Group, *Large Hadron Collider Conceptual Design*, CERN/AC 95-05, 1995.

[95] T. S. Virdee, *Detectors at LHC*, Phys. Rept. **403-404** (2004) 401-434.

[96] The ATLAS Collaboration : *ATLAS Detector and Physics - Performance Technical Design Report*, Vol. I, CERN/LHCC 99-14, 1999.

[97] The CMS Collaboration, *The Compact Muon Solenoid - Technical Proposal*, CERN/LHCC 94-38, 1995.

[98] ALICE collaboration, *ALICE technical proposal*, CERN/LHCC 95-71 LHCC / P3, 1995

[99] LHCb collaboration, *LHCb technical proposal*, CERN/LHCC 98-004 LHCC / P4, 1998.

[100] TOTEM Collaboration, *TOTEM - Technical Design Report*, CERN/LHCC 2004-002 (2004).

[101] M. Spira and P. M. Zerwas, *Electroweak Symmetry Breaking and Higgs Physics*, CERN-TH/97-379 (1997).

[102] B. Muller, *The physics of the Quark Gluon Plasma*, Lecture Notes in Physics (1985) 255.

[103] S.Luders, R.B.Flockhart, G. Morpurgo, S.M. Scheling: *The CERN Detector Safety System for the LHC experiments*, CERN,Geneve,Svizzera.

[104] CERN Safety Alarm Monitoring (CSAM), see http://st-div.web.cern.ch/st-div/Groups/ma/se/CSAM/CSAM.htm

[105] A. Daneels and W. Salter, *What is SCADA?*, Int. Conf. on Accelerator and Large Experimental Physics Control System, Trieste, 1999.

[106] Beate Briss, Matthias Schagginger, Leo Knipp *PVSS II - Getting Started - Basics* Version 2.0 (July 2004).

[107] JCOP Framework Team: *JOINT CONTROLS PROJECT (JCOP) FRAMEWORK SUB-PROJECT GUIDELINES AND CONVENTIONS*, CERN-JCOP-2000-008.

[108] CAEN: *User's Manual MOD. SY 1527 UNIVERSAL MULTICHANNEL POWER SUPPLY SYSTEM*, 6 October 2005 Revision n. 13, Italy.

[109] CAEN: *User's Manual MOD. EASY3000/4000 EMBEDDED ASSEMBLY POWER SUPPLY SYSTEM*, 9 May 2006 Revision n. 9, Italy.

[110] CAEN: *Technical Information Manual - OPC SERVER FOR CAEN POWER SUPPLIES Release 2.X*, Revision n. 4, 14 October 2003, Italy.

[111] CAEN: *Information Manual - MOD. A3009/A3009B 12 CH 8 V / 9 A / 45 W POWER SUPPLY BOARD*, Revision n. 7, 3 January 2006, Italy.